INNOVATIONS SUSTAINABILITY MODERNITY OPENNESS

MODERNITY IN ENGINEERING

**Edited by
Dorota Anna Krawczyk
Iwona Skoczko
Ewa Szatyłowicz**

**Politechnika
Białostocka**

INNOVATIONS – SUSTAINABILITY – MODERNITY – OPENNESS
MODERNITY IN ENGINEERING

Editied by
Dorota Anna Krawczyk
Iwona Skoczko
Ewa Szatyłowicz

Patronage

**Bialystok
Univeristy
of Technology**

**Silesian
University
of Technology**

University of Córdoba

**Faculty of Civil Engineering
and Environmental Sciences
Bialystok University
of Technology**

**Student's Branch
of the Polish Association
of Sanitary Engineers
and Technicians**

**Association
of Sanitary Engineers
and Technicians**

INNOVATIONS – SUSTAINABILITY – MODERNITY – OPENNESS
MODERNITY IN ENGINEERING

Editied by
Dorota Anna Krawczyk
Iwona Skoczko
Ewa Szatyłowicz

SERIES OF MONOGRAPHS
VOLUME 43

Table of contents

Authors

Yudum Biyik – Dokuz Eylül University, Engineering Faculty Environmental Engineering Department

Neval Baycan – Dokuz Eylül University, Engineering Faculty Environmental Engineering Department

Ciacci Cecilia – University of Florence, Faculty of Engineering Department of Civil and Environmental Engineering (DICEA)

Neri Banti – University of Florence, Faculty of Engineering Department of Civil and Environmental Engineering (DICEA)

Vincenzo Di Naso – University of Florence, Faculty of Engineering Department of Civil and Environmental Engineering (DICEA)

Frida Bazzocchi – University of Florence, Faculty of Engineering Department of Civil and Environmental Engineering (DICEA)

Francisco Comino – University of Cordoba, Escuela Politécnica Superior de Córdoba. Departament of Physical Chemistry and Applied Thermodynamics

María Jesús Romero – University of Cordoba, Escuela Politécnica Superior de Córdoba. Departament of Physical Chemistry and Applied Thermodynamics

Manuel Ruiz de Adana – University of Cordoba, Escuela Politécnica Superior de Córdoba. Departament of Physical Chemistry and Applied Thermodynamics

Jakub Copik – Silesian University of Technology, Faculty of Energy and Environmental Engineering Department of Water and Wastewater Engineering

Edyta Kudlek – Silesian University of Technology, Faculty of Energy and Environmental Engineering Department of Water and Wastewater Engineering

Mariusz Dudziak – Silesian University of Technology, Faculty of Energy and Environmental Engineering Department of Water and Wastewater Engineering

Diego Fernández-Cheliz – Universidad de Valladolid, School of Engineering Dept. Energy Engineering and Fluidmechanics

Eloy Velasco-Gómez – Universidad de Valladolid, School of Engineering Dept. Energy Engineering and Fluidmechanics

D. Juan Peral-Andrés – Universidad de Valladolid, School of Engineering Dept. Energy Engineering and Fluidmechanics

Ana Tejero-González – Universidad de Valladolid, School of Engineering Dept. Energy Engineering and Fluidmechanics

Ediz Kümük – Dokuz Eylül University, Engineering Faculty Environmental Engineering Department

Naval Baycan – Dokuz Eylül University, Engineering Faculty Environmental Engineering Department

Samten Lhendup – Jigme Namgyel Engineering College, Faculty Department of Mechanical Engineering

Adriana Małgorzata Dowbysz – Bialystok University of Technology, Faculty of Civil and Environmental Sciences. Department of Chemistry, Biology and Biotechnology

Mariola Samsonowicz – Bialystok University of Technology, Faculty of Civil and Environmental Sciences. Department of Chemistry, Biology and Biotechnology

María Jesús Romero – University of Cordoba, Escuela Politécnica Superior de Córdoba. Departament of Physical Chemistry and Applied Thermodynamics

Francisco Comino – University of Cordoba, Escuela Politécnica Superior de Córdoba. Departament of Physical Chemistry and Applied Thermodynamics

Manuel Ruiz de Adana – University of Cordoba, Escuela Politécnica Superior de Córdoba. Departament of Physical Chemistry and Applied Thermodynamics

Erjon Troja – University of Medicine of Tirana, Albania, Faculty of Medicine, Department of Pharmacy

Luljeta Pinguli – University of Tirana, Albania, Faculty of Natural Sciences, Department of Industrial Chemistry

Rozana Troja – University of Tirana, Albania, Faculty of Natural Sciences, Department of Industrial Chemistry

Eltion Dhamo – University of Tirana, Albania, Faculty of Natural Sciences, Department of Industrial Chemistry

Elena Muca – University of Tirana, Albania, Faculty of Natural Sciences, Department of Industrial Chemistry

Tetiana Vitenko – Ternopil Ivan Puluj National Technical University, Faculty of Engineering of Machines, Structures and Technologies Food Technologies Equipment Department

Nataliia Marynenko – Ternopil Ivan Puluj National Technical University, Faculty of Economics and Management Economics and Finance Department

Iryna Kramar – Ternopil Ivan Puluj National Technical University, Faculty of Economics and Management Economics and Finance Department

Anna Justyna Werner-Juszczuk – Bialystok University of Technology, Faculty of Civil Engineering and Environmental Sciences Heating, Ventilation, Air Conditioning Department

Comparison of Microplastic Detection Methods in Wastewater Treatment Plants

Abstract: A plastic can be turn to millions fragments of microplastic particles by anthropogenic activities and environmental events (such as wind, UV light, the water wave action). Due to their surface hydrophobicity, adsorb persistent organic pollutants, the potential to transport contaminants and persistent properties, microplastics have the potential to become widely dispersed in the water environment via hydrodynamic processes and water currents. Plastic materials are durable and rather than decomposing, they break down into small plastic particles over time. These small particles that are less than 5 mm usually defined as microplastic. As a consequence of large plastic production rates, plastic waste accumulation in natural environment rapidly increased all over the World. However, the effects of plastic wastes in different ecosystems are still largely unknown. Water and wastewater treatment plants are important facilities to estimate plastic waste release or retention amount to the environment. The field of microplastic pollution is in its infancy, and there are not yet widely accepted standards for sample collection, laboratory analyses, quality assurance/quality control (QA/QC) or reporting of microplastics in environmental samples. Up to date, few studies have quantified microplastics in wastewater. Moreover, the lack of a standardized and applicable method to identify microplastics in complex samples, such as wastewater, has limited the accurate assessment of microplastics and may lead to an incorrect estimation. In this study, microplastic sampling techniques, extraction methods and identification methods of microplastics in wastewater were compared. It was concluded that studies were mostly done with grap type sampling, wet peroxite oxidation and identification methods with microscope and Fourier Transform Infrared Spectrophotometer (FT-IR). In the FT-IR analysis to determine the polymer structure of microplastics, the most common type of polymer was found to be polypropylene (PP) and polyethylene (PE).

Introduction

The production of mass plastics dated back to 1950s. Since this date plastic production increase reached a current global production that exceeds 348 million tonnes and plastic production is estimated to double by 2035 [1, 2]. Plastics are a serious kind of pollution because of their accumulative and persisting characteristics, as the complete mineralization of polymers in plastic is a long process estimated to take hundreds of years [3]. Plastics are a huge category of synthetic materials in which diverse combinations of polymers and other chemicals results in the production of about 5000 grades of plastic materials [1].

Plastic particles that were not visible were detected in 2000's [4]. The broad classification of the plastics offered was mega-debris (>100 mm), macro-debris (>20 mm), meso-debris (20–5 mm) and micro-debris (<5 mm) [5]. Particles <5 mm was considered as microplastics and this classification is commonly used afterwards however, no lower limit was defined [6]. Different opinions for lowest size exist [7, 8, 9, 10] in the literature however, the term is generally used for particles smaller than 5 mm and larger than 1 μm [11].

Generally, MPs are divided into categories of either primary or secondary MPs. Primary MPs are manufactured as such and are used either as resin pellets to produce larger items or directly in cosmetic products such as facial scrubs and toothpastes or in abrasive blasting (e.g., to remove lacquers). Compared to this deliberate use, secondary MPs are formed from the disintegration of larger plastic debris [12].

Primary microplastics mostly originate from personal care products, drugs and pellets used for production of plastic consumer products [13, 14]. The microplastics present in personal care products entering the aquatic environments through effluent discharges of wastewater treatment plants [15] and run-off or mismanagement of industries producing or storing the pellets used in various products including the personal care products [16]. Fibers are the most occurring form of secondary microplastics, and they are most likely to be generated during washing activities of synthetic clothing [17]. Fibers enter the aquatic environment mostly with discharges from wastewater treatment plants.

Microplastics that are discharged from wastewater treatment plants can be transported to many compartments of the environment. Microplastics widely occur in the atmosphere [18], soil [19], ocean [20], freshwater [21] and even in the sediment of an Arctic freshwater lake [22]. They can adsorb pollutants, such as polycyclic aromatic hydrocarbons [23], heavy metals [24], polybrominated diphenyl ethers [25], pharmaceutical and personal care products [26, 27] from environmental media due to their small volume (particle debris size usually smaller than 5 mm) and high specific surface area [4, 11].

Wastewater treatment plants (WWTPs) are considered to be the main recipients of terrestrial microplastics before entering natural aquatic systems [28], which convert primary microplastics into secondary microplastics. The microplastics occurring in municipal wastewater commonly originate from daily human life activities. For example, polyester and polyamide components are commonly shed from clothing during the laundry process [14], and personal care products such as toothpaste, cleanser and shower gel enter WWTPs resulting from our daily use [11, 29].

Previous studies have identified the presence of MPs in wastewater effluents, but results comparisons are limited by the variability in the sampling methods and identification techniques. Presence of MPs has been frequently studied in marine ecosystems. However, there is limited data that involve wastewater samples. Urban waters differ from the marine waters in matrix and organic contents, surface area, MPs sources, and sizes.

This paper thus focuses mainly on reviewing the sampling, extraction and identification techniques used for microplastics analysis in the wastewater treatment plants. The objectives are to (1) compare the methodologies used for the analysis of MPs in wastewater and (2) identify the research gaps and limitations of current techniques; and (3) develop a ranking system to evaluate the information provided by the current study and by future studies.

Sampling and Processing Methods

The studies included in this review identified four types of sample collection techniques, that is, grab samples, composite samples, extraction pumps, and Neuston nets. Table 1 summarizes the studies presented in this section, including the advantages and disadvantages of each method.

TABLE 1. Comparison of MPs Sampling Techniques [30]

Sampling Method	Advantages	Disadvantages
Grab Sample	Easy to Perform Single time sample with less exposure to environmental contamination	Samples may not be representative of the various characteristics of WW influents due to patterns of use and seasonal effects
Extraction Pump	Samples can provide a better representation of the varying properties of WW than grab samples; large volumes can be collected	Sampling flow must be adjusted to the characteristics of the WW

Sampling Method	Advantages	Disadvantages
Composite Sample	Samples can represent the average performance of a WWTP during the collection period	Time-consuming and requires multiple sampling trips, limited volumes can be collected
Neuston/ Plankton Net	Easy	Smaller particles are underrepresented; possible cross contamination due to the plastic net

Sampling of wastewaters for microplastic studies can be conducted in several ways. One of which is grab sampling into containers. This can be done by collecting the wastewater with steel buckets, glass jars, metallic beakers, Ruttner samplers and automatic samplers into glass jars, glass bottles, steel buckets/containers and plastic containers. Some of these collected waters are directly transported to laboratories in the containers and stored at 4°C at dark. Some studies sieved the samples on site after collecting the water by grab samplers, before transporting them to the laboratory [29, 31, 32, 33, 34, 35, 36]. Other sampling method applied was collecting grab samples by direct sieving on stack of sieves in the wastewater treatment plant. The water was passed through the sieves with a connected pump applying a steady flow rate or directly pouring the sample onto the sieves [37, 38]. Sieve mesh size ranges differed from 400 µm to 20 µm and sieves were wrapped during and after completion of sieving. The sieves were then transported directly to the laboratory [30].

Composite sampling was also used for sampling wastewater with auto-samplers based on 24 hours with 15-minute intervals into plastic containers [39, 40]. Several studies used a mobile pumping and filtration device. Mintenig et al. (2017) used a membrane pump connected to a filter housing compartment with lid containing a 10 µm steel cartridge filter and a flowmeter for sampling effluent. Ziajahromi et al. (2017) used a pump connected to a contained vessel with 500 µm, 190 µm, 100 µm and 25 µm mesh screens to sample microplastics in primary, secondary and tertiary wastewater effluents. Talvitie et al. (2015, 2017a, 2017b) used a sampling device consisting of 200, 100 and 20 µm filter segments mounted on O-rings, in transparent tubing and connected to a pump for effluent sampling. These custom devices were generally suitable for effluent waters, due to clogging of the smaller mesh sized filters with high organic loads from other units of the wastewater treatment plants.

This sampling technique consists of using an electric pump, to pump water from the wastewater stream directly onto a stack of sieves with mesh sizes ranging from 20 to 5000 µm. Flow rates varied from 2 to 22 L/min, and the sampling time varied from 2 to 24 h. [37, 40, 44, 46]. The variability of both flow rates and sampling times led to sampling volumes ranging from 120 to 18 000 L [30].

MPs were collected using Neuston Nets or Plankton Nets. Neuston Nets consist of a net in a rectangular frame pulled by a rope, which collects particles in the upper 10 cm of the water column. The mesh sizes of the nets used in the studies ranged between 150 and 330 µm, limiting the detection of MPs to particles that are equal

to or larger than the mesh size. The smaller sizes of MPs can be underestimated. Other concerns of Neuston Nets are atmospheric deposition and cross-contamination from the net itself [37, 47, 48].

After sampling, MPs are processed to separate them from other particles, such as organic and inorganic colloids. Table 2 presents a summary of the studies as well as the advantages and limitations of each of the processing techniques described below.

TABLE 2. **Comparison of the Sample Processing Techniques [30]**

Processing Method	Advantages	Disadvantages
NOAA Method	Organic matter is dissolved, resulting in clean MPs Mps used by several studies	Might need more than one digestion step, increasing the time required different solutions were used to facilitate separation based on density through flotation; ZnCl2 and NaI had higher extraction efficiency than NaCl, but both are more expensive than NaCl
Simple Filtration	Easy, time-saving, and low cost	Difficulties in separating plastic particles from other organic or nonorganic particles
Centrifugation	Easy and simple to use	Fractioning and deformation of plastic particles, resulting in misrepresenting quantity, shape, and size
Staining Method	Easy and low cost	False affirmation of some MP polymers

Wastewaters have considerable amounts of organics and cellulose in their matrix, especially in influent wastewaters and early stages of treatment plants. Therefore, in order to investigate the microplastics in the wastewater, the organics have to be removed to facilitate a suitable condition for the identification and characterization of these particles.

The National Ocean and Atmospheric Administration (NOAA) method is the most used method for processing samples. This method involves digesting organic matter using hydrogen peroxide (H_2O_2) in the presence of an aqueous ferrous solution (Fe (II)) as a catalyst. The digestion step usually is followed by a separation step, which uses sodium chloride or zinc chloride solution to increase the density of the liquid phase. This allows the low-density MPs to float, and the highdensity particles to settle to the bottom. Then, the solution is filtered through mesh sizes [30].

Nuelle et al. (2014) proposed exposing wastewater the samples to 35% H_2O_2 for 7 days and stated that 92% of organic matter digestion or color removal was achieved through this process. Tagg et al. (2015) applied the method from Nuelle et al. (2014) and 15 mL 30% H_2O_2 was added to wastewater from aeration after centrifuging samples and filtering the extract on polycarbonate membranes (0.2 µm pore size). Masura et al. (2015) proposed an improved method for pre-treatment of samples from organic-rich environments. Sieving (5 mm–0.3 mm), collecting particles

and drying at 90°C followed by mass determination was the first step. Second part was the addition of 20 mL of 0.05 M Fe (II) aqueous solution and 20 mL of 30% H_2O_2 followed by heating and stirring at 75°C.

Filtration method, samples were either filtered directly through membrane filters or passed through sieves and followed by a vacuum filtration. The samples that passed through a stack of sieves in the range of 20–500 μm, were transferred using DI water into glass containers, and filtered using a vacuum pump [35, 36, 45, 53, 54]. Membrane filters have pore sizes that vary between 0.1 and 11 μm. This method does not differentiate MPs from other organic particles [30, 34, 35, 36, 53, 54]

Alternatively, some studies used centrifugation to process the samples, followed by sample filtration. Centrifugation conditions ranged from 4000 to 4500 rpm applied for a range of 2–20 min The main drawback was that centrifugation may have deformed, compressed, or broken plastic particles, resulting in an inaccurate determination of the number of MPs. The Rose bengal solution stains organic particles, such as natural fibers and other colloidal organic particles, but not plastics, allowing a visual differentiation between plastics and nonplastic particles [37, 40, 49].

Polymer Characterization

After processing, particles retained on filters or sieves are counted and identified using several techniques. MPs can have various colors, shapes, sizes, and composition; therefore, multiple characterization techniques can be used. The most commonly reported identification methods were visual inspection using an optical microscope, Fourier-transform infrared spectroscopy (FTIR), Raman spectroscopy, and scanning electron microscopy (SEM). Table 3 summarizes the advantages and disadvantages of each one of the identification methods.

Visual identification was done by the naked eye or by using an optical microscope with objectives ranging between 10× and 50× [35, 46, 55, 57]. In some cases, the microscope was coupled with image-analysis software, such as Histolab and Olympus stream. Although visual identification method is an easy and straightforward method, it is not a reliable identification of microplastics. This technique is susceptible to false positives resulting from interference by nonplastic particles; including cellulose, keratin, viscose rayon, coal/fly ash, and paint chips. Particles smaller than 100 μm and transparent particles are difficult to identify using this technique.

TABLE 3. **Advantages and Limitations of the Methods Used for Identifying MPs [30]**

Techniques	Advantages	Disadvantages
Microscope	Fast and easy Identifies shape, size, and colors	Lack of information on the plastic Composition; not confirmative of plastic nature of the particle
FT-IR	Identifies the composition of the polymer Confirmation of the composition of the MP Able to detect small plastic particles (~20 µm)	Expensive Tedious work and time-consuming to analyze all of the particles retained on the filter Wavelength radiation can be a limiting detection factor
Raman	Identification of the composition of the polymer; confirmation of the composition of the MP; detection of small microplastics (1 µm) and nanoplastic (<1 µm)	Expensive instrumentation Time-consuming Interference with pigments and contaminants
SEM/EDS	Clear and high-resolution images of particles facilitates differentiating between plastic and mineral particles due to the dominant inorganic elements (Si, Ca)	Nonaffirmative results in plastic particles; lack of information on the type of polymer

Raman spectroscopy and FT-IR were the most common analytical methods used to identify the composition of MPs, that is, polyethylene, polypropylene, polystyrene, or polyvinyl chloride. In both methods, molecules of the samples are investigated by vibrational spectroscopy producing a characteristic spectrum of the polymer that can be identified using a reference spectra library. For FT-IR, the infrared radiation that irradiates the molecular structure of the particle is partially absorbed and measured in transmission or reflection mode. For Raman spectroscopy, a monochromatic laser source interacts with the molecules of the sample upon the scattering of light, resulting in characteristic molecular vibrations depending on the chemical structure of the component. Similar to the FT-IR, Raman spectroscopy generates a spectrum that can be used to identify the polymer present in the particles [40, 57, 58, 59, 60].

Microplastic studies widely used FT-IR spectrometry for chemical characterization of the particles. 4000–600 cm−1 wave number range was used with spectral resolution of 8 cm−1 to 4 cm−1. Murphy et al. (2016) gathered 16 scans per spectrum, while Talvitie et al. (2017a, b) gathered 15 scans per spectrum. ATR module with diamond crystal was used by Carr et al. (2016) and Ziajahromi et al. (2017), where the spectral resolution was 8 cm−1 and 128 scans were taken to produce spectra. Gies et al. (2018) used wavelength range of 900–3800 cm−1 at spectral resolution of 8 cm−1, while 16 scans were accumulated for FTIR analysis.

Raman spectroscopy was another method widely used for microplastic research combined with a microscope (micro-Raman) [58]. 532 nm laser was used by Kappler et al. (2016) with 20x objective in wavenumber range of 160–3600 cm−1 with laser power of 0.5–10 mW. Integration time was 500 ms and 100 scans were accumulated to acquire spectra. 532 nm laser was also used by Ossmann et al. (2017) with 600 grooves per mm, 300 μm confocal hole width, 100 μm slit width and 50x objective 1.2 and 3.2 mW laser powers were used for the lasers in wavenumber range of 150–3500 cm−1 with 1 second acquisition time and 2 scans were taken per spectrum. Intensity correction was performed. Gündogdu et al. (2018) used 514 nm Ar+ laser with 20x objective to investigate particles. Lenz et al. (2015) used 455 nm laser with 1200 gratings/mm with 10–50x objective. Wavenumber range was 100–3500 cm−1 with 0.96 cm−1 spectral resolution. Integration time was 2 seconds and 3 or more scans per spectra accumulated. Dyachenko et al. (2017) used 632.8 nm laser with 600 lines/grating to confirm cellulose particles extracted. Ossmann et al. (2017) and Gündogdu et al. (2018) used 785 nm secondary lasers to verify particles scanned with 532 or 514 nm lasers and to scan unidentified particles with above-mentioned lasers.

A few studies used scanning electron microscopy (SEM), which visualizes the surface characteristics of the particles. This technique provides high-resolution images of a sample by scanning the surface with a focused electron beam.116 The detailed sample images (>0.5 nm) allow differentiation between particles.117 However, SEM does not identify the composition of the polymer. In addition, the samples require special preparation, such as cleaning, drying, applying a conductive coating, and mounting the sample on a stub using conductive tape [64, 65].

Units reported for MP are inconsistent in recording the sample location (influent, effluent, solids, upstream, downstream) and in the characteristics of the MPs (sizes, shapes, colors, and type of polymer). The various units that are used include MP particle number per volume (e.g., MP/L, MP/gal, MP/m^3), particle number per mass (e.g.MP/kg), particle number per area (e.g., MP/m^2), and concentration (e.g., mg/m^3).

Conclusion

Plastic and microplastic pollution with respect to their size, their invisibility to the naked eye and their durability in the environment is a fact that have attracted attention in the last decade. Structural properties of plastics provide manufacturers a great convenience and their production still continues in significant amounts and they are widely used in personal care products. Their direct effects on organisms in aquatic environments via feeding and indirect effect of releasing the additives, which are toxic to organisms of different levels present in their structure, are studied widely in the literature. Their potential to carry hydrophobic chemicals and antibiotics by sorption and desorption also, their potential to carry microorganisms over

long distances were evaluated. The microorganism layer attached to the microplastic particles and transport of chemicals and antibiotics with this layer have also been mentioned recently. Therefore, microplastics is an important pollutant for investigation in the environment.

Wastewater treatment plants are major potential receivers of primary microplastics such as beads in personal care products, fibers from washing of clothes in high amounts and secondary microplastics from combined sewage systems due to stormwater runoffs. Therefore, they must be investigated to prevent any damage to the environment. Wastewater treatment plants were generally reported successful for the removal of the microplastics (70%–99.9%). However, they still discharge considerable amount of microplastics into environment and considered to be as an important point source. Regarding to the structure of microplastics and the contents of wastewaters such as organic material, various microorganisms, potential chemicals from fugitive discharge of industrial plants and from chemicals used in cleaning and antibiotics used by people; queries of potential hazards arise and therefore, the assessment of microplastics in wastewater streams is crucial both for their direct hazards and indirect hazards to the organisms that they interact with.

Studies considering the determination of microplastics in wastewater treatment plants differentiate in data and sample collection and processing; report the MP concentrations in different units and use different compositional segmentation due to different analyzing methods. Variability of influent loads, temporal conditions and plant operational conditions make the assessments of microplastics difficult. Reviewed studies showed that microplastics in smaller sizes are most likely to be released into environments and detection of these microplastics would lead to a more realistic approach to the microplastics problem with wastewater treatment plants being a point source. The removal of MP may vary depending upon the various units and operations used in wastewater treatment plants.

Our results showed a lack of consistency among the studies with regards to quality assurance procedures, sample collection, sample processing, characterization and identification techniques, and reported results of MPs. Standardized procedures for all of the steps in the assessment of MPs in wastewater will increase the accuracy of the results, reduce time and effort required, and help to perform meaningful interpretations and comparisons between studies.

Literature

[1]   Turan N.B., *Microplastics in wastewater treatment plants: Occurrence, fate andidentification*, Process Safety and Environmental Protection, 2021 146, p. 77–84.

[2]   Walker, T., Gramlich, D., Dumont-Bergeron, A., *The case for a plastic tax: areview of its benefits and disadvantages within a circular economy*, Sustainability, 2020, Emerald Publishing Limited.

[3]   Shrivastava, A., *Introduction to Plastics Engineering*, William Andrew, Elsevier, 2018, ISBN: 978-0-323-39500-7.

[4]   Thompson, R., Moore, C., Andrady, A., Gregory, M., Takada, H., Weisberg S., *New directions in plastic debris*, Science, 2005 310, p. 1117.

[5]   Barnes, D.K.A., Galgani, F., Thompson, R.C., Barlaz, M., *Accumulation and fragmentation of plastic debris in global environments*. Philosophical Transactions of the Royal Society B: Biological Sciences, 2009, *364*(1526), p. 1985–1998.

[6]   Vardar, S. *Removal and Discharge of Microplastics From The Wastewater Treatment Plants In Istanbul*, Submitted to the Institute of Environmental Sciences in partial fulfillment of the requirements for the degree of Master of Science in Environmental Technology, 2020, Bogazici University, Istanbul.

[7]   Koelmans, A.A., Besseling, E., Shim, W.J., *Nanoplastics in the Aquatic Environment. Critical Review*, In: Bergmann M., Gutow L., Klages M. (eds) Marine Anthropogenic Litter, 2015, p. 325–340.

[8]   Kershaw, P. J., & Rochman, C. M., *Sources, fate and effects of microplastics in the marine environment: part 2 of a global assessment. Reports and Studies-IMO/FAO/Unesco-IOC/WMO/IAEA/UN/UNEP Joint Group of Experts on the Scientific Aspects of Marine Environmental Protection* (*GESAMP*), 2015, 93.

[9]   Eriksen, M., Lebreton, L.C.M., Carson, H.S., Thiel, M., Moore, C.J., Borerro, J.C., Galgani, F., Ryan, P.G., Reisser, J., *Plastic pollution in the world's oceans: more than 5 trillion plastic pieces weighing over 250,000 tons afloat at sea*. PLoS One,2014, 9(1), p.15.

[10] Liu, W., Zhang, J., Liu, H., Guo, X., Zhang, X., Yao, X., Cao, Z., Zhang, T., *A review of the removal of microplastics in global wastewater treatment plants: Characteristics and mechanisms, Environment International*, 2021, 146: 106277

[11] Wagner, M., Lambert, S., *The Handbook of Environmental Chemistry, Springer,*2018, p. 69–83.

[12] Browne, M.A., *Sources and pathways of microplastics to habitats,* In: Marine Anthropogenic Litter, Springer International Publishing, 2015, p. 229–244.

[13] Napper, I.E., Bakir, A., Rowland, S.J., Thompson, R.C., *Characterization, quantity and sorptive properties of microplastics extracted from cosmetics*, Marine Pollution Bulletin, 2015 99, p. 178–185.

[14] Anderson, P.J., Warrack, S., Langen, V., Challis, J.K., Hanson, M.L., Rennie, M.D., *Microplastic contamination in Lake Winnipeg, Canada. Environmental Pollution,* 2017, 225, p. 223–231.

[15] Sundt, P., Schulze, P., Syversen, F., *Sources of microplastic- pollution to the marine environment,* Norwegian Environment Agency. UNEP, Plastics in Cosmetics (A Fact Sheet. UNEP), 2014.

[16] Napper, I.E., Thompson, R.C., *Release of synthetic microplastic plastic fibres from domestic washing machines: effects of fabric type and washing condition,*. Marine Pollution Bulletin, 2016, 112, p. 39–45.

[17] Abbasi, S., Keshavarzi, B., Moore, F., Delshab, H., Soltani, N., Sorooshian, A., *Investigation of microrubbers, microplastics and heavy metals in street dust: a study in Bushehr city, Iran*. Environmental Earth Sciences, 2017, 76 (23), p. 1–19.

[18] Guo, J.J., Huang, X.P., Xiang, L., Wang, Y.Z., Li, Y.W., Li, H., Cai, Q.Y., Mo, C.H., Wong, M.H., *Source, migration and toxicology of microplastics in soil,* Environment International, 2019, 137, 105263.

[19] Wang, S.M., Chen, H.Z., Zhou, X.W., Tian, Y.Q., Lin, C., Wang, W.L., Zhou, K.W., Zhang, Y.B., Lin, H., *Microplastic abundance, distribution and composition in the mid--west Pacific Ocean*, Environmental Pollution 2020, 264, 114125.

[20] Han, M., Niu, X.R., Tang, M., Zhang, B.T., Wang, G.Q., Yue, W.F., Kong, X.L., Zhu, J.Q., *Distribution of microplastics in surface water of the lower Yellow River near estuary.* Science of the Total Environ. 2020, 707,135601.

[21] Gonz´alez-Pleiter, M., Vel´azquez, D., Edo, C., Carretero, O., Gago, J., Bar´on-Sola, ´A., Hern´andez, L.E., Yousef, I., Quesada, A., Legan´es, F., Rosal, R., Fern´andez-Pi˜nas, F., *Fibers spreading worldwide: Microplastics and other anthropogenic litter in an Arctic freshwater lake*, Science of the Total Environment, 2020, 722, 137904.

[22] Sørensen, L., Rogers, E., Altin, D., Salaberria, I., Booth, A.M., *Sorption of PAHs to microplastic and their bioavailability and toxicity to marine copepods under co-exposure conditions*, Environmental Pollution 2020, 258,113844.

[23] Foshtomi, M.Y., Oryan, S., Taheri, M., Bastami, K.D., Zahed, M.A., *Composition and abundance of microplastics in surface sediments and their interaction with sedimentary heavy metals, PAHs and TPH (total petroleum hydrocarbons)*, Marine Pollution Bulletin, 2019, 149, 110655.

[24] Singla, M., Díaz, J., Broto-Puig, F., Borr´os, S., *Sorption and release process of polybrominated diphenyl ethers (PDBEs) from different composition microplastics in aqueous medium: Solubility parameter approach.* Environ. Pollution, 2020, 262, 114377.

[25] Liu, G.Z., Zhu, Z.L., Yang, Y.X., Sun, Y.R., Yu, F., Ma, J., *Sorption behavior and mechanism of hydrophilic organic chemicals to virgin and aged microplastics in freshwater and seawater.* Environmental Pollution, 2019, 246, p. 26–33.

[26] Ma, J., Zhao, J.H., Zhu, Z.L., Li, L.Q., Yu, F., *Effect of microplastic size on the adsorption behavior and mechanism of triclosan on polyvinyl chloride*, Environmental Pollution, 2019, 254, 113104.

[27] Sun, J., Dai, X.H., Wang, Q.L., van Loosdrecht, M.C.M., Ni, B.J., *Microplastics in wastewater treatment plants: Detection, occurrence and removal,* Water Research, 2019, 152, p. 21–37.

[28] Magni, S., Binelli, A., Pittura, L., Avio, C.G., Torre, C.D., Parenti, C.C., Gorbi, S., Regoli, F., *The fate of microplastics in an Italian wastewater treatment plant. Science of the Total Environment*, 2019, 652, p. 602–610.

[29] Gies, E.A., LeNoble, J.L., Noël, M., Etemadifar, A., Bishay, F., Hall, E.R., Ross, P.S., *Retention of microplastics in a major secondary wastewater treatment plant in Vancouver, Canada*, Marine Pollution Bulletin,2018, 133, p. 533–561.

[30] Elkhatib, D., Oyanedel-Craver, V. *A Critical Review of Extraction and Identification Methods of Microplastics in Wastewater and Drinking Water*, Environmental Science & Technology, 2020, 54, p. 7037–7049.

[31] Lares, M., Ncibi, M.C., Sillanpää, M., Silanpää, M., *Occurrence, identification and removal of microplastic particles and fibers in conventional activated sludge process and advanced MBR technology,* Water Research, 2018, 133, p. 236–246.

[32] Lares, M., Ncibi, M.C, Sillanpää, M., Sillanpää, M., *Intercomparison study on commonly used methods to determine microplastics in wastewater and sludge samples,* Environmental Science and Pollution Research, 2019, 26, p. 12109–12122.

[33] Leslie, H.A, Brandsma, S.H., van Velzen, M.J.M., Vethaak, A.D., *Microplastics en route: Field measurements in Dutch river delta and Amsterdam canals, wastewater treatment plants, North Sea sediments and biota.* Environmental International, 2017, 101, p. 133–142.

[34] Michielssen, M.R., Michielssen, E.R., Ni, J., Duhaime, M.B., *Fate of microplastics and other small anthropogenic litter (SAL) in wastewater treatment plant depends upon unit process employed.* Environmental Science: Water Research and Technology,2016, 2, p. 1064–1073.

[35] Murphy, F., Ewins, C., Carbonnier, F., Quinn, B., *Wastewater Treatment Works (WwTW) as a source of microplastics in the aquatic environment,* Environmental Science and Technology,2016, 50, p. 800−5808.

[36] Carr, S.A., Liu, J., Tesoro, A.G., *Transport and fate of microplastic particles in wastewater treatment plants,* Water Research, 2016, 91, p. 174–182.

[37] Lee, H., Kim, Y., *Treatment characteristics of microplastics at biological sewage treatment facilities in Korea,* Marine Pollution Bulletin, 2018, 137, p. 1–8.

[38] Simon, M., Alst, N., Vollertsen, J., *Quantification of microplastic mass and removal rates at wastewater treatment plants applying Focal Plane Array (FPA)-based Fourier Transform Infrared (FT-IR) imaging,* Water Research, 2018, p. 142, p. 1–9.

[39] Dyachenko, A., Mitchell, J., Arsem, N., *Extraction and identification of microplastic particles from secondary wastewater treatment plant (WWTP) effluent.* Analytical Methods, 2017, 9, p. 1412–1418.

[40] Mintenig, S.M., Int-Veen, I., Löder, M.G., Primpke, S., Gerdts, G., *Identification of microplastic in effluents of waste water treatment plants using focal plane array-based micro--Fourier-transform infrared imaging,* Water Research, 2017, 108, p. 365–372.

[41] Ziajahromi, S., Neale, P.A., Rintoul, L., Leusch, F.D.L., *Wastewater treatment plants as a pathway for microplastics: Development of a new approach to sample wastewater-based microplastics,* Water Research, 2017, 112, p. 93–99.

[42] Talvitie J., Heionen M., Pääkkönen J-P., Vahtera E., Mikola A., Setälä O., Vahala R., *Do wastewater treatment plants act as a potential point source of microplastics? Preliminary study in the coastal Gulf of Finland, Baltic Sea* Water Science and Technology, 2015, 72 (9), p. 1495–1504.

[43] Talvitie J., Mikola A., Setälä O., Heionen M., Koistinen A., *How well is microlitter purified from wastewater? – A detailed study on the stepwise removal of microlitter in a tertiary level wastewater treatment plant,* Water Research, 2017, 109, p.164–172.

[44] Talvitie J., Mikola A., Koistinen A., Setälä O*., Solutions to microplastic pollution – Removal of microplastics from wastewater effluent with advanced wastewater treatment technologies,* Water Research, 2017, 123, p. 401–407.

[45] Mason, S. A.; Garneau, D.; Sutton, R.; Chu, Y.; Ehmann, K.; Barnes, J.; Fink, P.; Papazissimos, D.; Rogers, D. L. *Microplastic pollution is widely detected in US municipal wastewater treatment plant effluent,* Environmental Pollutution, 2016, 218, p. 1045–1054.

[46] McCormick, A. R.; Hoellein, T. J.; London, M. G.; Hittie, J.; Scott, J. W.; Kelly, J. J, *Microplastic in surface waters of urban rivers: concentration, sources, and associated bacterial assemblages,* Ecosphere 2016, 7 (11), e01556.

[47] Barrows, A. P. W.; Neumann, C. A.; Berger, M. L.; Shaw, S. D. *Grab vs. neuston tow net: a microplastic sampling performance comparison and possible advances in the field*, Analytical Methods, 2017, 9 (9), p. 1446–1453.

[48] Tagg, A. S.; Harrison, J. P.; Ju-Nam, Y.; Sapp, M.; Bradley, E. L.; Sinclair, C. J.; Ojeda, J. J. *Fenton's reagent for the rapid and efficient isolation of microplastics from wastewater*, Chemical Commununications, 2017, 53 (2), p. 372–375.

[49] Nuelle, M.T., Dekiff, J.H, Remy, D., Fries, E., *A new analytical approach for monitoring microplastics in marine sediments.* Environmental Pollution, 2014, 184, p. 161–169.

[50] Tagg, A.S., Sapp, M., Harrison, J.P., Ojeda, J.J., *Identification and quantification of microplastics in wastewater using focal plane array-based reflectance micro-FT-IR imaging*, Analytical Chemistry, 2015, 87(12), p. 6032–6040.

[51] Masura, J., Baker, J., Foster, G., Arthur, C., *Laboratory Methods for the Analysis of Microplastics in the Marine Environment: Recommendations for Quantifying Synthetic Particles in Waters and Sediments,* NOAA Technical Memorandum, Silver Spring, Maryland, USA, 2015.

[52] Mahon, A. M.; O'Connell, B.; Healy, M. G.; O'Connor, I.; Officer, R.; Nash, R.; Morrison, L. *Microplastics in Sewage Sludge: Effects of Treatment*, Environmental science & technology, 2017, 51 (2), p. 810–818.

[53] Majewsky, M.; Bitter, H.; Eiche, E.; Horn, H. *Determination of microplastic polyethylene (PE) and polypropylene (PP) in environmental samples using thermal analysis (TGA-DSC)*, Science of the Total Environment, 2016, 568, p. 507–511.

[54] Dris, R.; Gasperi, J.; Rocher, V.; Saad, M.; Renault, N.; Tassin, B. *Microplastic contamination in an urban area: a case study in Greater Paris,* Environmental Chemistry, 2015, 12 (5), 592–599.

[55] Sutton, R.; Mason, S. A.; Stanek, S. K.; Willis-Norton, E.; Wren, I. F.; Box, C. *Microplastic contamination in the San Francisco Bay, California. Marine Pollution Bulletin,* 2016, 109 (1), p. 230–235.

[56] Ivleva, N. P.; Wiesheu, A. C.; Niessner, R., *Microplastic in Aquatic Ecosystems,* 2017,56, p. 1720–1739.

[57] Gündoğdu, S.; Çevik, C.; Güzel, E.; Kilercioğlu, S. *Microplastics in municipal wastewater treatment plants in Turkey: a comparison of the influent and secondary effluent concentrations,* Environmental monitoring and assessment, 2018, 190 (11), p. 1–10.

[58] Wolff, S.; Kerpen, J.; Prediger, J.; Barkmann, L.; Müller, L., *Determination of the microplastics emission in the effluent of a municipal wastewater treatment plant using Raman microspectroscopy*, Water research X, 2019, 2,100014.

[59] Imhof, H. K.; Laforsch, C.; Wiesheu, A. C.; Schmid, J.; Anger, P. M.; Niessner, R.; Ivleva, N. P. *Pigments and plastic in limnetic ecosystems: A qualitative and quantitative study on microparticles of different size classes.* Water Research, 2016, 98, p. 64–74.

[60] Kappler, A., Windrich, F., Löder, M.G.J., Malanin, M., Fischer, D., Labrenz, M., Eichhorn, K-J, Voit, B., *Identification of microplastics by FTIR and Raman microscopy: a novel silicon filter substrate opens the important spectral range below 1300 cm−1 for FTIR transmission measurements*, Analytical and Bioanalytical Chemistry, 2015, 407 (22), p. 6791–6801.

[61] Ossmann, B.E., Sarau, G., Scmitt, S.W., Holtmannspötter, H., Christiansen, S.H., Dicke, W., *Development of an optimal filter substrate for the identification of small microplastic particles in food by micro-Raman spectroscopy*, Analytical and Bioanalytical Chemistry, 2017, 409, p. 4099–4109.

[62] Lenz, R., Enders, K., Stedmon, C.A., Mackenzie, D.M., Nielsen, T.G., *A critical assessment of visual identification of marine microplastic using Raman spectroscopy for analysis improvement.* Marine Pollution Bulletin, 2015, 100, p. 82–91.

[63] Kalčíková, G.; Alič, B.; Skalar, T.; Bundschuh, M.; Gotvajn, A. Ž. *Wastewater treatment plant effluents as source of cosmetic polyethylene microbeads to freshwater*, Chemosphere, 2017, 188, p. 25–31.

[64] Zarfl, C., *Promising techniques and open challenges for microplastic identification and quantification in environmental matrices,* Analytical and bioanalytical chemistry, 2019, 411(17), p.3743–3756.

Cost-optimal methodology for energy requalification of "raffaello" school in Pistoia

Abstract: In 2017, 46.5% of school buildings in Italy needed urgent maintenance regarding architectural usability and accessibility, but also concerning structural, energy and environmental aspects. 36% of the energy needs during the operational and management phase of the Italian school sector is required by secondary schools. The main objective of this paper is to propose an integrated (architectural, energy and environmental) redevelopment for the "Raffaello" School in Pistoia (Italy) aimed at improving the environmental and technological system and decreasing the building's primary energy demand. Here, for the sake of brevity, we will only deal explicitly with energy rehabilitation. The results show that the replacement of the artificial lighting system with LED lamps alone leads to a 45% decrease in primary energy demand. Moreover, for the sake of completeness a cost-optimal analysis was performed referred to both heating and lighting system and technological solution for the external envelope. The cost-optimal analysis points out that the substitution of artificial lighting system is the upgrade measure that satisfy both economic and energy sustainability, confirming previous findings. Regarding external envelope redevelopment the more advantageous solution is the one with external insulation layer in wood fiber with aerated concrete blocks for load-bearing functional layer.

Introduction

The Italian school heritage is undoubtedly old, obsolete, inadequate and above all characterized by limited energy efficiency and poor environmental sustainability. Several problems characterize the existing schools, and they are linked not only to the internal

organization, which does not at all meet the requirements of new teaching and pedagogical methods, usability, and safety, but also mainly to energy and environmental issues. This condition of the existing Italian schools is primarily related to the construction period of these buildings. Indeed the 63% of Italian schools are built before 1974 and the 23% before 1940, when there are not any standards concern energy saving, low environmental impact, and legislations about seismic construction.

Actually, school buildings are characterized by an excessive yearly primary energy demand (primarily energy needs for heating), mainly due to the non-use of renewable sources for energy production, inefficient heating and/or cooling systems and inadequate technological solutions for the external envelope. In Italy in 2018 only 1% of school buildings were in energy class A, while 45.3% were in energy class G ($EP_{gl,ren}$ > 3.50 $EP_{gl,nren,rif,standard}$) [1].

Due to this context and the ongoing climate change, it is essential complying with the requirements of "*2030 climate and energy package*", the *Paris Agreement* and the European *17 Sustainable Developments Goals* with the aim at obtaining safe and sustainably built schools. This aim can be achieved both by building new schools according to nZEB (Nearly Energy Building) and low-carbon standards and by planning suitable structural, energy and environmental upgrading of existing school's heritage. Certainly, this leads to a significant decrease in both primary energy demand and environmental impact during operational phase and consequently to the reduction of costs during building management for Public Administrations.

The main objective of this research work is to propose an integrated requalification (architectural, energetical and environmental) for the secondary school "Raffaello", designed by Luigi Pellegrin (1925–2001) and built by the company Fratelli Bortolaso of Verona in Pistoia in 1967, taken as a case study.

Here, for the sake of brevity, the chapter only deals specifically with the energy requalification. Once identified the possible energy and enviornmental requalification strategies to be used in the case study, mainly related to the external envelope technological solutions, a cost-optimal methodology was performed, with the help of BIM (Building Information Modeling) [2] especially to specify materials quantities.

This analysis makes it possible to define for the considered school building the better upgrade strategies considering both environmental and economic sustainability.

State of the art

As regard to existing school buildings, the analysis of the literature shows that many studies on existing school buildings (primary and secondary schools) deal with the evaluation of the best energy and environmental refurbishment strategies adopted to obtain a lower annual primary energy demand (especially in terms of energy demand for heating considering Italy). The Italian education sector energy

needs is equal to 1 Mtoe/year (data from 2012) [3]. The 36% of the total energy demand is for public secondary schools, as for instance the level of the school considered as a case study. Regarding primary energy demand and upgrading strategies, some studies consider obviously the cost parameter as well.

Different analyses are used to outline the type of measure to carry out: the comparative cost-optimal methodology proposed directly by the European Directive 2010/31/EU [4][5][6][7] and combined very often with the calculation of the payback period and the CO_2 emissions released into the atmosphere [8].

The cost-optimality procedure allows to identify the possible requalification strategies to be applied on an existing building to obtain a better performance considering both energy and economic performance. Usually, the different energy measures are related in a graph to both the primary energy demand of the building [kWh/m^{2}a] and the global cost (initial investment, operational, servicing, substitution, energy and disposal) of the different measure applied [€/m^2].

For instance, Becchio et al. [9]for buildings, on the cost-optimal level. In Italy, the EPBD recast was transposed in a document (published in GU 2012/C 115 applied the cost-optimal methodology to evaluate the most energy efficient measure (mainly concerning external envelope and systems together to renewables for energy production) for an industrial building in northern Italy considering 21 different scenarios. They would change the intended use in house and office. They concluded that for a better performance an internal insulation layer for the external envelope must be used combined with condensing boiler and chiller with radiant floor for residential space and with fan coils for office building. With an appropriate global cost (of about 1000 €/m^2), the energy needs would be reduced by about 15 kWh/m^{2}a with these energy retrofitting measures.

Instead, some authors applied the cost-optimal procedure to evaluate the optimal thickness of insulation layer in building with different intended use and located in different climate zone [10][11]. For instance, Raimundo et al. considered 5 different intended use of building and different climate zone in Portugal in order to define the best solution of insulation layer (material and thickness) considering both economic and energy sustainability. They stated that the EPS (sintered expanded polystyrene) located in the middle of the external envelope stratigraphy is the best solution and the residential building required a higher thickness of insulation materials due to the permanent occupation of internal functional units.

In some cases, authors [12] resort to using BIM as a support tool for the cost-optimal analysis thanks to the parametric nature of the model it can be exploited to extract bill of materials ensuring reliable cost estimation. Moreover, because of its interoperability with energy simulation tools the model can be used for primary energy demand assessment.

Or to define the better upgrade strategy for existing buildings many authors performed the comparison through simulation in dynamic regime between the existing state and the design state with a proposal of upgrading according to nZEB standards

considering the interventions also in terms of cost [13] and performing monitoring on the existing building to validate the simulation models [14] or through the life cycle assessment (LCA) or the application of certification protocols [15]. For instance, Elkhapery et al. [16] proposed a method to consider the cost-effective measure, especially for water and electricity savings, for 9 different schools in Dubai with respect to the level of LEED (Leadership in Energy and Environmental Design) energy certification (certified, silver, gold and platinum). They stated that there is not a significant difference in terms of cost between the 3 first levels along with the same energy savings and so they advised a requalification to gold level.

Instead, Doulos et al. [17] considering different energy retrofitting for a school building located in Pisa to evaluate the needed energy upgrade to obtain a nZEB building, according to current Italian standard, also evaluating the cost of each different requalification measure. If they considering a whole retrofitting action (for instance substitution of the external envelope, upgrade of artificial lighting system, installation of solar protection and retrofitting of heating, cooling and ventilation systems also using renewables), they obtain a decrease in both electric (70%) and thermal energy demand (48%).

Finally, many authors point out that to significantly reduce primary energy demand, it is necessary to work on the artificial lighting system and on the management of shading systems [18] [19].

Method

The methodology for the study of the energy requalification proposal (which is part of an integrated requalification process) is divided into 4 different phases:
- Identification of the energy strategies for the rehabilitation of existing schools. From the analysis of several case studies of secondary schools that are characterized by energy upgrading after 2008 and the state of the art, recurring energy strategies to improve the energy performance of an existing school building were defined.
- Detailed analysis of the case study. The energy performance of the existing state was defined through modelling of the school and energy simulation in a dynamic regime with hourly time step using Design Builder [20]. Heating, cooling, and lighting consumptions were considered because they are the most important contributions to the energy balance of a school building.
- Proposal for the energy requalification of the "Raffaello" School. First of all, different strategies for the energy requalification, according to the most recurrent ones in literature, have been proposed and validated through the energy simulations; replacement of the external envelope, replacement of the artificial lighting system (22 lm/W – fluorescent lamps) with a more efficient LED system

(120 lm/W with control on natural lighting), replacement of the existing heating system (gas boiler with 50% efficiency) and introduction of cooling one maintaining a natural ventilation of the rooms and two design proposals related to the system: design proposal 1 replacement of the boiler with an air-water heat pump (coefficient of performance = 3. 8 and energy efficiency ratio = 3.5) for heating and cooling with radiant panel as distribution system and design proposal 2 equal to design proposal 1 in addition to the replacement of the mechanical ventilation system (integrated with heat recovery with 60% efficiency) currently not working.

- To deeper study the external envelope in terms of different technological solutions to be applied, and some measures for lighting and heating system, a cost-optimal methodology [4] was performed to identify the retrofitting solutions that could ensure the best compromise between economic investment and energy saving.

The UNI EN 15459: 2018 [21] define the global cost with the following equation that lets considering both financial and macroeconomic scenario:

$$C_G(\tau) = C_I + \sum_j \left[\sum_{i=1}^{\tau} \left(C_{a,i}(j) \cdot R_d(i) + C_{c,i}(j) \right) - V_{f,r}(j) \right]$$

where: $C_G(\tau)$ is the global cost, referred to the first year $\tau = 0$, C_I are the initial investment costs, $C_{a,i}(j)$ is the annual cost for the year i for the component j, $R_d(i)$ is the discount factor for year i, $V_{f,r}(j)$ residual value of component j at the end of the calculation time, $C_{c,i}(j)$ is the cost of CO_2 emissions for the component j.

So, the initial investment cost for building materials was obtained recurring to price lists available on Italian Regional price list or other nationally trusted price list (for instance DEI prince list 2018) and, for the missing elements, referring to producers' websites. The cost of labor was included in the cost of the manufacturing. As it concerns the quantification of the amount of materials to be used in each of the alternative configuration, BIM models comprehensive of all the different stratigraphies to be compared were realized. An accurate calculation of materials was then provided thanks to the parametric nature of the model and the table sheets exported in Excel format.

As far as the period for the cost-optimality procedure concerns it was considered equal to 30 years as specified for public buildings in the Delegate Regulation n. 244/2012 [22]. Moreover, in the calculation of the annual cost for the year (i) for the component or measures (j) the cost of servicing for components maintenance, the cost of substitution of materials with lower service life than the period of calculation (for instance for the heating system) and the cost of energy for building operational phase are included. The cost for the substitution of the materials is considered equal to the initial investment costs while the cost of energy was defined with ARERA (Authority of Regulation for energy grid and environment) that gives costs of electricity and gas composed by a fixed part based on the Italian Region and by a variable part based on energy consumption of the building.

The discount factor for year depends on the real discount factor that was considered for both the economic scenarios: financial and macroeconomic. The difference is that for the first one the VAT and excise duties were considered but in the equation the cost of CO_2 emissions was not, by contrast for the second one the cost of CO_2 emissions for energy consumption was considered while VAT and excise duties were not. As the regulation detailed the cost of CO_2 emissions is equal to 20 €/tCO_2 within 2025, 35 €/tCO_2 until 2030 and 50 €/tCO_2 after 2030. In order to calculate the CO_2 emissions for energy consumption for both gas and electricity the following conversion factor referred to each energy vector are considered as reported in the ISPRA Report 317/2020: 0.201 kgCO_2/kWh for natural gas and 0.360 kgCO_2/kWh for electricity. For the value of VAT and excise duties the Italian standard was considered.

As previously mentioned, for completeness both financial and macroeconomic scenarios are considered, so the discounting factors are equal to 4% and 5% for the first scenario and 3% and 4% for the second one. In this way also a sensitivity analysis of data was performed, as required by the European regulation.

In the following table (Table 1) the different measures for the redevelopment of the existing school used for the cost-optimal methodology are showed, firstly the single upgrade and secondly a combination of some of them (5 different kind of combinations).

TABLE 1. **Differet upgrade measure for cost-optimal analysis**

Abbreviation	Upgrade measure description
GF_N1 + GF_N2	Insulation and waterproofing of the ground floor stratigraphy for the whole existing school building
EW_N1	Substitution of the external envelope with aerated concrete for load-bearing functional layer, rock wool insulation and advanced ventilated façade (thermal transmittance equal to the reference building)
EW_N1.1	The same of EW_N1 but characterised by half of the thermal transmittance
EW_N2.1	Substitution of external envelope with dry solution with rock wool insulation and gypsum fibre panel as external finishing (characterised by half of the thermal transmittance with respect to reference building)
EW _N3	The same of PPV_N1.1 but with wood fibre insulation
EW _N3.1	The same of PPV_N2.1 but with wood fibre insulation
EW_N3.2	The same of EW_N1.1 but with ETICS (External Thermal Insulation Composite System) external finishing
W_N1	Substitution of all windows in the whole building (Glazing + frame)
RF_N1	Insulation and waterproofing of roof stratigraphy with external finishing with gravel
RF_N2	Insulation and waterproofing of roof stratigraphy with technological solution of green roof

Abbreviation	Upgrade measure description
Syst_1	Substitution of gas boiler with condensing one characterised by a performance equal to 90%
Syst_2	Substitution of artificial lighting system with one more efficient (LED)
Combinations of upgrade measure	
1	EW_N3.1.2 + W_N1 + RF_N1
2	EW_N3.1.2 + W_N1 + RF_N1 + Syst_1
3	EW_N3.1.2 + W_N1 + RF_N1 + Syst_2
4	EW _N3.1 + W_N1 + RF_N1 + Syst_1
5	EW_N3.1 + W_N1 + RF_N1 + Syst_2

The different types of technological solutions proposed are more detailed in tables 7–12 and A.1-A.4 and figures 3–5.

FIG. 1. Aerial view (up on the left – https://www.google.it/maps) and plan of the standard floor of Secondary school Raffaello with the indications of the main functional units.

The secondary school "Raffaello" built in 1967 is located in the municipality of Pistoia, belonging to the climatic zone D [23] with a degree day number equal to 1885. Italy, in fact, is divided in 6 climate zones based on the number of the degree day. The building is characterized by a very complex planimetric configuration that also includes a swimming pool, a gym and an auditorium, perfectly integrated with the remaining part dedicated exclusively to the school. Although the building is characterized by a very articulated architectural design, it can be inscribed in a rectangle with main dimensions of 80 m x 60 m; it has total surface area equal

to 7196 m² and volume of about 37600 m³. The architectural and structural design is based exclusively on the repetition of elements with a module of 1.20 m. The school develops on to 3 floors and a basement (Figures 1–2), which there is the central heating and air conditioning system.
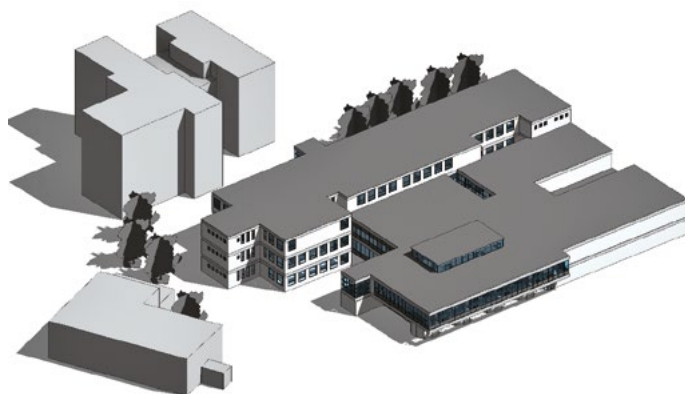
FIG. 2. **Axonometric view of the BIM model in Revit of the Secondary School Raffello.**

The existing building is characterized by a metal load-bearing structure and the only parts in reinforced concrete are the load-bearing structure of the stairs and auditorium. The external walls are mainly made of insulated precast reinforced concrete panel and the roof stratigraphy was characterized by a prefabricated panel in reinforced concrete 0.8 m thick (RAP patent) that was recurrently used in Italy during the period of construction of this school. For a better understanding of the current characteristics of the external envelope the following tables (tables 2–6) and corresponding figures (figures 3–5) show the detailed stratigraphy of each technological solution found in the building (from the external layer to internal one) and the main thermodynamic characteristics considering the requirements imposed by current Italian legislation. The thermal conductivity are mainly found, when they are not available, in the UNI 10351:2015 [24].

TABLE 2. **Existing ground floor stratigrafy (GF_E1) for gym functional unit**

Technological solution	Layer	T [m]	λ [W/mK]	R [m²K/W]
Ground floor type 1 (Gym) – GF_E1	Brick slab	0.06		0.14
	Screed	0.05	1.910	
	Wood finishing	0.02	0.15	
Thermal transmittance [W/m²K]				1.963

TABLE 3. Existing ground floor stratigrafy (GF_E2) for the whole building except gym

Technological solution	Layer	T [m]	λ [W/mK]	R [m²K/W]
Ground floor type 2 (Whole building) − GF_E2	Brick slab + reinforced concrete slab	0.26	−	0.35
	Screed	0.06	1.91	−
	Linoleum finishing	0.03	0.22	−
Thermal transmittance [W/m²K]				1.653

TABLE 4. Existing external wall stratigrafy (PPV_E1)

Technological solution	Layer	T [m]	λ [W/mK]	R [m²K/W]
External wall (prefabricated panel) − PPV_E1	Vibrated and reinforced concrete conglomerate panel	0.03	1.91	−
	Air cavity	0.10	−	0.15
	Resin foam	0.04	0.032	
	Aluminium sheet	−	−	−
	Gypsum laminate	0.018	0.21	
Thermal transmittance [W/m²K]				1.671
Periodic thermal transmittance [W/m²K]				0.57
Time shift [h]				1.90

TABLE 5. Existing roof floor stratigrafy (RF_E1)

Technological solution	Layer	T [m]	λ [W/mK]	R [m²K/W]
Roof floor − RF_E1	Waterproof sheet	0.003	0.5	−
	Resin foam	0.03	0.032	−
	Precast reinforced concrete slab	0.03	1.91	−
Thermal transmittance [W/m²K]				0.912

TABLE 6. Existing windows characteristics (W_E1)

Technological solution	Existing windows description
Windows − W_E1	The existing windows are characterised by a wooden frame and a single glazing (5 mm thick) with thermal transmittance that does not meet the Italian requirements

For performing cost-optimality methodology the following technological solutions for the external envelope in tables 7–12 and tables A.1–A.4 in the appendix A and figures 4–6 were investigated.

TABLE 7. Upgraded ground floor stratigrafy (GF_N1) for gym functional unit

Technological solution	Layer	T [m]	λ [W/mK]	R [m²K/W]
Ground floor type 1 (Gym) – GF_N1	Brick slab	0.06		0.14
	Screed	0.05	1.91	
	Vapour barrier polyethylene	0.00005	0.40	
	Wood fiber	0.14	0.037	
	Lightweight Screed	0.04	0.25	
	Wood finishing	0.02	0.15	
Thermal transmittance [W/m²K]				0.225

TABLE 8. Possible redevelopment measure for external wall (PPV_N1) with same transmitance of the reference building

Technological solution	Layer	T [m]	λ [W/mK]	R [m²K/W]
External wall – PPV_N1	Advance screen façade	–	–	–
	Air cavity	–	–	–
	Aerated concrete	0.30	0.07	
	Gypsum fibre panel	0.015	0.3	
	Gypsum fibre panel	0.015	0.3	
Thermal transmittance [W/m²K]				0.22
Periodic thermal transmittance [W/m²K]				0.042
Time shift [h]				13.37

TABLE 9. Possible redevelopment measure for external wall with dry solution (rock wool insulation) characterised by the half value of the thermal transmittance of the reference building (PPV_N2.1)

Technological solution	Layer	T [m]	λ [W/mK]	R [m²K/W]
External wall – PPV_N2.1	Cement board	0.013	0.13	
	Vapour barrier	0.0002	0.38	
	Rock wool	0.20	0.035	
	Gypsum panel	0.015	0.21	
	Rock wool	0.04	0.035	
	Gypsum fibre panel	0.015	0.3	
	Gypsum fibre panel	0.015	0.3	
Thermal transmittance [W/m²K]				0.137
Periodic thermal transmittance [W/m²K]				0.092
Time shift [h]				6.44

Rock wool insulation

Gypsum panel

Rock wool insulation

Cement Board

Vapour Barrier

Metal substructure

Gypsum fibre panel
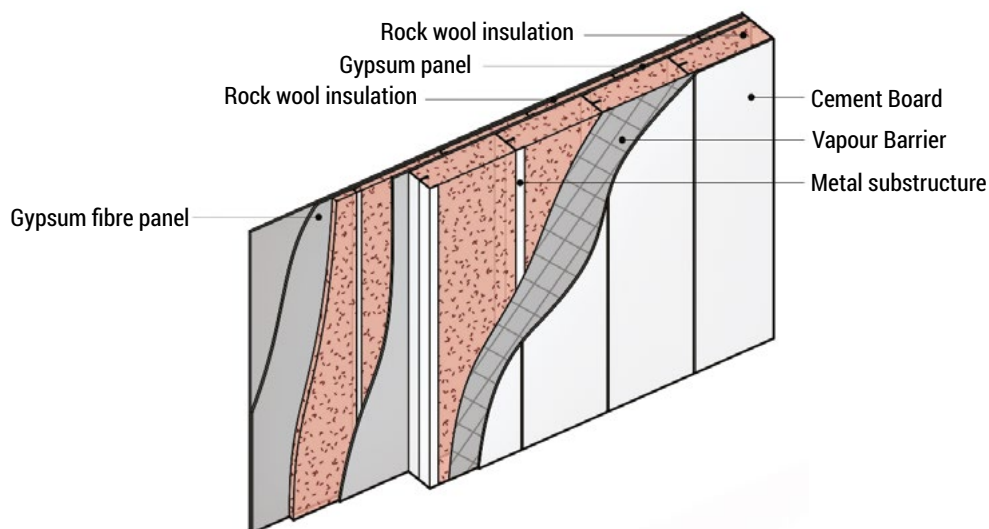
FIG. 3. Sketch of PPV_N2.1 stratigraphy

TABLE 10. **Possible redevelopment measure for external wall characterised by the half value of the thermal transmittance of the reference building with ETICS as external finishing (PPV_N3.2)**

Technological solution	Layer	T [m]	λ [W/mK]	R [m²K/W]
External wall – PPV_N3.2	External plaster	0.03	0.43	
	Wood fibre	0.04	0.034	
	Aerated concrete	0.30	0.07	
	Gypsum fibre panel	0.015	0.3	
	Gypsum fibre panel	0.015	0.3	
Thermal transmittance [W/m²K]				0.177
Periodic thermal transmittance [W/m²K]				0.019
Time shift [h]				15.83

FIG. 4. Sketch of PPV_N3.2 stratigraphy

TABLE 11. Possible redevelopment measure for roof floor with gravel as fnishing layer (RF_N1)

Technological solution	Layer	T [m]	λ [W/mK]	R [m²K/W]
Roof floor – RF_N1	Gravel	0.05	–	–
	Waterproof sheet	0.003	0.5	–
	Wood fiber	0.14	0.037	
	Vapour barrier	0.0005	0.4	–
	Precast reinforced concrete slab	0.03	1.91	–
Thermal transmittance [W/m²K]				0.253
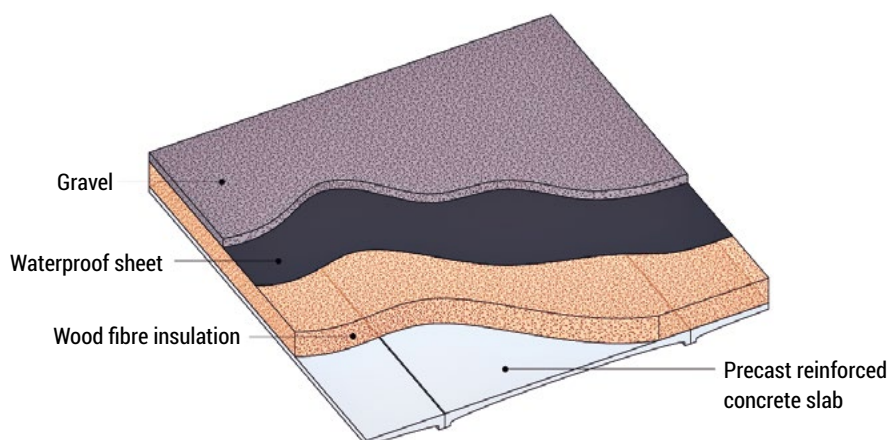
FIG. 5. Sketch of RF_N1 stratigraphy

TABLE 12. **Upgrade windows characteristics (W_E1)**

Technological solution	Existing windows description
Windows − W_E1	The new glazing is type AGC 66.2A(16AR)44.2A with solar factor equal to 31% and U = 1 W/m^{2}K

Results and Discussion

The main energy requalification strategies to obtain a reduction of primary energy demand identified in the study of the analyzed buildings and in the literature are: improvement of the shading system with both fixed and mobile solar shading ones, replacement of windows, creation of an external insulation layer for the external wall, integration with renewables, installation of more efficient artificial lighting system, use of rainwater collection systems, installation of a cooling system to maintain adequate internal comfort conditions even during the summer season.

From an energy point of view, the analysis of the current state of the building highlights the following main problems: the technological solutions for the external wall are not verified in terms of thermodynamic properties and thermal transmittance as demonstrated in the values showed in previous tables about existing technological solutions, the artificial lighting system is outdated and obsolete and characterized by neon lamps with no automated control according to the level of illumination guaranteed by natural light. The heating system with gas boiler (peak power equal to about 1200 kW) does not guarantee the average minimum setpoint temperature of 20°C in the building, the mechanical ventilation system is currently not working, and therefore the air exchange required occurs only through natural ventilation. Consequently, the main proposals for the energy upgrading are: the replacement of the external wall made of prefabricated slabs with a solution characterised by a load-bearing layer made of aerated autoclaved concrete blocks (0.24 m), an insulation layer with rock wool (0.6 m) and an advanced screen façade with stoneware finishing, the replacement of windows that do not meet the requirements of current energy and safety regulations for schools, the replacement of the artificial lighting system and a double proposal for upgrading the system, as already described.

The graph in Figure 6 shows the annual energy demand in [kWh/m^{2}year] for heating, cooling, and lighting for the existing and design proposal 1 and 2.
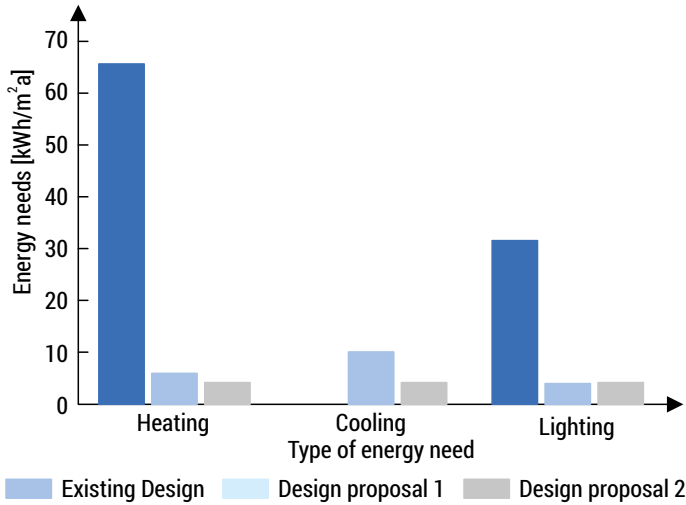
FIG. 6. **Energy needs [kWh/m²year] for heating, cooling and artificial lighting.**

The graph shows that the energy requalification of the building leads to a significant decrease in both energy consumption for heating, by about 90%, and lighting, by about 85%. These results in a clear improvement in the environmental performance of the building during operational phase, with a decrease in CO_2 emissions of about 22 kgCO_2/m²year (for heating alone). The energy demand for cooling obviously only appears in design proposal 1 and 2 and it is not significant, thanks to the use of solar shading systems on both the South and East façades of the building. Comparing design proposal 1 and 2, the former has a slightly higher value of energy demand for electricity. This is due to the presence of natural ventilation inside the rooms to ensure air exchange rates and the absence of heat recovery due to mechanical ventilation during the winter season.

The graph in Figure 7 shows the primary energy demand for heating, cooling and lighting for the existing state; design proposal 1 and 2; the replacement of the external envelope; the heating/cooling system and the artificial lighting system considered separately.

The graph (Figure 7) highlights that between the existing state and the design proposal 1 and 2 there is a difference for the primary energy demand, considering the conversion factors for each energy vector (gas or electricity from grid without renewables), equal to 66% and 79% respectively. As already pointed out, the decrease in primary energy demand in design condition 2 is due to the presence of mechanical ventilation with heat recovery. However, just the replacement of existing lamps with a more efficient lighting system with natural lighting control leads to a decrease in primary energy demand of about 45%.
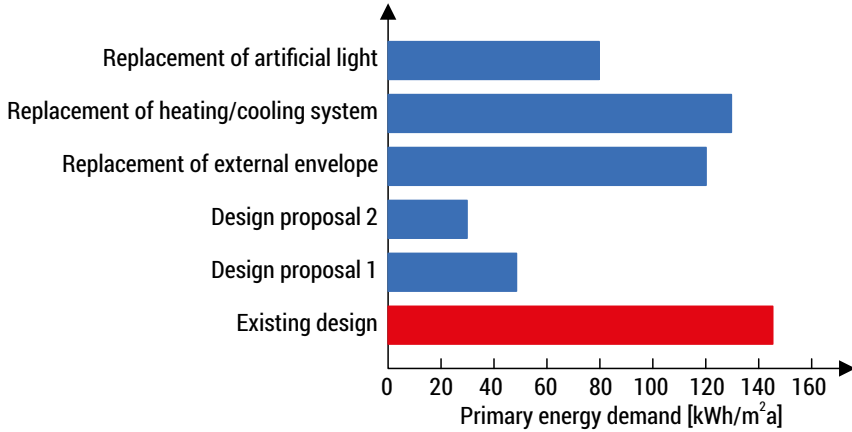
FIG. 7. **Primary energy demand [kWh/m²year]. In red the yearly primary energy demand for existing design.**

As far as cost-optimal analysis concerns Figure 8 shows the results of the financial scenario of the cost-optimality methodology with the discount factor equal to 4%.
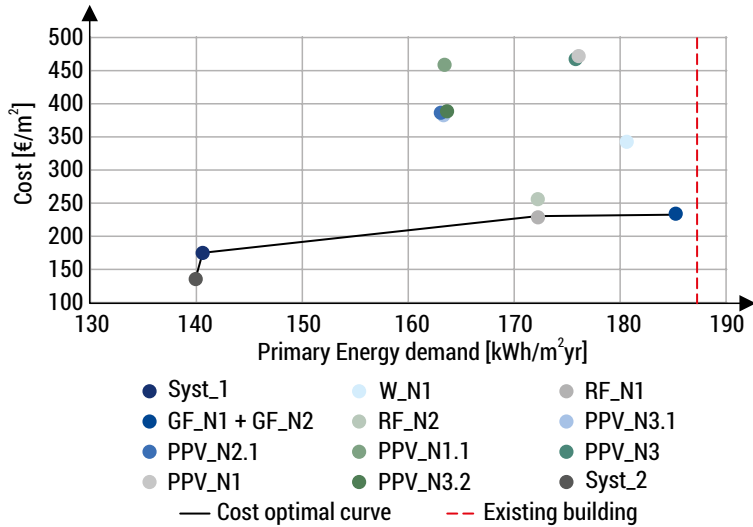
FIG. 8. **Cost-optimality method results for financial scenario and discount factor equal to 4%. The red line in the graph shows the primary energy consumption for existing building.**

Firstly, the graph highlights that all the solutions characterized by the external finishing with ventilated façade have higher cost with respect to other solutions linked to the used of metal substructure and the materials for the external cladding. Indeed, as regards energy performance in term of primary energy demand [kWh/m²year],

the ETICS solution and the ventilated façade are equivalent because they are characterized by the same thermal transmittance. So, the choice of technological solution with ventilated façade as external finishing is mainly related to an esthetical requirement of the designer or the administration.

At the same time, it is important to point out that all the upgrade measures for the external envelope are above the cost-optimal curve because of the higher cost of windows (frame and glazing) substitution. These measures result in a significant cost of all proposed redevelopment of the external wall.

Moreover, the graph shows that the solution GF_N1 + GF_N2 with waterproofing and insulation of the ground floor stratigraphy does not lead to a significant reduction in primary energy demand despite the cost of the solution. The same thing happens if we consider the only substitution of windows keeping the external wall the existing one, because this does not result in a considerable advantage in terms of energy performance.

Furthermore, regarding the technological solution for the external envelope, the solution PPV_N3.2 with ETICS satisfy the cost-optimal requirements of financial scenario, along with the same energy performance of PPV_N2.1 and PPV_N3.1.

Finally considering the cost optimal curve at 4% also the retrofitting measure related to the roof floor with gravel finishing (RF_N1) is not despicable as it lets achieving a decrease in annual primary energy demand with a lower cost than the upgrade measures for the external wall. As well as the same energy performance the solution with green roof finishing is characterised by a slight increase in cost.

Confirming previous findings, the Syst_2 upgrade measure with the redevelopment of the artificial lighting system is the better one because it is characterised by the lower cost along with the better energy performance.

The following graph in Figure 9 shows the sensitivity analysis of the cost-optimality financial scenario, considering a discounting factor equal to 5%. This analysis is fundamental to understand how the most variable parameters affect the global cost considering a range of time equal to 30 years.

The graph points out that the cost noticeably decreases for a value equal to about 25 €/m². The upgrading measure Syst_2 is always the better one but with respect to the others over time it is distinguished by a less decrease in cost due to the cost of maintenance of other solutions (for instance Syst_1) that considerably affect the global cost. Indeed, the LED solution does not have this component.
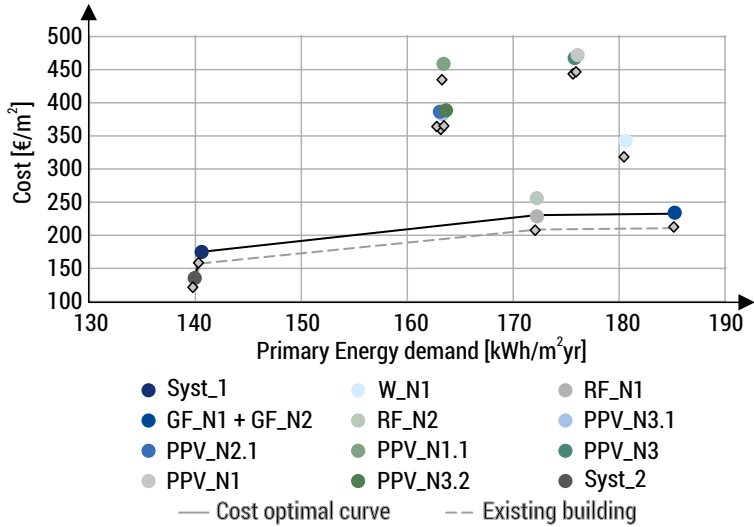
FIG. 9. Cost-optimality sensitivity analysis for financial scenario and discount factor equal to 5%.

Figure 10 shows the cost-optimality procedure considering some combinations of parameters (Table 1) as well to consider the variation in the period of the analysis (30 years) of the global cost for financial scenario with discount factor equal to 4%.
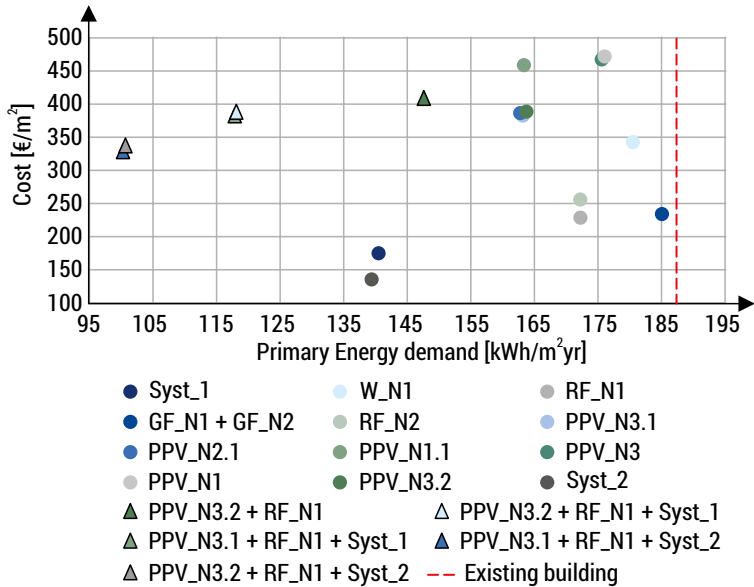
FIG. 10. Cost-optimal results for financial scenario with discount rate euqal to 4% considering some combinations of parameters.

As well as in previous graph in Figure 8, Figure 10 shows that combining some different solutions of upgrade measures for the external envelope, included obviously the substitution of windows, with retrofitting of systems, the higher cost of windows (both initial investment cost and maintenance one over time) significantly influences the results of cost-optimal analysis. Indeed, all the solutions with the retrofitting of the external wall are over the cost-optimal curve. The solutions PPV_N3.1 + RF_N1 + Syst_2 and PPV_N3.2 + RF_N1 + Syst_2, the first one with dry solution and the other one with the aerated concrete blocks, are the best combinations of parameters in terms of both cost and energy demand mainly related to the substitution of artificial lighting that lets to obtain a noticeable decrease in primary energy demand with affordable cost of initial investment.

For the sake of completeness, also the macroeconomic scenario was considered for the cost-optimality methodology. The graph in Figure 11 illustrates the sensitivity analysis of macroeconomic scenario for both values of discount factor: 3% and 4%.
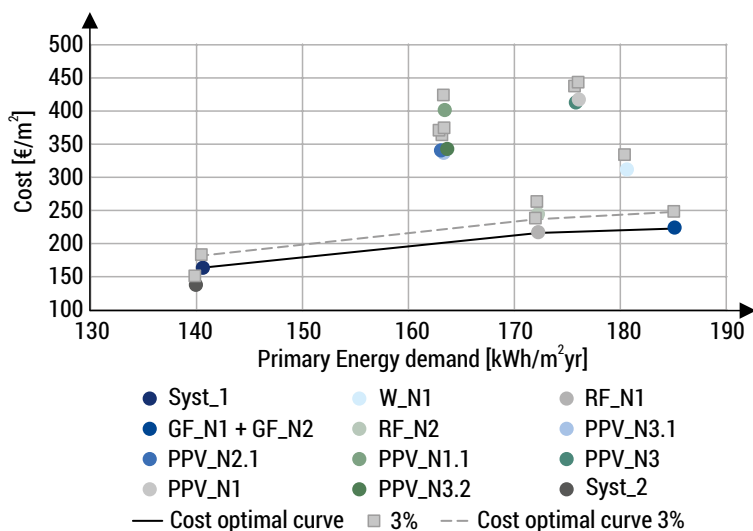

FIG. 11. **Cost-optimality method results for macroeconomic scenario and discount factor equal to 3% and related sensitivity analysis at 4%.**

It is possible to affirm that in general for each improvement measures proposed, the global cost of the cost-optimality methodology decreased in this macroeconomic scenario with respect to financial one. This is mainly due to the VAT and excise duties that in this scenario were not considered as required by legislation. In this case the cost of CO_2 emissions were included but they have less influence than taxes because they are applied exclusively to energy consumption. Indeed, the graph shows that the cost of the solutions with many components (for instance the dry solution for the external envelope) significantly decrease because of there are not taxes

for materials components. For instance, for the solution with ventilated façade the cost of the financial scenario is equal to about 450 €/m^2, by contrast for the macroeconomic one is equal to about 400 €/m^2.

Moreover, as it possible to see in table in Figure A.1 and A.2 with respect to the existing building, the solution Syst_2 is the better one in terms of cost-optimal for both scenarios because it halves the global cost over time. If we consider the macroeconomic scenario, it is also possible stating that all the considered retrofitting measures lets to obtain a decrease in CO_2 emissions over time (30 years) and this is fundamental taking into account the European aim at achieving carbon-free economy within 2050, especially for a public building with this intended use.

Conclusion

In conclusion, the main energy redevelopment proposals of the case study concern 3 main aspects: the external envelope, the artificial lighting system and the plant system (heating, cooling and mechanical ventilation). A complementary economic assessment was not carried out to determine the economic sustainability of the different proposed interventions. For this reason, the benefits obtained by considering separately the 3 main aspects of the proposed energy requalification were analyzed, as for hypothesis even only one of the 3 could be carried out without involving the others. The one that has the greatest benefit in terms of primary energy demand is the replacement of the neon lighting system with LED lighting, which leads to a reduction of about 45% in annual primary energy demand. The replacement of the external envelope and the heating/cooling system results in a reduction of 17% and 11% respectively. The energy requalification defined as "design proposal 2", although the most expensive in terms of cost of the interventions, is certainly the one that ensures adequate conditions of well-being for the occupants, a correct air exchange and certainly an undoubted advantage from an environmental point of view during the operation and management costs of the building: the primary energy demand can be reduced to about 39 kWh/m^{2}year compared to the existing design of the building which needs 145 kWh/m^{2}year.

The cost-optimal analysis confirms the results of the energy simulations because the solution Syst_2 with the retrofitting measure of the artificial lighting system and the substitution of the existing one with more efficient one it is possible to achieve both economic and energy sustainability. Indeed, there is a significant decrease in primary energy consumption along with an affordable initial investment cost.

With respect to the performed cost optimal analysis the upgrade measures that consider the substitution of the external envelope with the inclusion of windows retrofitting are the most expensive solution, by contrast the influence on energy demand is not noticeable comparable with global cost.

Moreover, the calculation of both financial and macroeconomic scenario let to point out that the global cost is more influence by VAT and excise duties rather than the cost of CO_2 emissions over time. But in the context of the Paris Agreement all the proposed retrofitting measure significantly decrease the environmental impact over time with respect to the existing building.

The research can be deepened considering both other retrofitting measures for the existing building and another building with the same intended use in order to make a comparison between 2 different buildings in the same climate zone. At the same time, it is important to consider the evaluation of more efficient system for heating and cooling (for instance heating pump) and the integration with renewables for energy supply.

Finally, since it is an existing school building dates to 1967, a comparison between two different scenarios, and so demolition and construction of a new school building or combination of retrofitting measures for the existing one, would be evaluated in terms of both economic and environmental sustainability also considering payback period and the possible economic advantages due to renewables.

Literature

[1] Legambiente, *Ecosistema Scuola. XIX Rapporto di Legambiente Sulla Qualità Dell'edilizia Scolastica, delle Strutture e dei Servizi*, 2018.

[2] Autodesk. (2020c). Revit (No. 2020).

[3] ENEA, *Guida per il contenimento della spesa energetica nelle scuole*, 2012.

[4] Parlamento Europeo, *Direttiva 2010/31/UE del Parlamento Europeo e del consiglio del 19 maggio 2010 sulla prestazione energetica dell'edilizia*, 2010.

[5] Stocker E., Tschurtschenthaler M., Schrott L., *Cost-optimal renovation and energy performance: Evidence from existing school buildings in the Alps.* Energy and Buildings 2015, 100, p. 20–26. 10.1016/j.enbuild.2015.04.005. https://doi.org/10.1016/j.enbuild.2015.04.005.

[6] Mora T.D., Righi, A., Peron, F., Romagnoni, P., *Cost-Optimal measures for renovation of existing school buildings towards nZEB.* Energy Procedia 2017, 140, p. 288–302. https://doi.org/10.1016/j.egypro.2017.11.143.

[7] Di Giuseppe E., D'Orazio M. *Livelli ottimali di costo per involucri ad alta efficienza energetica.* Costruire in Laterizio 2015, CIL 159: verso nZEB, p. 52–56. Available online: http://www.laterizio.it/pubblicazioni/costruire-in-laterizio/cil-159-verso-nzeb.html.

[8] Moazzen N., Ashrafian T., Yilmaz Z, Karagüler M.E., *A multi-criteria approach to affordable energy-efficient retrofit of primary school buildings.* Applied Energy 2020, 268, p. 115046. https://doi.org/10.1016/j.apenergy.2020.115046.

[9] Raimundo A.M., Saraiva N.B., Oliveira A.V.M., *Thermal insulation cost optimality of opaque constructive solutions of buildings under Portuguese temperate climate.* Building and Environment 2020, 182, p. 107107. https://doi.org/10.1016/j.buildenv.2020.107107.

[10] D'Agostino D., De Rossi F., Marigliano M., et al., *Evaluation of the optimal thermal insulation thickness for an office building in different climates by means of the basic and modified "cost-optimal" methodology.* Journal of Building Engineering Build 2019, 24, p. 100743. https://doi.org/10.1016/j.jobe.2019.100743.

[11] Farina M., Tesi di laurea magistrale, Politecnico di Torino, *Metodologie innovative nell'era digitale: il BIM per la "cost optimal analysis"*, Relatore: Prof.ssa Osello A., 2018.

[12] Marrone P., Gori P., Asdrubali F., et al., *Energy benchmarking in educational buildings through cluster analysis of energy retrofitting.* Energies 2018, 11, p. 1–20. https://doi.org/10.3390/en11030649.

[13] Dall'O G., Sarto L., *Potential and limits to improve energy efficiency in space heating in existing school buildings in northern Italy.* Energy and buildings 2013, 67, p. 298–308. https://doi.org/10.1016/j.enbuild.2013.08.001.

[14] Gamarra A.R., Istrate I.R., Herrera I., et al., *Energy and water consumption and carbon footprint of school buildings in hot climate conditions. Results from life cycle assessment.* Journal of Cleaner Production 2018, 195, p. 1326–1337. https://doi.org/10.1016/j.jclepro.2018.05.153.

[15] Elkhapery B., Kianmehr P., Doczy R. *Benefits of retrofitting school buildings in accordance to LEED v4.* Journal of Building Engineering 2021, 33, p. 101798. https://doi.org/10.1016/j.jobe.2020.10179817.

[16] Doulos L.T., Kontadakis A., Madias E.N., et al., *Minimizing energy consumption for artificial lighting in a typical classroom of a Hellenic public school aiming for near Zero Energy Building using LED DC luminaires and daylight harvesting systems.* Energy and Buildings 2019, 194, p. 201–217. https://doi.org/10.1016/j.enbuild.2019.04.033.

[17] Tsikra P., Andreou E., *Investigation of the Energy Saving Potential in Existing School Buildings in Greece. The role of Shading and Daylight Strategies in Visual Comfort and Energy Saving.* Procedia Environmental Sciences 2017, 38, p. 204–211. https://doi.org/10.1016/j.proenv.2017.03.107.

[18] Lourenço P., Pinheiro M.D., Heitor T., *Light use patterns in Portuguese school buildings: User comfort perception, behaviour and impacts on energy consumption.* Journal of Cleaner Production 2019, 228, p. 990–1010. https://doi.org/10.1016/j.jclepro.2019.04.144.

[19] Design Builder v6.1. Available online: https://www.designbuilderitalia.it/.

[20] Italian Organization for Standardization (UNI) UNI EN 15459–1: *Prestazione energetica degli edifici – Sistemi di riscaldamento e sistemi di raffrescamento idronici negli edifici – Parte 1: procedura di valutazione economica per i sistemi energetici negli edifici*, Modulo M1–14, 2018.

[21] Commissione Europea, *Regolamento delegato UE N. 244/2012* della commissione del16 gennaio 2012 che integra la direttiva 2010/31/UE del Parlamento europeo e del Consiglio sulla prestazione energetica nell'edilizia istituendo un quadro metodologico comparativo per il calcolo dei livelli ottimali in funzione dei costi per i requisiti minimi di prestazione energetica degli edifici e degli elementi edilizi, 2012.

[22] Governo Italiano, *Regolamento recante norme per la progettazione, l'installazione, l'esercizio e la manutenzione degli impianti termici degli edifici ai fini del contenimento dei consumi di energia*, 1998.

[23] Italian Organization for Standardization, *UNI 10351 – Materiali e prodotti per edilizia – Proprietà termoigrometriche – procedure per la scelta dei valori di Progetto*, 2015.

Appendix A

TABLE A. 1. Possible redevelopment measure for external wall characterised by the half value of the thermal transmittance of the reference building (PPV_N1.1)

Technological solution	Layer	T [m]	λ [W/mK]	R [m²K/W]
External wall – PPV_N1.1	Advance screen façade	–	–	–
	Air cavity	–	–	–
	Rock wool	0.04	0.035	
	Aerated concrete	0.30	0.07	
	Gypsum fibre panel	0.015	0.3	
	Gypsum fibre panel	0.015	0.3	
Thermal transmittance [W/m²K]				0.175
Periodic thermal transmittance [W/m²K]				0.019
Time shift [h]				15.30

TABLE A. 2. Possible redevelopment measure for external wall characterised by the half value of the thermal transmittance of the reference building with advanced screen facade as external finishing (PPV_N3)

Technological solution	Layer	T [m]	λ [W/mK]	R [m²K/W]
External wall – PPV_N3	Advance screen façade	–	–	–
	Air cavity	–	–	–
	Wood fibre	0.04	0.034	
	Aerated concrete	0.30	0.07	
	Gypsum fibre panel	0.015	0.3	
	Gypsum fibre panel	0.015	0.3	
Thermal transmittance [W/m²K]				0.177
Periodic thermal transmittance [W/m²K]				0.019
Time shift [h]				15.83

TABLE A. 3. Possible redevelopment measure for external wall with dry solution (wood fibre insulation) characterised by the half value of the thermal transmittance of the reference building (PPV_N3.1)

Technological solution	Layer	T [m]	λ [W/mK]	R [m²K/W]
External wall – PPV_N3.1	Cement board	0.013	0.13	–
	Vapour barrier	0.0002	0.38	–
	Wood fibre	0.014	0.035	
	Gypsum panel	0.015	0.21	
	Rock wool	0.04	0.035	
	Gypsum fibre panel	0.015	0.3	
	Gypsum fibre panel	0.015	0.3	
Thermal transmittance [W/m²K]				0.186
Periodic thermal transmittance [W/m²K]				0.083
Time shift [h]				8.72

TABLE A. 4. Possible redevelopment measure for roof floor with green roof as fnishing layer (RF_N2)

Technological solution	Layer	T [m]	λ [W/mK]	R [m²K/W]
	Earth	0.12	–	0.3
	Filter layer	0.001	–	–
Roof floor – RF_N2	Accumulation layer (EPS)	0.04	–	0.71
	Waterproof sheet	0.003	0.5	–
	Wood fiber	0.10	0.037	
	Vapour barrier	0.0005	0.4	–
	Precast reinforced concrete slab	0.03	1.91	–
Thermal transmittance [W/m²K]				0.253

SOLUTION	Initial Investment Costs	Substitiution costs	Annual costs [€/yr]				Annual costs over the reference period [€/m²yr]	Residual value	Primary Energy demand [kWh/m²yr]		
			Heating	Electricity	Maint.	Total			Heating	Electricity	Total
Existing building	-	-	30,787	43,103	-	73,890	1,277,712	-	104.95	82.23	187.18
W_N1	719,551 €	- €	28,830	43,103	7,011	78,944	1,365,105	- €	98.25	82.23	180.18
PPV_N1	1,520,173 €	- €	27,505	43,103	7,011	77,619	1,342,189	- €	93.71	82.23	175.94
PPV_N1.1	1,504,310 €	- €	23,836	43,103	7,011	73,950	1,278,744	- €	81.15	82.23	163.39
PPV_N2.1	1,066,181 €	- €	23,728	43,103	7,011	73,843	1,276,887	- €	80.79	82.23	163.02
PPV_N3	1,498,462 €	- €	27,440	43,103	7,011	77,554	1,341,075	- €	93.49	82.23	175.72
PPV_N3.1	1,047,866 €	- €	23,796	43,103	7,011	73,910	1,278,054	- €	81.02	82.23	163.25
PPV_N3.2	1,075,006 €	- €	23,885	43,103	7,011	73,999	1,279,593	- €	81.32	82.23	163.55
GF_N1 + GF_N2	152,913 €	- €	30,186	43,103	-	73,289	1,267,315	- €	102.89	82.23	185.12
RF_N1	196,924 €	- €	26,406	43,103	-	69,509	1,201,960	- €	89.95	82.23	172.19
RF_N2	349,671 €	- €	26,412	43,103	59	69,575	1,203,095	- €	89.97	82.23	172.21
Syst_1	20,853 €	9,517 €	17,159	43,103	417	60,679	1,049,272	3,214.76 €	58.30	82.23	140.53
Syst_2	31,228 €	- €	34,487	11,971	-	46,457	803,343	- €	117.61	22.31	139.92
PPV_N3.2 + RF_N1	1,271,930 €	- €	19,464	42,726	7,011	69,201	1,196,629	- €	66.19	81.51	147.70
PPV_N3.2 + RF_N1 + Syst_1	1,302,301 €	9,517 €	10,871	42,726	7,428	61,026	1,055,255	3,214.76 €	36.78	81.51	118.29
PPV_N3.2 + RF_N1 + Syst_2	1,303,158 €	- €	23,075	11,971	7,011	42,057	727,244	- €	78.55	22.31	100.86
PPV_N3.1 + RF_N1 + Syst_1	1,275,161 €	9,517 €	10,834	42,726	7,011	60,572	1,047,406	3,214.76 €	36.66	81.51	118.16
PPV_N3.1 + RF_N1 + Syst_2	1,276,018 €	- €	23,004	11,971	7,011	41,986	726,024	- €	78.31	22.31	100.62

FIG. A. 1. Summary table of cost-optimal methodology for financial scenario with discount rate equal to 4%

SOLUTION	Initial Investment Costs	Substitution costs	Annual costs [€/yr]				Annual costs over the reference period [€/m²yr]	Emissions		Residual value	Primary Energy demand [kWh/m²yr]		
			Heating	Electricity	Maint.	Total		CO₂ [ton]	CO₂ costs [€]		Heating	Electricity	Total
Existing building	-	-	24,048	32,753	-	56,801	982,202 €	196.151	250,092	-	104.95	82.23	187.18
W_N1	589,796 €	- €	22,519	32,753	5,747	61,019	1,055,146 €	188.368	240,170	- €	98.25	82.23	180.18
PPV_N1	1,246,043 €	- €	21,485	32,753	5,747	59,984	1,037,250 €	183.099	233,451	- €	93.71	82.23	175.94
PPV_N1.1	1,233,041 €	- €	18,619	32,753	5,747	57,119	987,703 €	168.511	214,851	- €	81.15	82.23	163.39
PPV_N2.1	873,919 €	- €	18,535	32,753	5,747	57,035	986,253 €	168.084	214,307	- €	80.79	82.23	163.02
PPV_N3	1,228,248 €	- €	21,434	32,753	5,747	59,934	1,036,380 €	182.843	233,125	- €	93.49	82.23	175.72
PPV_N3.1	858,907€	- €	18,588	32,753	5,747	57,088	987,164 €	168.352	214,649	- €	81.02	82.23	163.25
PPV_N3.2	881,153 €	- €	18,658	32,753	5,747	57,157	988,366 €	168.706	215,100	- €	81.32	82.23	163.55
GF_N1 + GF_N2	148,417 €	- €	23,578	32,753	-	56,331	974,083 €	193.760	247,044	- €	102.89	82.23	185.12
RF_N1	161,413€	- €	20,627	32,753	-	53,380	923,044 €	178.732	227,884	- €	89.95	82.23	172.19
RF_N2	286,615 €	- €	20,632	32,753	49	53,433	923,970 €	178.757	227,915	- €	89.97	82.23	172.21
Syst_1	17,093 €	7,801 €	13,405	32,753	342	46,500	804,081 €	141.965	181,005	2,635.05 €	58.30	82.23	140.53
Syst_2	25,596 €	- €	26,937	9,113	-	36,050	623,376 €	156.769	199,880	- €	117.61	22.31	139.92
PPV_N3.2 + RF_N1	1,042,566 €	- €	15,205	32,466	5,747	53,419	923,716 €	150.474	191,854	- €	66.19	81.51	147.70
PPV_N3.2 + RF_N1 + Syst_1	1,067,460 €	7,801 €	8,495	32,466	6,089	47,050	813,589 €	116.308	148,292	2,635.05 €	36.78	81.51	118.29
PPV_N3.2 + RF_N1 + Syst_2	1,068,162 €	- €	18,025	9,113	5,747	32,885	568,641 €	111.393	142,027	2,635.05 €	78.55	22.31	100.86
PPV_N3.1 + RF_N1 + Syst_1	1,045,214 €	7,801 €	8,466	32,466	5,747	46,679	807,181 €	116.161	148,106	2,635.05 €	36.66	81.51	118.16
PPV_N3.1 + RF_N1 + Syst_2	1,045,916 €	- €	17,970	9,113	5,747	32,829	567,688 €	111.113	141,699	- €	78.31	22.31	100.62

FIG. A. 2. Summary table of cost-optimal methodology for macroeconomic scenario with discount rate equal to 4%

Cooling potential assessment
of a regenerative indirect evaporative cooler

Abstract: Regenerative indirect evaporative cooling (RIEC) systems are an interesting alternative to conventional air-cooling systems based on direct expansion units. In the present work, the main objective was to experimentally determine the performance of a RIEC air-cooling system under different inlet air conditions. Moreover, a mathematical RIEC model based on modified ε-NTU numerical method was developed and validated. The experimental RIEC results showed high cooling capacity, with dew point effectiveness values up to 0.91. The accuracy obtained of the mathematical model was more than acceptable. Therefore, it can be used properly to study the global behaviour of a RIEC. These air-cooling systems would contribute to achieve the European objectives of nZEB.

Introduction

Development of very low energy consumption HVAC (Heating, Ventilation and Air Conditioning) systems are required in the European frame of NZEB (Nearly Zero Energy Building). Evaporative cooling systems could be an effective alternative to conventional technologies, due to their high efficiency and reduced primary energy consumption [1]. There are two main types of evaporative coolers: the direct evaporative cooler (DEC), and the indirect evaporative cooler (IEC) [2, 3]. DEC is based on direct contact between air and water, while IEC is based on heat and mass transfer between two streams of air, separated by a heat transfer surface with a dry side, where only air is cooling, and a wet side, where water is evaporated into air.

Different experimental and numerical research works have been carried out in order to study the operational parameters that influence the overall performance of regenerative indirect evaporative coolers (RIEC) [4]. Experimental results established that RIEC systems could achieve high COP values COP [5–7]. Other experimental studies of RIEC showed high cooling capacities [8, 9].

The main objective of this study was to experimentally determine the performance of a RIEC air-cooling system under different inlet air conditions. Moreover, a mathematical RIEC model based on modified ε-NTU numerical method was developed and validated.

Materials and Methods

Experimental test rig

An experimental test rig was built to study the performance of a regenerative indirect evaporative cooler (RIEC) under different working conditions. A schematic representation of the experimental setup is shown in Fig. 1. The inlet temperature, relative humidity and air flow rate of process stream were set using cooling and heating coils (CC, HC), a steam humidifier (SH) and a variable speed fan (F), located upstream of the RIEC. The data of temperature, humidity and air flow rate were measured and recorded for each experimental test. The sensor locations are shown in Fig. 1.
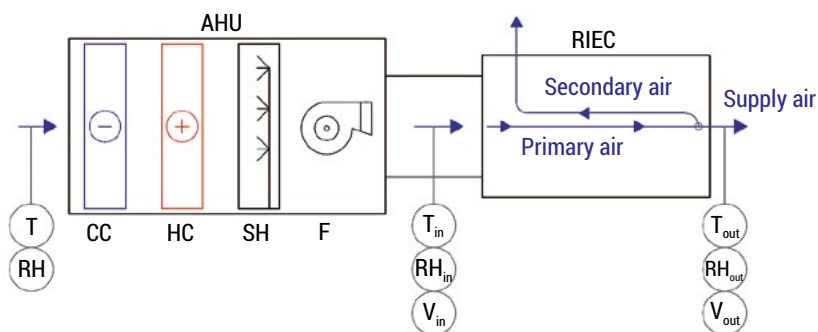
AHU − Air handling unit, HC − Heating coil, CC − Cooling coil
SH − Steam humidifier, F − Centrifugal fan, RIEC Reg. indirect evap. cooler
T − Dry bulb temperature, RH − Relative humidity, V − Volumetric air flow rate

FIG. 1. Layout of the test facility of the regenerative indirect evaporative cooler

The RIEC system consists of a counter-flow heat and mass exchanger, a water distributing system and an outer casing. The primary air of the device, T_{in}, is cooled along the dry channels without moisture increase and subsequently discharged (supply air), T_{out}. Through the perforations located at the end of channels, a portion of the primary air is diverted into the adjacent wet channels. Flowing in counter direction to the primary air in dry channels, the secondary air of wet channels is humidified, heated and finally exhausted to outside. A damper was used to regulate the discharge air pressure and control the supply air flow.

25 experimental tests of the RIEC system were performed for the study and validation of a mathematical RIEC model. The ranges of the experimental test carried out is shown in Table 1. The input variables were the inlet air primary temperature, T_{in}, inlet air primary humidity ratio, ω_{in}, primary air flow rate, V_{in}, and ratio of secondary air flow rate to primary air flow rate, R. Each state point was taken under steady-state conditions and all the measured values were average values over a period of 20 minutes with sampling time steps of 5 seconds.

TABLE 1. **Ranges of the experimental tests carried out**

Range	T_{in} [ºC]	ω_{in} [g/kg]	V_{in} [m³/h]	R [−]
Lower value	33	8.5	3000	0.3
Upper value	43	13	4500	0.7

Mathematical model of the indirect evaporative cooler

A mathematical RIEC model based on modified ε-NTU numerical method to determine the optimal geometrical and operating parameters was developed. The main equations of the model are expressed by (1)–(3).

$$NTU = U \cdot dA / C_{min,i} \tag{1}$$

$$U \cdot dA = \left(a \cdot \left[\frac{1}{\alpha_{d,i}} + \frac{\delta}{K} + \frac{\delta_w}{K_w} \right] + \frac{1}{\beta_i} \right)^{-1} \cdot N_{ch} \cdot W \cdot dx \tag{2}$$

$$\varepsilon = f\left(NTU, C_{r,i} \right) \tag{3}$$

Validation and evaluation of the indirect evaporative cooler

The validation of mathematical model and the performance study of the RIEC were carried out in terms of variation of primary air temperature, ΔT, and of dew point effectiveness, ε_{dp}. Such indexes were defined through the following equations:

$$\Delta T = T_{in} - T_{out} \tag{4}$$

$$\varepsilon_{dp} = \frac{T_{in} - T_{out}}{T_{in} - T_{dp,out}} \tag{5}$$

Where T is dry bulb temperature and T_{dp} is dew point temperature.

Results and Discussion

The experimental and numerical results of variation of primary air temperature, ΔT, and of dew point effectiveness, ε_{dp}, are shown in Fig. 2, corresponding to the 25 tests carried out. As shown in Fig. 2, there is a very good agreement between numerical and experimental primary air temperature variation, being the deviation always within 0.45°C, see Fig. 2a. The accuracy of the dew point effectiveness results has also been found to be appropriate, with deviations less than ± 0.025, see Fig. 2b.

The experimental results showed high ΔT values, up to 26.5°C for values of T_{in}, ω_{in}, V_{in} and R equal to 43°C, 8.5 g/kg, 4000 m^3/h and 0.5, respectively, see Fig. 2a. The ε_{dp} results showed that the supply air conditions were close to the dew point. The highest ε_{dp} value was 0.91 for values of T_{in}, ω_{in}, V_{in} and R equal to 43°C, 13 g/kg, 3000 m^3/h and 0.35, respectively, see Fig. 2b.

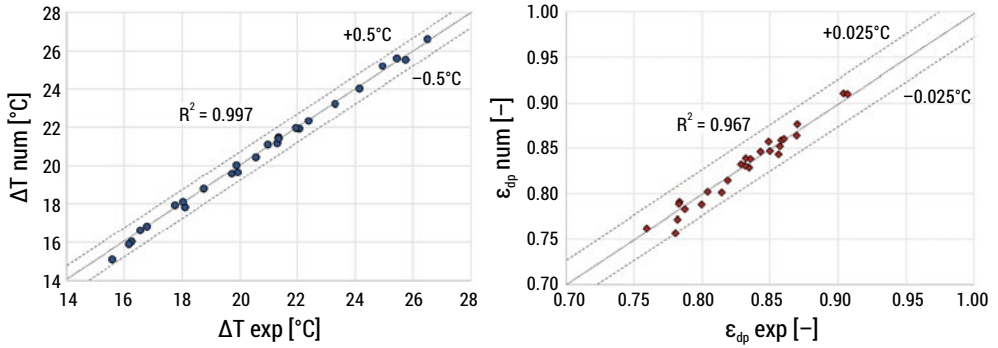FIG. 2. Parity plots of experimental and numerical results of (a) ΔT and (b) ε_{dp}

The validated model allowed to obtain the temperature, enthalpy and humidity distributions inside the exchanger. The air conditions of the primary and secondary air flows for each computational element of the exchanger are shown in Fig. 3. For this example, 100 computational elements were used for the numerical modelling.
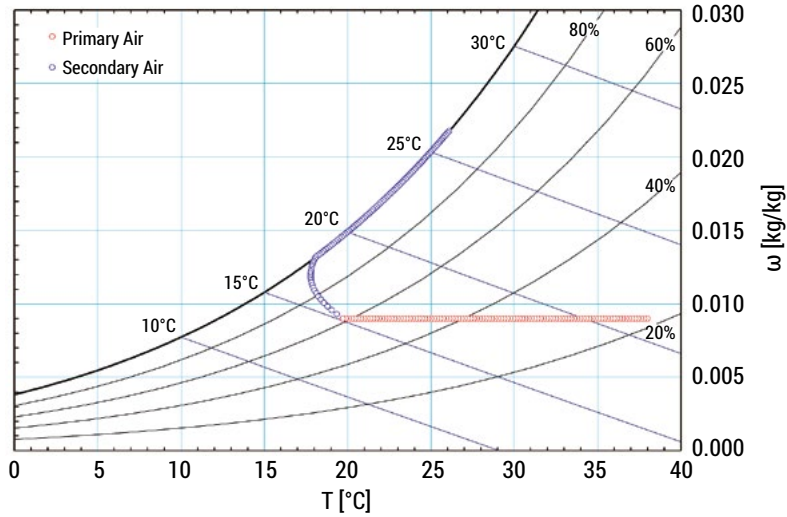
FIG. 3. **Psychrometric chart with the primary and secondary air flows for each computational element**

Conclusions

The experimental results showed that the studied RIEC system reached high cooling capacity, with dew point effectiveness values up to 0.91. The numerical results suggested that the proposed mathematical model can be valid to study the air-cooling system in detail, achieving suitable accuracy. The maximum deviations of ΔT and ε_{dp} were always within 0.45ºC and 0.025, respectively. Moreover, the model allowed to obtain the temperature, enthalpy and humidity distributions inside the exchanger.

Therefore, the results suggested that RIEC systems can be considered as a serious alternative to conventional air-cooling systems composed of direct expansion units, to cool air in hot air conditions, such as in South European climatic conditions. Moreover, these systems would contribute to achieving the European objectives of NZEB.

Literature

[1]   B. Porumb, P. Ungureşan, L.F. Tutunaru, A. Şerban, M. Bălan, A Review of Indirect Evaporative Cooling Operating Conditions and Performances, Energy Procedia. 85 (2016) 452–460. doi:10.1016/j.egypro.2015.12.226.

[2]   B. Porumb, P. Ungureşan, L.F. Tutunaru, A. Şerban, M. Bălan, A Review of Indirect Evaporative Cooling Technology, Energy Procedia. 85 (2016) 461–471. doi:10.1016/j.egypro.2015.12.228.

[3]   D. Pandelidis, S. Anisimov, P. Drag, Performance comparison between selected evaporative air coolers, Energies. 10 (2017) 1–20. doi:10.3390/en10040577.

[4]   Y. Wang, X. Huang, L. Li, Comparative study of the cross-flow heat and mass exchangers for indirect evaporative cooling using numerical methods, Energies. 11 (2018). doi:10.3390/en11123374.

[5]   D. Pandelidis, S. Anisimov, Application of a statistical design for analyzing basic performance characteristics of the cross-flow Maisotsenko cycle heat exchanger, Int. J. Heat Mass Transf. 95 (2016) 45–61. doi:10.1016/j.ijheatmasstransfer.2015.11.060.

[6]   Z. Duan, X. Zhao, J. Li, Design, fabrication and performance evaluation of a compact regenerative evaporative cooler: Towards low energy cooling for buildings, Energy. 140 (2017) 506–519. doi:10.1016/j.energy.2017.08.110.

[7]   J. Lin, R. Wang, C. Li, S. Wang, J. Long, K.J. Chua, Towards a thermodynamically favorable dew point evaporative cooler via optimization, Energy Convers. Manag. 203 (2020) 112224. doi:10.1016/j.enconman.2019.112224.

[8]   J. Lin, D.T. Bui, R. Wang, K.J. Chua, The counter-flow dew point evaporative cooler: Analyzing its transient and steady-state behavior, Appl. Therm. Eng. 143 (2018) 34–47. doi:10.1016/j.applthermaleng.2018.07.092.

[9]   M. Ali, W. Ahmad, N.A. Sheikh, H. Ali, R. Kousar, T. ur Rashid, Performance enhancement of a cross flow dew point indirect evaporative cooler with circular finned channel geometry, J. Build. Eng. (2020) 101980. doi:10.1016/j.jobe.2020.101980.

Removal of PAHs from road drainage system by ultrasonication

Abstract: Polycyclic aromatic hydrocarbons (PAHs) due to natural and anthropogenic processes are widely spread substances in the environment. It was proved that some of these pollutants can cause serious humans health problems such as hemolytic anemia, liver, cataracts and retina damage, neurological diseases, and primarily some PAHs are cancerogenic. These substances are hardly removable biologically so modern techniques such as ultrasonication should be developed. The articles reveal the removal effectiveness of 7 polycyclic aromatic hydrocarbons (PAHs) which were recognized in water from highway drainage system by using the ultrasound treatment process. Results showed that after 45 min of sonication, the average removal of PAHs reached 59%. The reduction of analyzed substances was proportional to treated time and irradiation amplitude. Furthermore, because of ozone addition to the sonicated samples, the efficiency of the treatment was significantly higher. The average PAHs degradation rate at the 10 mgL^{-1} dosage of O$_3$ assisted with ultrasonication was equal to 96%.

Introduction

The group of organic compounds which consist of two or more benzene rings are called polycyclic aromatic hydrocarbons (PAHs). As known, they are mainly colorless, white, or yellow solids with high melting and boiling points, low vapor pressure, and high molecular weight. Moreover, they have relatively low solubility in aqueous media. Worthnoty, some of the PAHs were recognized as mutagenic and cancerogenic substances [1, 2]. Due to anthropogenic and natural processes such as fires,

volcano eruptions, petroleum spills PAHs are ubiquitous substances in the environment. However, incomplete combustions of the fuels are considered as the main source of these compounds. The occurrence of PAHs in the environment is also related to transportation because of vehicles, road dust, and abrasion of road surfaces. Mentioned substances are used commercially mainly in agriculture and photographic products, the plastic and chemical industry, and in pharmaceuticals [3]. As a consequence, PAHs can migrate to air, soil, and water and undergo dynamic physical changes [4]. Although over 100 PAHs were identified in the environment, most studies and regulations are focused on a limited number of these substances, commonly from 14 to 20 [5]. For example, U.S. Environmental Protection Agency (USEPA) distinguished 16 PAHs according to their effects on human health and impact on the environment [6]. The concentration of these 16 PAHs in rainwater can varies from a few hundred to a few thousand ngL^{-1} [7].

Recently, there is a tendency to search for innovative PAHs removal techniques because mentioned substances are hard degradable biologically [3]. One of these techniques can be ultrasound treatment which was found to be an effective tool in PAHs removal from water both at low and moderate ultrasound frequencies. For instance, Manariotis et al. [8] reported that Phenanthrene and pyrene removal efficiency after 100 min of sonication was higher than 90% at a frequency of 582 kHz while naphthalene degradation in the same conditions was higher than 85%. They found also that using higher frequencies in the case of naphthalene was less effective. This study was carried out to determine PAHs in the samples from one of the highway rainwater drainage system and established the relation between operational parameters of ultrasonication on PAHs removal efficiency. Moreover, this work examines the effect of ozone treatment assisted with ultrasonication process on above mentioned identified in the samples substances.

Fundamentals of ultrasound treatment

In general, ultrasound water and wastewater treatment is related to acoustic cavitation phenomena which is the formation, growth, and implosion of bubbles formed due to intensive ultrasonic waves. The occurrence of the bubble is connected with the so-called rarefaction phase in which pressure oscillation amplitude is large enough. As a result of the collapse of the bubble which occurs in the so-called compression phase, several physical and chemical effects take place, namely shearing forces, micro-jets, shock waves, and very high temperature and pressure conditions [9–14]. Fig. 1 shows the bubble behavior during acoustic cavitation phenomena.
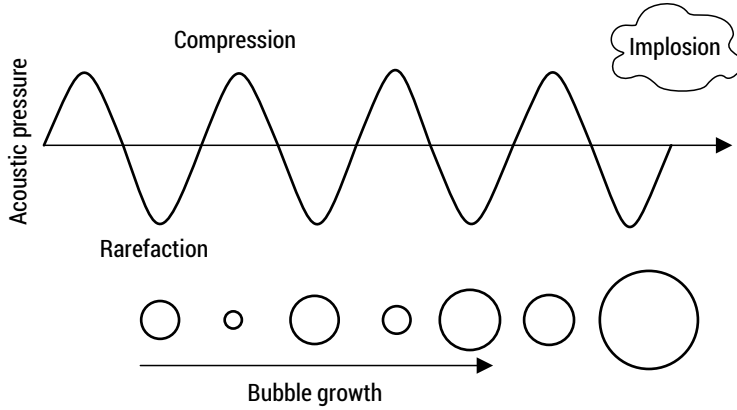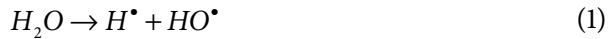
FIG. 1. Formation, growth, and collapse of the bubble during acoustic cavitation phenomena
SOURCE: Own source based on [15]

During the acoustic cavitation process, pollutants can be removed as a consequence of mechanical destruction, oxidation (e.g. due to hydroxyl radicals and ozone generation), and extreme temperature and pressure conditions (about 5000 K and 100 MPa, respectively) [16]. The hydroxyl radicals and hydrogen peroxide generation follows the equation [17, 18].

$$H_2O \rightarrow H^\bullet + HO^\bullet \tag{1}$$

$$H^\bullet + HO^\bullet \rightarrow H_2O \tag{2}$$

$$H^\bullet + H^\bullet \rightarrow H_2 \tag{3}$$

$$HO^\bullet + HO^\bullet \rightarrow H_2O_2 \tag{4}$$

In the acoustic cavitation process, inaudible sounds i.e. greater than 20 kHz are used and for that purpose, most often ultrasonic horns or baths are used. Generally, depends on frequency, the removal mechanism of substances is different. At higher frequencies, bubbles have a shorter lifetime and smaller radius than in the case of lower frequency conditions treatment. There are many factors influencing ultrasound treatment efficiency such as type of the treated substance, sonication time, sample volume, intensity, frequency, temperature, initial concentration, etc.[3, 19–22]. Nowadays, due to some limitations of ultrasonic treatment, there is a tendency to combine ultrasonication with other advanced oxidation processes such as O_3 or H_2O_2 addition which can lead to significantly enhance the pollutants degradation efficiency [23, 24].

Materials and methods

The PAHs concentration collected from the highway drainage system was determined by using the 7890B gas chromatograph (GC) provided by Perlan Technologies (Warsaw, Poland). Before measurement samples were prepared according to Bohdziewicz et al. [25] by using the solid phase extraction method (SPE) applying Supelclean™ ENVI™-18 cartridges supplied by Sigma-Aldrich (Poznan, Poland) with an Octadecylsilane (C_{18}) as a cartridge bed. For that purpose 5 mL of Methanol (MeOH) and pure water (H_2O) was used in conditioning and 3 mL of dichloromethane (DCM) in the elusion process. The process was carried out under 5 min. drying time in vacuum, 1 mL/min. flow rate and the negative pressure was set to 5–10 kPa. During GC analysis, helium was used as the carrier gas. The temperature of the ion trap was set to150°C while the temperature of the ion source was equal to 230°C. The temperature of the oven varied from 80°C to 280°C and the injector temperature was set to 250°C. The flow rate of helium was 1.1 mL/min. The water samples were tested for basic parameters, namely pH value, turbidity, conductivity, and color.

After identified the PAHs present in the drainage samples, the study was carried out to evaluate the ultrasonication effectiveness on its removal. Therefore, an ultrasonic processor Sonics VCX 500 (Vibra Cell Sonics, Sonics & Materials, USA) with a 20 kHz frequency and 13 mm diameter probe was used. The processor is also characterized by 114 μm amplitude and a maximum net power of 500 W. Experimental setup which was used in the experiments are shown in fig. 2.
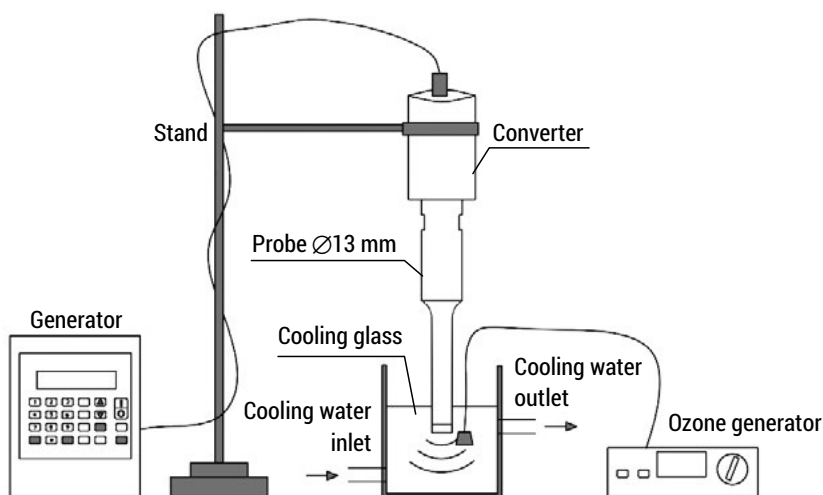

FIG. 2. Experimental setup used in the study

SOURCE: Own data

To increase the precision of PAHs removal efficiency determination additionally 1 mL of identified substances was added to the treated solution. In this study, irradiation time (at maximum amplitude) and irradiation amplitude (during 1 min sonication) effect on PAHs removal efficiency was established. The volume of the treated sample was 100 mL and 50 mL, respectively. Moreover, by using ozoner FM500 (WRC Multiozone, Gdansk, Poland) impact of 1, 3, 5, and 10 mgL^{-1} ozone addition on the degradation rate of PAHs were tested during 1 min ultrasonication, at maximum amplitude, and in 100 mL volume of the sample. In all experiments, to prevent overheating cooling system was used. Acoustic power P [W] in this study was calculated as (1):

$$P = \frac{E}{t} \tag{1}$$

where E [J] is the sonication energy given by the ultrasonic processor and t [s] is the sonication time. The intensity of ultrasound I [W/cm^2] as a function of acoustic power and sonication surface area follows the equation (2):

$$I = \frac{P}{A} \tag{2}$$
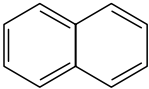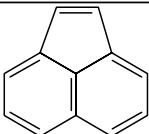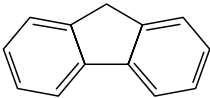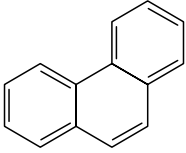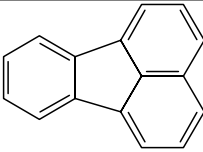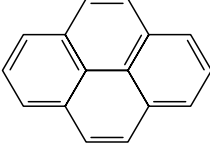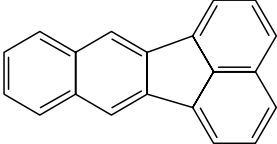
where A [cm^2] is the area of the sonication surface ($A = 1.33$ cm^2)

Results and discussion

To initially evaluate the quality of the sample, as an indirect indicators of harmful substances presence, conductivity (204.5 µm/cm), pH (7.80), turbidity (26.2 NTU), and color (242 mg Pt L^{-1}) were measured.

As can be seen in Table 1, GC analysis revealed that in sample 7 of PAHs were identified, namely Naphthalene, Acenaphthylene, Fluorene, Phenanthrene, Fluoranthene, Pyrene, and Benzo[k]fluoranthene. Some of them can cause serious health effects on human health. According to International Agency for Research on Cancer (IARC) [26], Benzo[k]fluoranthene and Naphthalene are classified as possibly cancerogenic for humans. Moreover, some of the identified substances cause hemolytic anemia, liver, neurological, cataracts, and retina damage [6, 27].

TABLE 1. The chemical characteristic of PAHs identified in the water

Name	Molecular formula	Molecular mass (gmol^{-1})	Chemical structure	CAS No
Naphthalene	$C_{10}H_8$	128.17		91−20−3
Acenaphthylene	$C_{12}H_8$	152.19		208−96−8
Fluorene	$C_{13}H_{10}$	166.22		86−73−7
Phenanthrene	$C_{14}H_{10}$	178.23		85−01−8
Fluoranthene	$C_{16}H_{10}$	202.25		206−44−0
Pyrene	C_6H_{10}	202.25		129−00−0
Benzo[k]fluoranthene	$C_{20}H_{12}$	252.30		207−08−9

SOURCE: [27].

During treatment of the samples at the amplitude of 23, 68, 91 and 114 μm results indicated that increasing amplitude results in higher removal efficiency of PAHs. This relation is caused by the fact, that as amplitude increases, the energy, power, and intensity of the process are higher, thus more hydroxyl radicals and other oxidants are generated. In table 2 parameters corresponding to individual amplitude levels are shown.

TABLE 2. Energy, power, and intensity of the process corresponding to applied amplitude levels

Amplitude (µm)	Energy (J)	Power (W)	Intensity (W/cm^2)
23	816	13.6	10.25
68	3407	56.8	42.78
91	4815	80.3	60.46
114	6704	111.7	84.18

The average removal efficiency of 7 identified PAHs at maximum amplitude was equal to 76%. At the amplitude of 23, 68 and 91 µm average degradation rate was 29, 53, and 66%, respectively. The effect of amplitude on PAHs removal efficiency is illustrated in fig. 3.
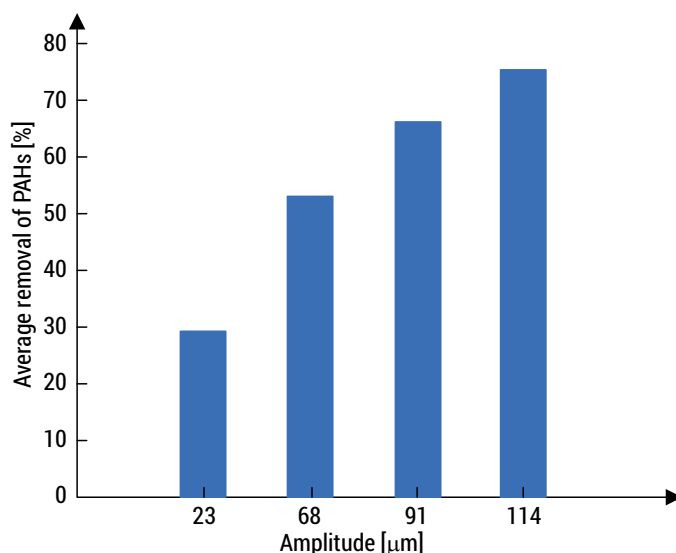
FIG. 3. Effect of irradiation amplitude on PAHs average removal efficiency
SOURCE: Own data

In the study, the effect of irradiation time was investigated during 1, 5, 15, 30, and 45 min of sonication. As a well-known fact, sonication time was proportional to the effectiveness of PAHs removal. As illustrated in fig. 4, the minimum degradation rate was obtained after 1 min of sonication (18%) and maximum after 45 min. (59%).

At the maximum time, the highest efficiency was obtained in the case of phenanthrene and the lowest in the case of pyrene which could be caused by the different number of aromatic rings and molecular weight.
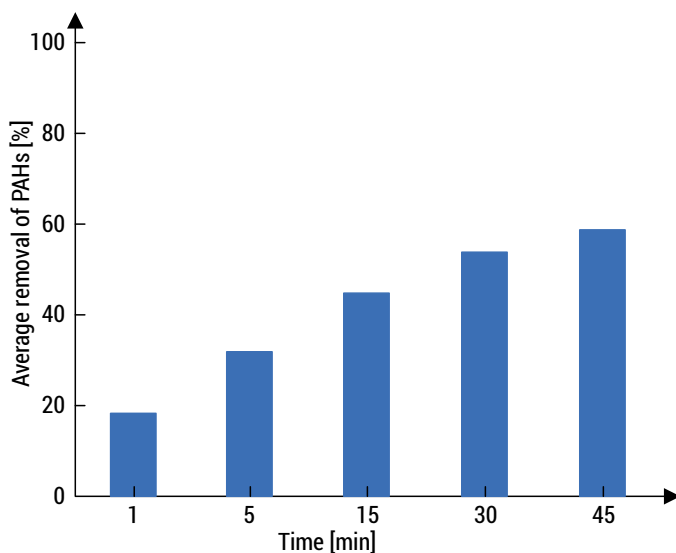
FIG. 4. Effect of irradiation time on PAHs average removal efficiency
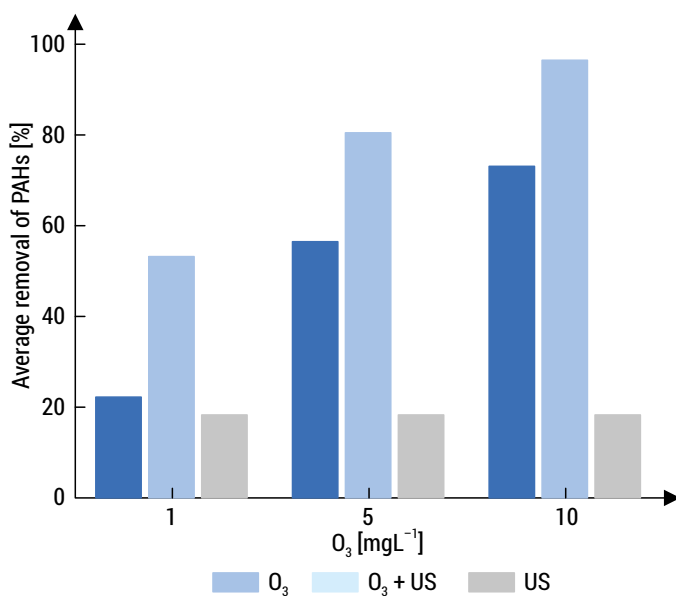
SOURCE: Own data

FIG. 5. Comparison of O_3, O_3 assisted with ultrasound (US) and US treatment impact on PAHs removal efficiency (at 1 min sonication time and maximum amplitude)

SOURCE: Own data

As a consequence of 1, 5 and 10 mg L^{-1} addition of ozone to the treated samples, the average removal efficiency of identified PAHs was 22, 56, and 73%, respectively. However, ozone treatment with ultrasonic assistance resulted in significantly higher average PAHs removal efficiency. It was about 30% more effective than the ozonation process alone.

Results of ozone treatment as a single process and ozonation with ultrasound assistance are shown in fig. 5. It was noted that the maximum average degradation of identified PAHs was obtained during 10 mg L^{-1} of O$_3$ addition assisted with ultrasonication process and it was 96%.

Both ozonation used alone and with ultrasound treatment assistance were more efficient than 1 min ultrasonication as a single process (removal of 18%). It is a well-known fact that ozone is a powerful oxidant, especially in the case of double C=C bonds in water. Furthermore, due to its decomposition more hydroxyl radicals in sonicated aqueous media can be generated. It was proved that in alkaline conditions, this conversion is relatively fast. However, ultrasound assistance could significantly improve the speed of the decomposition which is connected with O$_3$ pyrolysis inside the acoustic bubble or at the bubble interface [28–32].

Summary

In conclusion, the results of this study reveal that in the road drainage system sample 7 of PAHs were detected, namely Naphthalene, Acenaphthylene, Fluorene, Phenanthrene, Fluoranthene, Pyrene, and Benzo[k]fluoranthene. These substances are ubiquitous in the environment and can cause serious health problems. Naphthalene and Benzo[k]fluoranthene were found to be possibly cancerogenic for humans. Moreover, they are considered as substances hardly removal biologically. Performed experiments indicated that ultrasonication was the effective process in PAHs removal, especially while it was combined with O$_3$ addition. The degradation rate in the experiments was as follows: O$_3$ addition + ultrasound treatment > O$_3$ as a single process > ultrasound as a single process. In all cases, PAHs removal efficiency was proportional to the irradiation time, amplitude, and O$_3$ dosage. Maximum average PAHs reduction (96%) was obtained during ultrasound treatment and the addition of 10 mg L^{-1} O$_3$. As a result of 45 min ultrasound treatment as a single process, 59% average degradation rate of selected PAHs were obtained. Although ultrasound is considered as a promising technology, there are some limitations such as scale effect and high energy demand that need to be explored in further research.

Literature

[1] Abdel-Shafy H. I.,Mansour M. S. M., *A review on polycyclic aromatic hydrocarbons: Source, environmental impact, effect on human health and remediation*, Egypt. J. Pet., 2016, 25 (1), pp. 107–123, doi: 10.1016/j.ejpe.2015.03.011.

[2] IARC, *Chemical agents and related occupations.*, 100, 2012.

[3] Gupta P.,Suresh S.,Jha J. M.,Banat F.,Sillanpää M., *Sonochemical degradation of polycyclic aromatic hydrocarbons: a review*, Environ. Chem. Lett., 2021, doi: 10.1007/s10311-020-01157-9.

[4] Gbeddy G.,Goonetilleke A.,Ayoko G. A.,Egodawatta P., *Transformation and degradation of polycyclic aromatic hydrocarbons (PAHs) in urban road surfaces: Influential factors, implications and recommendations*, Environ. Pollut., 2020, 257, p. 113510, doi: 10.1016/j.envpol.2019.113510.

[5] Fan Z.,Lin L., *Exposure science: Contaminant mixtures*, in *Encyclopedia of Environmental health*, 2019, pp. 805–815.

[6] USEPA, *Polycyclic Aromatic Hydrocarbons (PAHs).* 2008.

[7] Forsgren A. J., *Wastewater treatment: Occurrence and fate of polycyclic aromatic hydrocarbons (PAHs).* 2015.

[8] Manariotis I. D.,Karapanagioti H. K.,Chrysikopoulos C. V., *Degradation of PAHs by high frequency ultrasound*, Water Res., 2011, 45 (8), pp. 2587–2594, doi: 10.1016/j.watres.2011.02.009.

[9] Dular M. *et al.*, *Use of hydrodynamic cavitation in (waste)water treatment*, Ultrason. Sonochem., 2016, 29, pp. 577–588, doi: 10.1016/j.ultsonch.2015.10.010.

[10] Zupanc M.,Pandur Ž.,Stepišnik Perdih T.,Stopar D.,Petkovšek M.,Dular M., *Effects of cavitation on different microorganisms: The current understanding of the mechanisms taking place behind the phenomenon. A review and proposals for further research*, Ultrason. Sonochem., 2019, 57, (April), pp. 147–165, doi: 10.1016/j.ultsonch.2019.05.009.

[11] Yasui K., *Acoustic Cavitation and Bubble Dynamics.* 2018. [Online]. Available: http://www.springer.com/series/15634

[12] Ashokkumar M., *The characterization of acoustic cavitation bubbles – An overview*, Ultrason. Sonochem., 2011, 18 (4), pp. 864–872, doi: 10.1016/j.ultsonch.2010.11.016.

[13] Fetyan N. A. H.,Salem Attia T. M., *Water purification using ultrasound waves: application and challenges*, Arab J. Basic Appl. Sci., 2020, 27 (1), pp. 194–207, doi: 10.1080/25765299.2020.1762294.

[14] Warade A.,Gaikwad R., *Review on wastewater treatment by hydrodynamic cavitation*, IOSR J. Environ. Sci., 2016, 10 (12), pp. 67–72.

[15] Merouani S.,Hamdaoui O.,Rezgui Y.,Guemini M., *Modeling of ultrasonic cavitation as an advanced technique for water treatment*, Desalin. Water Treat., 2015, 56 (6), pp. 1465–1475, doi: 10.1080/19443994.2014.950994.

[16] Doosti M. R.,Kargar R.,Sayadi M. H., *Water treatment using ultrasonic assistance : A review*, Ecology, 2012, 2 (2), pp. 96–110.

[17] Zhang K. *et al.*, *Degradation of bisphenol – A using ultrasonic irradiation assisted by low – concentration hydrogen peroxide*, J. Environ. Sci., 2011, doi: 10.1016/S1001-0742(10)60397-X.

[18] Nie M.,Wang Q.,Qiu G., *Enhancement of ultrasonically initiated emulsion polymeriza-tion rate using aliphatic alcohols as hydroxyl radical scavengers*, Ultrason. Sonochem., 2008, doi: 10.1016/j.ultsonch.2007.03.010.

[19] Muñoz-Calderón A.,Zúñiga-Benítez H.,Valencia S. H.,Rubio-Clemente A.,Upegui S. A.,Peñuela G. A., *Use of low frequency ultrasound for water treatment: Data on azithro-mycin removal*, Data Br., 2020, 31, pp. 0–6, doi: 10.1016/j.dib.2020.105947.

[20] Peterson R. V.,Pitt W. G., *The effect of frequency and power density on the ultrasoni-cally-enhanced killing of biofilm-sequestered Escherichia coli*, Colloids Surfaces B Biointerfaces, 2000, 17 (4), pp. 219–227, doi: 10.1016/S0927-7765(99)00117-4.

[21] Ghasemi N.,Gbeddy G.,Egodawatta P.,Zare F.,Goonetilleke A., *Removal of polycyclic aromatic hydrocarbons from wastewater using dual-mode ultrasound system*, Water Environ. J., 2020, 34 (1), pp. 425–434, doi: 10.1111/wej.12540.

[22] Xiao R.,Diaz-Rivera D.,Weavers L. K., *Factors influencing pharmaceutical and personal care product degradation in aqueous solution using pulsed wave ultrasound*, Ind. Eng. Chem. Res., 2013, 52 (8), pp. 2824–2831, doi: 10.1021/ie303052a.

[23] Nikfar E. *et al.*, *Removal of Bisphenol A from aqueous solutions using ultrasonic waves and hydrogen peroxide*, J. Mol. Liq., 2016, doi: 10.1016/j.molliq.2015.08.053.

[24] Gągol M.,Przyjazny A.,Boczkaj G., *Wastewater treatment by means of advanced oxida-tion processes based on cavitation – A review*, Chem. Eng. J., 2018, 338, pp. 599–627, doi: 10.1016/j.cej.2018.01.049.

[25] Bohdziewicz J.,Dudziak M.,Kamińska G.,Kudlek E., *Chromatographic determina-tion and toxicological potential evaluation of selected micropollutants in aquatic envi-ronment—analytical problems*, Desalin. Water Treat., 2016, 57 (3), pp. 1361–1369, doi: 10.1080/19443994.2015.1017325.

[26] *International Agency for Research on Cancer List of classifications*, https://monographs.iarc.fr/list-of-classifications.

[27] Kim S. *et al.*, *PubChem substance and compound databases*, Nucleic Acids Res., 2016, doi: 10.1093/nar/gkv951.

[28] Wu Z.,Abramova A.,Nikonov R.,Cravotto G., *Sonozonation (sonication/ozonation) for the degradation of organic contaminants – A review*, Ultrason. Sonochem., 2020, 68, pp. 1–23, doi: 10.1016/j.ultsonch.2020.105195.

[29] Wu Z. *et al.*, *Enhanced effect of suction-cavitation on the ozonation of phenol*, J. Hazard. Mater., 2011, 190 (1–3), pp. 375–380, doi: 10.1016/j.jhazmat.2011.03.054.

[30] Wu Z.,Ondruschka B.,Zhang Y.,Bremner D. H.,Shen H.,Franke M., *Chemistry driven by suction*, Green Chem., 2009, 11 (7), pp. 1026–1030, doi: 10.1039/b902224d.

[31] Wu Z.,Cravotto G.,Ondruschka B.,Stolle A.,Li W., *Decomposition of chloroform and suc-cinic acid by ozonation in a suction-cavitation system: Effects of gas flow*, Sep. Purif. Technol., 2016, 161, pp. 25–31, doi: 10.1016/j.seppur.2016.01.031.

[32] Wu Z.,Shen H.,Ondruschka B.,Zhang Y.,Wang W.,Bremner D. H., *Removal of blue-green algae using the hybrid method of hydrodynamic cavitation and ozonation*, J. Hazard. Mater., 2012, 235–236, pp. 152–158, doi: 10.1016/j.jhazmat.2012.07.034.

Energy performance optimization in a condensing boiler

Keywords: condensing boiler, Domestic Hot Water, space heating, energy performance, excess air.

Abstract: In Europe, primary energy consumption in buildings accounts for up to 25%–40%, depending on the climate conditions. Space heating and Domestic Hot Water (DHW) contribute significantly to this energy consumption. Among the most common sources for heat generation in these appliances is natural gas. Condensing boilers can surpass the 100% energy performance over the lower heating value if the operating conditions enable the water vapor in the exhaust gases to condensate. Consequently, optimizing the operating parameters of condensing boilers is necessary to decrease the fuel consumption without hindering the water heating needs. The present work presents an experimental approach to the operating parameters of a condensing boiler that works with natural gas. The aim is to develop a theoretical model that relates the energy performance to the water temperature, set by the final user, and the excess air set by the maintenance staff.

Introduction

Given the primary energy consumed in buildings [1], the building stock is a key target to improve energy use. The substitution of old boilers that use solid or liquid fossil fuels by condensing boilers fueled by natural gas, has noticeably improved the energy performance in water heating, hence the environmental impact [2].

Although increasing the percentage of hydrogen in the natural gas achieves lower CO_2 emissions [3], its composition is determined by the supplier and thus cannot be controlled. Condensation of the water vapor in the exhaust gases depend on the water vapor pressure and the saturation vapor pressure at the cooling temperature. Water

vapor pressure depends on the atmospheric pressure, the composition of the natural gas used and the excess air in the combustion process. The temperature at which the exhaust gases cool depends on the DHW set temperature and the supply and return water temperatures from the heating system. Consequently, set values of these parameters will be determinant for the boiler performance, hence the fuel consumption. As optimizing the combustion process minimize the energy consumed to achieve the required heating and DHW needs, this work develops an experimental study to validate a theoretical model that enables identification of the optimal operating parameters. The theoretical model is implemented in Excel. First, total combustion is considered. Operating conditions are then modified to compare the results yielded by the theoretical model to the actual experimental values observed.

Materials and Methods

The target natural gas condensing boiler for the experimental tests is a Vaillant Ecotech PLUS. During the tests, DHW is generated at 45°C set temperature and supply water to the heating system is set at 50°C. Temperature is measured at the supply tap water temperature, actual DHW temperature, supply and return water temperatures from the heater system and the gas exhaust. Temperature and Relative Humidity are measured at the air inlet to the combustion process. Further measured variables are the gas consumption and the amount of water condensed from the exhaust gases. Figure 1 shows the target condensing boiler and the temperature sensors used at some of the measuring points.

(a)   (b)   (c)
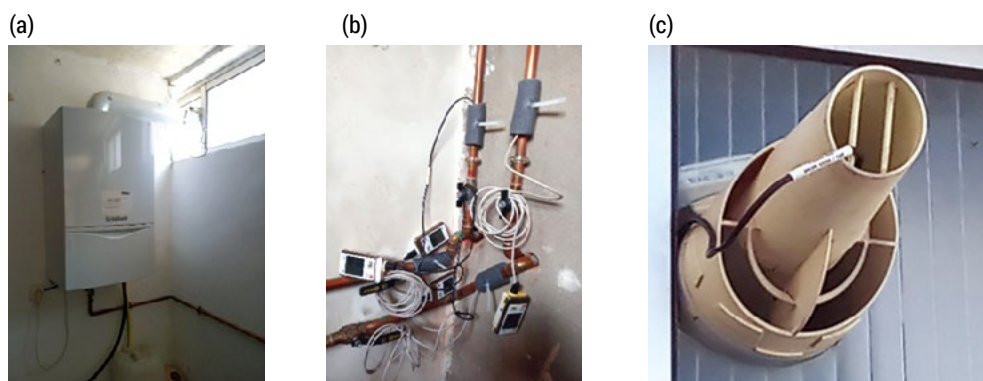
FIG. 1. **Views of the (a) condensing boiler; (b) temperature sensors at the water supply and return; (c) Temperature measurement at the gas exhaust**

Temperature sensors are Testo Data Loggers, model 175 T2. Air temperature and relative humidity are measured with a Testo Data Logger model 175 H1. The measuring interval and storage cycle is 10s. Figure 2 shows the values registered along a typical day.
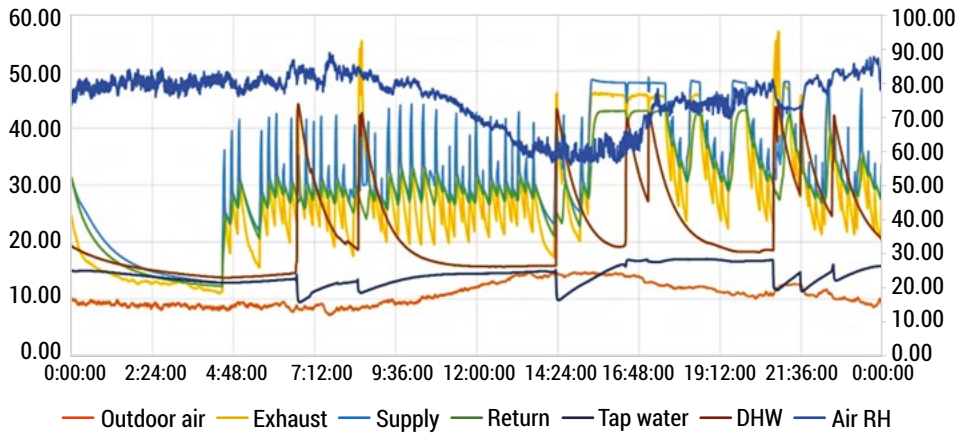
FIG. 2. Experimental values registered during one typical day

During periods of continuous space heating, it can be observed that the exhaust gas temperature maintains between the heating system supply and return water temperatures. This demonstrates that the temperature at which the exhaust gases can get cooled is always lower than the supply water for space heating. Although the average temperature of the exhaust gases keeps below that water temperature, it can occasionally exceed it due to the boiler start-up.

TABLE 1. This is a table. Tables should be placed in the main text near to the first time they are cited. Note: please refer to the table in the main text

Parameter	Measured value
Instant exhaust gases temperature Average variation	52.5°C 30−56.8°C
Air temperature	12.4°C
Performance	99.1%
Excess air	1.27
Losses (%)	0.9%
$[CO_2]$	9.41%
$[O_2]$	4.4%
$[CO]$	68 ppm

Besides, an analysis of combustion is performed to determine the exhaust gases composition and the excess air in the combustion process. Results are gathered in Table 1. The analyzer is a TESTO model 330–2 that calculates the boiler performance through the Sieggert equation. The average fuel consumption is also measured. Water condensed during five days is weighted, obtaining an average condensing rate of 840 g/Nm³ of natural gas.

Results and discussion

A theoretical model is developed to calculate the temperature at which condensation of water vapor in the exhaust gases starts, condensed water mass flow, the condensing boiler energy performance and the energy recovered in the boiler. Parameters studied are fuel mass rate and composition, excess air, and ambient air psychrometric conditions.

First, the stoichiometric combustion is calculated assuming a non-fixed composition of the natural gas [4], whose components are methane, ethane, propane, n-butane, isobutane, n-pentane, isopentane, hexane, heptane, nitrogen and carbon dioxide. Assuming no unburnt combustibles, stoichiometric oxygen is calculated. Excess air is used to calculate the air rate supplied to the boiler and the composition of the exhaust gases.

Next, an energy balance is constructed in the burner. Provided an adiabatic process, this energy balance provides the Adiabatic Flame Temperature. Assuming steady flow [5], this energy balance is given by equation (1):

$$\dot{Q} + \dot{n}_r \cdot \overline{C}_{p,r} \cdot \left(T_r - 25\right) - \dot{n}_p \cdot \overline{C}_{p,p} \cdot \left(T_p - 25\right) - \sum_{i=1}^{N} \dot{n}_i \cdot \Delta H^{\circ}_{r,i} = 0 \qquad (1)$$

Where $\dot{Q}$ is the heat losses to the environment (equal to zero, provided an adiabatic process), $\dot{n}_r$ is the molar rate of the reactants supplied to the burner, $\overline{C}_{p,r}$ is the reactants average isobaric specific heat, T_r is the temperature of the reactants at the burner inlet, $\dot{n}_p$ is the molar rate of products in the exhaust gases, $\overline{C}_{p,p}$ is the products average isobaric specific heat, T_p is the products temperature (corresponding to the Adiabatic Flame Temperature, provided an adiabatic process), $\dot{n}_i$ is the molar rate of each reactive component i of the natural gas and $\Delta H^{\circ}_{r,i}$ is the enthalpy of combustion for each component of the natural gas. Super index N in the summation denotes the number of reactive components considered for the supplied natural gas.

Then, a value for the exhaust gases temperature is set. This value may correspond to a measured, experimental value, or rather be an arbitrary temperature. Composition of the exhaust gases enable calculation of the temperature at which

water vapor condensation starts (dew point temperature): if this temperature is over that of the exhaust gases, then condensation occurs. Both the dew point temperature and the water molar fraction in the exhaust gases are calculated from the Raoult-Dalton Law (2) and the Antoine equation (3) [6]:

$$P_{H2O} = y_{H20} \cdot P = P_{H20}^{\circ} \qquad (2)$$

$$\log_{10}\left(P_{H20}^{\circ}\right) = A - \frac{B}{T + C - 273.15} \qquad (3)$$

In equation (2), P_{H2O} is the partial water vapor pressure in the exhaust gases, y_{H20} is the water molar fraction in the exhaust gases, P is the total pressure and P_{H20}° is the saturation vapor pressure of water. Concerning equation (3), T is the absolute temperature in Kelvin, whereas A, B and C are constants dependent from the component. It should be noted that the only possible condensable component considered in the exhaust gases is the water vapor, which has its molar fraction changed as it condenses. The amount of water condensed is calculated through equation (4):

$$\dot{n}_{H2O} = \dot{n}_p \cdot \left(y_{H20,p} - y_{H20,s}\right) \qquad (4)$$

Where $\dot{n}_{H2O}$ is the condensed water molar rate, $\dot{n}_p$ is the exhaust gases molar rate, $y_{H20,p}$ is the water molar fraction in the exhaust gases at the burner outlet, and $y_{H20,s}$ is the water molar fraction in the exhaust gases at the boiler outlet.

Finally, the boiler performance is calculated through the sensible heat transferred from the exhaust gases and the water latent heat (λ):

$$\eta = \frac{\dot{n}_p \cdot \overline{C}_{p,p} \cdot \left(T_p - T_{p,s}\right) + \dot{n}_{H2O} \cdot \lambda}{\dot{n}_{NG} \cdot LHV_{NG}} \qquad \left(Ec-5\right)$$

Where T_p and $T_{p,s}$ are the temperature of the exhaust gases at the burner and at the chimney outlet, respectively, $\dot{n}_{GN}$ is the natural gas molar flow and LHV_{NG} is its Lower Heating Value.

Table 2 gathers compares the results obtained through the theoretical model and the experimental measurements. It must be noted that the theoretical model considered a fixed value of the excess air and composition of the natural gas [4]. Temperature of exhaust gases at the boiler outlet is fixed at 40°C, considered a more typical value during the most steady operating periods of the boiler observed in Figure 2. Results provided in Table 2 show slight deviations due to differences in the concentration of carbon dioxide in the exhaust gases, whose cause relies in the unknown actual composition of the natural gas used.

TABLE 2. **Comparative of results obtained through the theoretical model and the experimental study**

Procedure	Excess air	Tp,s (°C)	$[O_2]$ %vol.	$[CO_2]$ %vol.	Condensed water (g/Nm³)	η (%)
Theoretical model	1.27	40	4.46%	8.56%	864.64	99.58%
Experimental results	1.27	30−56.8	4.4%	9.41%	840	99.10%

Results provided in Table 2 show slight deviations due to differences in the concentration of carbon dioxide in the exhaust gases, whose cause relies in the unknown actual composition of the natural gas used.

Summary

A theoretical model describing the operation of a natural gas condensing boiler is validated with the experimental measurements performed in a real appliance. The model provides information on the expected performance for the operating air dry bulb temperature, relative humidity and atmospheric pressure. Excess air can be adjusted to control the Flame Adiabatic Temperature, hence the emission of pollutants like NOx and optimize the performance of the boiler. This model thus provides a tool to improve the operation of existing condensing boilers, achieving larger energy and economic savings with positive environmental impact.

Literature

[1] IEA *energy efficiency 2018 – analysis and outlooks to 2040*, Mark. Rep. Ser. 1–143 (2017).

[2] Jiri Horaka, Lenka Kubonova, Kamil Krpec, et all. *PAH emissions from old and new types of domestic hot water boilers.* Environmental Pollution. Volume 225, June 2017. https://doi.org/10.1016/j.envpol.2017.03.034.

[3] M.S. Boulahlib, F. Medaerts, M.A. Boukhalf. *Experimental study of a domestic boiler using hydrogen methane blend and fuel-rich staged combustion.* International Journal of Hydrogen Energy. Available online March 2021. https://doi.org/10.1016/j.ijhydene.2021.01.103.

[4] Kuczynski, Szymon, Mariusz Łaciak, Adam Szurlej, and Tomasz Włodek. 2020. *Impact of Liquefied Natural Gas Composition Changes on Methane Number as a Fuel Quality Requirement.* Energies 13 (19) https://doi.org/10.3390/en13195060.

[5] Smith, Robin. 2005. *Chemical Process Design and Integration.* Edited by John Wiley & Sons Ltd. Second Edition.

[6] E. Poling, Bruce, John M. Prausnitz, and John P. O'Connell. 2001. *The Propierties of Gases and Liquids.*

Determination and removal of perfluorinated alkyl compounds (PFAs) in industrial wastewaters

Abstract: Perfluorinated Alkyl Compounds (PFAs) are highly produced and used materials in various fields. Due to their unique properties like water repellence and grease repellence, they are very useful as surfactants and surface protectors. However, since having a strong structure these materials are highly resistant and accumulative in the environment. Because of their persistent nature and harmful potential, they are listed within materials in Stockholm Convention as persistent organic pollutants (POPs) and all uses of PFAs and derivatives are restricted. Since PFAs cannot be treated biologically, advanced treatment processes like advanced oxidation, adsorption, and membrane filtration are utilized for their removal. Within this work, their occurrence and treatment situations will be evaluated according to the literature data.

Introduction

Perfluorinated Compounds (PFC) have been produced in high amounts since 1950s for a wide range of applications like carpet coating, food packaging, paper products, metal coating, medical devices, insecticides, dye, polish, toner and printing cartridges, sealants, and firefighting foams [1, 2]. PFCs are very good surfactants and surface protectors due to having both aquaphobic and lipophobic properties. Some of these compounds are persistent, but some could be reduced and converted to other materials that have low persistency environmentally [3]. PFCs can cause mutagenic effects

and birth abnormalities. These properties derive from their content of elemental fluorine atom, which is the most electronegative element among the halogens [4]. These properties induce C-F covalent bonding, resulting in a frame highly resistant to hydrolysis, photolysis, metabolism, and biodegradation [5]. These properties are the reason why PFCs are highly persistent and bioaccumulative [6].

Perfluorooctane sulfonic acid (PFOS) is a completely fluorinated anion, usually added to bigger polymers and used as salts in some cases, that belong to PFCs. PFOS, their salts, and Perfluorooctane sulfonyl fluoride (PFOSF) are listed within the materials in the Stockholm Convention and production and utilization of PFOS and related materials are restricted. PFOS can be derived synthetically by the resolution of PFOSF and their salts. "PFOS related materials" term is used for all materials containing one or more PFOS groups or materials that can be reduced to PFOS environmentally. These materials are restricted via listing PFOS and PFOSF in the framework of this convention.

This work presents an overview of the occurrence of PFAs in the environment and water sources and current advanced treatment techniques used on their removal. Our main goal is to compare the concentrations of PFAs in various sources and evaluate treatment efficiencies of techniques used to remove PFAs and their derivatives.

Materials and Methods

Analytical methods for quantitative measurement of PFAs are still under development and there are few technical standards defined yet. Analysis of PFAs is very challenging work because of their low volatility and high solubility in water. The preferred analytical detection method for PFAS is Liquid Chromatography-Mass Spectrometry (LC-MS) and LC-MS/MS for anionic compounds (including PFOS and PFOA). However, both LC-MS(MS) and Gas Chromatography-Mass Spectrometry (GC-MS) could be used for the detection of neutral per- and poly-fluorinated alkyl compounds including most of the PFOS precursors.

Sampling

Sampling for polyfluorinated compounds is crucial because analysis results are highly affected by the type of sampling method, sampling period, sampling container, and sampling depth. Bottle sampling, ship inlet system, rosette type sampling, and glass plate sampling are the most used sampling techniques. Grab sampling and composite sampling are common sampling periods. It is reported by various researchers that as the depth rise, fewer PFC concentrations are observed for samples [7, 8].

Before sampling containers must be pretreated with sample water, methanol, or purified water. Thus, any possible contaminations will be hindered.

Commonly used materials for sampling are glass, polypropylene, stainless steel, polyethylene, and polyvinylchloride and samples generally kept within polyethylene, polyethylene terephthalate (PET), polypropylene, and amber bottles.

PFCs can be adsorbed on glass in an aqueous medium. Furthermore, polyfluorinated materials or false applications may result in contamination of samples [7, 9]. Polyfluorinated materials are like;

- Polytetrafluoroethylene (PTFE) includes Teflon and Hostaflon.
- Polyvinylidene fluoride (PVDF) includes Kynar.
- Polychlorotrifluoroethylene (PCTFE) includes Neoflon.
- Ethylene-tetrafluoro-ethylene (ETFE) includes Tefzel.
- Fluorinated ethylene propylene (FEP) includes Teflon FEP and Hostaflon FEP.

After sampling, sample transportation must be carried out at 4°C via insulated boxes filled with ice. Samples are usually kept at 4°C to prevent microbial growth. Samples that will be kept for a longer period before analysis should be frozen at 20°C for storage.

Characterization

Before the detection phase, samples must be prepared using the appropriate method (e.g., dilution of water samples, extraction of solid samples). First, samples are diluted 1:1 with methanol. Then samples must be filtered via glass fiber filters and must be extracted by C18 extraction cartridges. According to the literature, Oasis (HLB and WAX) and Sep-Pak Plus brands are widely preferred cartridge brands. After extraction, cartridges will be eluded with methanol to move extracts to a solution. Acetic acid is added for some analytes to adjust pH to ~3–4 for improving the sensitivity of analytes. Then solutions are treated with the required procedure for analysis and prepared for LC-MS/MS or GC-MS.

Samples with high content of suspended solids (SS) necessitate filtration to prevent plugging of solid-phase extraction cartridges. Furthermore, separate analysis of dissolved phase and particulate phase enables analysis of PFCs partition behavior. On the other hand, because of the adsorption possibility of PFCs to filters, filtration devices can be a source of contamination.

It is not possible to analyze PFCs directly via GC-MS because of their high polarity and carboxylic acidic group content. High polarity results with wide and tailed peaks and thus relatively high detection limits [10]. Furthermore at neutral pH evaporation of anionic PFCs during GC analysis becomes harder because of their low volatility [11].

Derivation processes are required before GC analysis to raise volatility and thermal stability and to lower boiling points of PFCs [12]. Furthermore, via derivation processes less tailed and better peaks can be achieved. Additionally, the selectivity of GC analysis can be enhanced. The main purpose of derivation processes is to decrease the polarity. Derivation in mass spectrometry can increase molecular ion intensity and can affect fractionation or enhance ionization efficiency. Acetylation, alkylation, and silylation are the most common derivation techniques [13].

Occurrence of PFAs in water samples

There are many types of research for the occurrence of PFOS and related materials in especially Europe and the Far East. PFOS and related materials were observed in various water samples (seawater, rivers, lakes, tap waters, and wastewater). Concentrations of various PFAs from various researches overall the world are given in Table 1.

TABLE 1. Concentrations of PFAs from various sources according to literature

Chemicals	Source	Region	Findings	References
PFOS	River	Japan	PFOS range: 0.30–157 ng/L	Saito et al. [14]
	Coast		PFOS range: 0,20–25,2 ng/L	
PFOS	Bay	Japan	PFOS range: 9.00–59.0 ng/L	Taniyasu et al. [15]
	Lake		PFOS range: 4.00–7.40 ng/L	
PFOS, PFOA	Lake, river, coast	South Korea	PFOS range: 4.11–450 ng/L PFOA range: 2.95–68.6 ng/L	Naile et al. [16]
PFOS, PFOA	Lake	South Korea	PFOS range: 2.24–651 ng/L PFOA range: 0.9–62 ng/L	Rostkowski et al. [17]
	River		PFOS range: 8.03–651 ng/L PFOA range: 5.21–61.7 ng/L	
PFOS, PFOA	Lake	United States	PFOS range: 15–121 ng/L PFOA range: 15–70 ng/L	Boulanger et al. [18]
PFOS, PFOA	Creek	Canada	PFOS range: n.d.–2210 ng/L PFOA range: n.d.–10.60 ng/L	Moody et al. [19]
PFOS, PFOA	Coast	China	PFOS range: 0.09–3.1 ng/L PFOA range: 0.73–5.5 ng/L	So et al. [20]
	Ocean	South Korea	PFOS range: 0.04–2.30 ng/L PFOA range: 0.24–11.0 ng/L	
	River	China	PFOS range: 0.02–12 ng/L PFOA range: 0.24–16 ng/L	

Chemicals	Source	Region	Findings	References
PFOS, PFOA	River	China	PFOS range: 0.90−99.0 ng/L PFOA range: 0.85−13.0 ng/L	So et al. [21]
PFOS, PFOA	River	Japan	PFOS range: 7.90−110 ng/L PFOA range: 5.12−10.0 ng/L	Senthilkumar et al. [22]
PFOS, PFOA	Surface water	Japan	PFOS range: 0.40−123 ng/L PFOA range: 26.00−29.9 ng/L	Lein et al. [23]
PFOS, PFOA	Freshwater	United states	PFOS range: n.d.−2.30 ng/L PFOA range: n.d.−116 ng/L	Schultz et al. [24]
PFOS, PFOA	Sewage effluent	Japan	PFOS range: 42−635 ng/L PFOA range: 10−68.0 ng/L	Murakami et al. [25]
PFOS, PFOA	Coast	China	PFOS range: 0.10−0.96 ng/L PFOA range: 0.27−2.12 ng/L	Ju et al. [26]
PFOS, PFOA	Ocean	South Korea	PFOS range: 0.04−2.53 ng/L PFOA range: 0.24−11.4 ng/L	Yamashita et al. [27]
		China	PFOS range: 0.01−9.68 ng/L PFOA range: 0.14−15.3 ng/L	
		Japan	PFOS range: 0.04−57.7 ng/L PFOA range: 0.14−192 ng/L	
PFOS, PFOA	Tap water	China	PFOS range: 0.24−0.30 ng/L PFOA range: 0.10−0.92 ng/L	Zhang et al. [28]
PFOS, PFOA	Tap water	China	PFOS mean: 7.60 ng/L PFOA mean: 78.0 ng/L	Mak et al. [29]
		Japan	PFOS mean: 1.60 ng/L PFOA mean: 18.0 ng/L	
PfPeA, PFHxA, PFHpA, PFOA, PFNA, PFDA, PFUnDA, PFBS, PFHxS, PFOS, PFDS, PFHxPA, PFOPA, PFDPA	Tap water	Sweden	Maximum concentrations were measured as 8.81, 6.18, 2.86, 2.50 ng/L for PFOS, PFOA, PFHxA, PFHxS respectively.	Ullah et al. [30]
		Italy	Maximum concentrations were measured as 6.92, 4.92, 2.10 ng/L for PFOS, PFOA, PFHxA respectively.	
		Belgium	Maximum concentrations were measured as 3.00, 2.94, 2.71, 2.70 ng/L for PFHxA, PFBS, PFOS, PFOA respectively.	
		Netherlands (Amsterdam University)	Maximum concentrations were measured as 8.56, 7.61, 3.06 ng/L for PFOA, PFBS, PFHxA respectively.	

Chemicals	Source	Region	Findings	References
		Netherlands (VU University)	Maximum concentrations were measured as 18.8, 5.66, 5.15, 2.69, 1.91 ng/L for PFBS, PFOA, PFHxA, PFPeA, PFHpA respectively.	
		Norway	Maximum concentrations were measured as 2.20 ng/L for PFOA.	
		Germany	Maximum concentrations were measured as 0.85 ng/L for PFOS.	
PFPeA, PFHxA, PFHpA, PFOA, PFNA, PFDA, PFBS, PFHxS, PFOS	Tap water	Greece	Maximum concentrations were measured as 5.9, 3.63 ng/L for PFPeA and PFOA respectively. PFOS range: <0.6 ng/L PFOA range: 0.8−3.63 ng/L	Zaffirini et al. [31]
		Netherlands	Maximum concentrations were measured as 19.8, 13.7, 11.1, 5.0, 4.9, 3.0, 2.3 ng/L for PFPeA, PFBS, PFOA, PFOS, PFHxA, PFHpA, PFHxS respectively. PFOS range: 3.0−5.0 ng/L PFOA range: 1.4−11.1 ng/L	
PFBA, PFPeA, PFHxA, PFHpA, PFOA, PFNA, PFDA, PFBS, PFHxS, PFOS	Tap water	Netherlands	Maximum concentrations were measured as 11, 10, 7.1, 5.9, 5.1, 3.2, 2.6 ng/L for PFBS, PFBA, PFOA, PFHxA, PFPeA, PFHpA, PFOS respectively. PFOS range: 1.1−2.6 ng/L PFOA range: 1.9−7.1 ng/L	Brandsma et al. [32]
PFHpA, PFOA, PFBS, PFHxS, PFOS	Tap water	United States	Maximum concentrations were measured as 108, 98.6, 11.7, 10.0, 6.0 ng/L for PFOA, PFOS, PFBS, PFHpA, PFHxS respectively. PFOS range: 1.9−98.6 ng/L PFOA range:2.5−108 ng/L	Dasu et al. [33]
PFBA, PFPeA, PFHxA, PFHpA, PFOA, PFNA, PFDA, PFBS, PFHxS, PFOS	Tap water	Turkey	Maximum concentrations in tap waters were measured as 2.90, 2.37, 2.18, 2.04, and 1.93 ng/L, for PFHxA, PFOA, PFHxS, PFOS, PFBA, respectively. PFOS range: 0.09−2.04 ng/L PFOA range: 0.10−2.37 ng/L	Ünlü Endirlik et al. [34]

Chemicals	Source	Region	Findings	References
PFHxA, PFHpA, PFOA, PFNA, PFDA, PFHxS, PFOS	Tap water	Spain	Maximum concentrations were measured as 6.28, 3.02 ng/L for PFOA and PFHpA respectively. PFOS range: 0.39−0.87 ng/L PFOA range: 0.32−6.28 ng/L	Ericson et al. [35]
PFHxA, PFHpA, PFOA, PFNA, PFDA, PFHxS, PFOS	Tap water	Spain	Maximum concentrations were measured as 58.21, 58.12, 57.43, 18.40, 10.00, 8.55, 5.30 ng/L for PFNA, PFOS, PFOA, PFHpA PFDA, PFHxA, PFHxS respectively. PFOS range: 0.12−58.12 ng/L PFOA range:0.85−57.43 ng/L	Ericson et al. [36]
PFBA, PFPeA, PFHxA, PFHpA, PFOA, PFNA, PFDA, PFBS, PFHxS, PFOS	Tap water	Faroe Islands	Maximum concentrations were measured as 0.610, 0.250, 0.220, 0.170 ng/L for PFOS, PFOA, PFHpA, PFNA respectively. PFOS range: 0.170−0.610 ng/L PFOA range: 0.230−0.250 ng/L	Eriksson et al. [37]
PFPeA, PFHxA, PFHpA, PFOA, PFDA, PFOS	Tap water	Ghana	Maximum concentrations were measured as 190, 168 ng/L for PFOA and PFOS respectively. PFOS range: 16.2−168 ng/L PFOA range: 66−190 ng/L	Essumang et al. [38]
PFBA, PFPeA, PFHxA, PFHpA, PFOA, PFNA, PFDA, PFBS, PFHxS, PFOS	Tap water	Sweden	Maximum concentrations were measured as 4.64, 2.92, 2.31, 2.15 ng/L for PFOS, PFBA, PFBS, PFHxS respectively. PFOS range: 0.03−4.64 ng/L PFOA range:0.07−1.50 ng/L	Filipovic and Berger [39]
PFPeA, PFHxA, PFHpA, PFOA, PFBS, PFOS	Tap water, river, surface waters	Germany	Maximum concentrations were measured as 519, 77, 56, 26, 23 22 ng/L for PFOA, PFPeA, PFHxA, PFBS, PFHpA, PFOS respectively. PFOS range: 3−22 ng/L PFOA range: 22−519 ng/L	Skutlarek et al. [40]
PFBA, PFPeA, PFHxA, PFHpA, PFOA, PFNA, PFDA, PFBS, PFHxS, PFOS	Tap water	Germany	Maximum concentrations were measured as 12.1, 6.4, 6.1, 5.8, 5.2, 4.7, 4.4 ng/L for PFHxS, PFHxA, PFOA, PFBS, PFPeA, PFOS, PFBA respectively. PFOS range: 1.0−4.7 ng/L PFOA range: 1.1−6.1 ng/L	Gellrich et al. [41]
PFOS, PFOA	Tap water	China	PFOS range: 0.1−14.8 ng/L PFOA range: 0.1−45.9 ng/L	Jin et al. [42]

Chemicals	Source	Region	Findings	References
PFBA, PFPeA, PFHxA, PFHpA, PFOA, PFNA, PFDA, PFBS, PFHxS, PFOS	Tap water	Burkina Faso	Maximum concentrations were measured as 3.85, 3.52, 1.89 ng/L for PFOS, PFBA, PFOA respectively. PFOS range: 0.12–3.85 ng/L PFOA range: 0.22–1.89 ng/L	Kaboré et al. [43]
		Ivory Coast	Maximum concentrations were measured as 1.32 ng/L for PFOS. PFOS range: 0.23–1.32 ng/L PFOA range: 0.30–0.35 ng/L	
PFHpA, PFOA, PFNA, PFDA, PFOS	Tap water	Italy	Maximum concentrations were measured as 9.7, 2.9 ng/L for PFOS and PFOA respectively. PFOS range: 6.2–9.7 ng/L PFOA range: 1.0–2.9 ng/L	Loos et al. [44]
PFBA, PFPeA, PFHxA, PFHpA, PFOA, PFNA, PFDA, PFBS, PFHxS, PFOS	Tap water	China	Maximum concentrations were measured as 115.4, 41.2, 29.0, 7.2, 6.9, 6.67, 5.6, 5.2 ng/L for PFOA PFHxA, PFBS, PFPeA, PFHxS, PFOS, PFBA, PFHpA respectively. PFOS range: 1.6–6.67 ng/L PFOA range: 5.6–115.4 ng/L	Lu et al. [45]
PFPeA, PFHxA, PFHpA, PFOA, PFNA, PFDA, PFBS, PFHxS, PFOS	Tap water	South Korea	Maximum concentrations were measured as 189.6, 27.7, 24.1, 17, 13.5, 5.74, 2.95, 1,78 ng/L for PFHxS, PFOA, PFHxA, PFPeA, PFHpA, PFBS, PFNA, PFOS respectively. PFOS range: 0.315–1.78 ng/L PFOA range: 0.75–27.7 ng/L	Park et al. [46]
PFBA, PFPeA, PFHxA, PFHpA, PFOA, PFNA, PFDA, PFBS, PFHxS	Tap water	Germany	Maximum concentrations were measured as 6.50 ng/L for PFOA. PFOA range: 22–519 ng/L	Shafique et al. [47]

Chemicals	Source	Region	Findings	References
PFHxA, PFHpA, PFOA, PFNA, PFDA, PFBS, PFHxS, PFOS	Tap water	Brazil	Maximum concentrations were measured as 46.75, 45.62, 43.83, 36.11, 19.65, 16.48, 15.90 ng/L for PFNA, PFOA, PFOS, PFHpA, PFDA, PFBS, PFHxA respectively. PFOS range: 4.58−43.83 ng/L PFOA range: 2.98−45.62 ng/L	Schwanz et al. [48]
		France	Maximum concentrations were measured as 32.87, 29.99, 17.55, 14.98, 11.87, 6.81 ng/L for PFHpA, PFOS, PFOA, PFBS, PFDA, PFHxA respectively. PFOS range: 11.99−29.99 ng/L PFOA range: 8.75−17.55 ng/L	
		Spain	Maximum concentrations were measured as 140.48, 58.21, 46.33, 41.58, 28.75, 24.99, 23.82 ng/L for PFOS, PFHxA, PFNA, PFHpA, PFOA, PFDA, PFBS respectively. PFOS range: 1.99−140.48 ng/L PFOA range: 3.85−28.75 ng/L	
PFHxA, PFHpA, PFOA, PFNA, PFDA	Tap water	Japan	Maximum concentrations were measured as25.55, 9.53, 7.03, 6.57, 2.50 ng/L for PFOA, PFHpA, PFNA, PFHxA, PFDA respectively. PFOA range: 6.17−25.55 ng/L	Shiwaku et al. [49]
PFOA, PFOS	Tap water	Japan	PFOS range: 0.16−22 ng/L PFOA range: 2.3−40 ng/L	Takagi et al. [50]
PFPeA, PFHxA, PFHpA, PFOA, PFBS, PFHxS, PFOS	Tap water	Australia	Maximum concentrations were measured as 15.6, 14.4, 9.66, 5.53, 4.23 ng/L for PFOS, PFHxS, PFOA, PFHxA, PFPeA respectively. PFOS range: 0.76−15.6 ng/L PFOA range: 0.54−9.66 ng/L	Thompson et al. [51]
PFOA	Tap water	Italy	PFOA range: 2−47 ng/L	Castiglioni et al. [52]
PFOS, PFOA	Rainwater	China	PFOS range: 9.92−113 ng/L PFOA range: 32.9−40.8 ng/L	Liu et al. [53]
	Snow		PFOS range: 10.8−138 ng/L PFOA range: 7.74−56.7 ng/L	

Removal/degradation of PFAs

Despite having many types of research for the occurrence of these materials, limited works have been reported for their removal. Active carbon adsorption, membrane filtration, and advanced oxidation processes are highly utilized techniques for their removal.

Adsorption

Liang et al. [54] observed sorption behaviors of PFOS in aqueous solutions using powdered activated carbon (PAC). PAC adsorptions were better than Ni/PAC for equilibrium concentrations. An increase in absorbance is related to PFOS concentration increase for lower concentrations (50–100 ppm). However, for higher concentrations (100–150 ppm) PAC adsorbance decreased with an increase of PFOS concentration. For Ni/PAC an opposite behavior was observed. As a result, it is determined that the occurrence of Ni decreases the adsorption capacity of PACs.

Qu et al. [55] observed removal of PFOA from aqueous solutions via PAC with batch experiments. With an increase of PAC concentration from 0,1 g/L to 10,0 g/L, the removal efficiency of PFOA increased from 51,1% to 99,9%.

Ochoa-Herrera and Sierra-Alvarez [56] examined the adsorption of PFOS, PFOA, and PFBS from aqueous solutions onto various commercial-grade granular activated carbon (GAC). For an equilibrium concentration of surfactant as 27 mg/L in aqueous phase adsorbed PFOA, PFBS, and PFOS concentrations measured as 57 mg/g GAC, 48 mg/g GAC, and 182 mg/g GAC respectively. Higher adsorptions of PFOS demonstrate the effect of chain lengths of long fluorocarbons and structures of functional groups on the sorption of anionic surfactants.

Hansen et al. [57] evaluated the adsorption of waters contaminated with PFCs onto PAC and GAC. PAC usually demonstrated a better performance according to GAC and sulfonates displayed more powerful sorption behavior than carboxylic acids. Results demonstrated that activated carbon is an efficient adsorption method for the removal of PFC from contaminated waters.

Yu et al. [58] investigated sorption behaviors of PFOS and PFOA onto commercial adsorbents including activated carbon and resin and evaluated the feasibility of these adsorbents' PFOS and PFOA removal from water. For the same equilibrium concentration sorption amounts of PFOS and PFOA for these adsorbents sorted from smallest to largest as GAC < Al400 < PAC vet GAC < PAC < Al400. The sorption rate is increased as the pH value is lowered. The highest PFOS sorption capacity of PAC was observed as 1,04 mmol/g and the highest PFOA sorption capacity of Al400 was observed as 2,92 mmol/g.

Deng et al. [59] investigated the effects of resin properties, solution pH, and rival anions on PFOS adsorption onto anion exchange resins. The highest values observe for polyacrylic resins at an equilibrium state. After that highest values were observed for microporous polystyrene resins and gel-type polystyrene resins respectively. PFOS sorption capacities of polyacrylic resins reached 4–5 mmol/g. Results demonstrated that anion exchange resins are efficient for the removal of PFOS from wastewaters.

Seneviratne et al. [60] investigated and compared PFOS sorption behaviors onto nonionic exchange adsorbents like activated carbon and commercial ionic exchange adsorbents at low equilibrium concentrations. Sorption capacities sorted from the largest to smallest as ion exchange polymers > nonionic exchange polymers > GAC for a 1 μg/L equilibrium concentration. Nonionic exchange polymers exhibit higher adsorption capacities for further lower equilibrium concentrations.

Chen et al. [61] investigated sorption behaviors of PFOS onto single-walled carbon nanotubes (SWCNT), multi-walled carbon nanotubes (MWCNT), and coal produced with the pyrolysis of corn starch and willow chips at 400 °C with limited oxygen conditions. Both CNTs and corn ash displayed high sorption capacities (<170 mg/g). This might have resulted from their lower BET surface area.

Liang et al. [54] observed PFOS sorption behaviors onto PAC-based adsorbents in aqueous solutions. For equilibrium concentration, PAC adsorption was better than Ni/PAC. With an increase of PFOS concentration adsorbance of PAC is decreased and the adsorbance of Ni/Pac is increased.

Wang et al. [62] investigated the adsorption behaviors of PFOS and PFOA onto aluminum oxide. Maximum adsorption capacities of PFOS and PFOA onto alumina were measured as 0,252 μg/L and 0,157 μg/L respectively. With an increase in pH adsorption onto alumina is lowered. This might be caused by the decrease in electrostatic interactions. Furthermore, as the ionic strength increased adsorption capacity is decreased.

Yu and Hu [63] observed the effect of effluent organic matter (Enform) on PFOS and PFOA adsorption onto PAC for low concentrations. Results demonstrated that EfOM lowers the adsorption capacity of PAC significantly.

Rattanaoudom et al. [64] investigated the effective removal of PFOS and PFOA. PAC and hydrotalcite exhibited more dan 97% removal efficiency of all adsorbents used. Results showed that pH affects the initial sorption rate.

Appleman et al. [65] compared GAC and nanofiltration techniques for removal of PFAAs including PFCAs and PFSAs from waters. Clean and plugged NF270 membranes achieved more than 93% removal efficiency for all conditions. GACs adsorption capacity decreased in the occurrence of resolved organic carbon.

Filtration

Steinle-Darling and Reinhard [66] researched the importance of membrane type, solvent size, pH, ionic strength, sorption, and occurrence of clogged layers for removal of 15 PFC species within four nanofiltration membranes. PFC removal for clean membranes was 93.3% and this value was 95.3% for clogged membranes. Removals for pH 2.8 were 70% and for pH 10 it is increased over 99%.

Tang et al. [67] investigated PFOS discrimination of reverse osmosis and nanofiltration and the effect of membrane properties and hydrodynamic conditions, furthermore mechanism of flow decrease during PFOS removal. While reverse osmosis membranes achieved over 99% PFOS removal, nanofiltrations membranes ranged between 90–99%. With a decrease in the flow (< 16%) longer filtration times were achieved, thus PFOS removal increased.

Schröder et al. [68] investigated PFS removal efficiencies of membrane bioreactors and tried to improve oxidation techniques for removal if permeates contain PFS. MBR processes achieved 75–81% PFOS and PFOA removal. With transformation-Fenton and phenomenon, 70% removal efficiency was achieved. Activated sludge, GAC or reverse osmosis achieved 77%, 99%, and 86% removal efficiencies respectively.

Advanced Oxidation

Magyar et al. [69] investigated the degradation efficiency of PFCs via ozonation and photocatalytic ozonation processes. With ozonation 50% PFOS removal and 10% PFOA removal were achieved. In the case of photocatalytic ozonation, 51% PFOS removal and 10% PFOA removal were achieved.

Huang et al. [70] researched photocatalytic ozonation of PFOAs. After 4 hours of reaction, 91% degradation efficiency was achieved. Defluorination efficiency was achieved as only up to 44,3%.

Lin et al. [71] researched pretreatment and ozonation capacities for the removal of PFOS and PFOA under alkali conditions. Without pretreatment with ozone removal efficiencies after 4 hours were 33% and 43% for PFOA and PFOS respectively. After a pretreatment removal efficiency increased to 90% and 85% respectively.

Dai et al. [72] observed removal efficiencies of PFAS for UV, ozonated air fractionation, air fractionation, and UV/ozone combination. While removal efficiency for air fractionation was 81%, it was 95% for ozonated air fractionation. The removal efficiency of PFAS was 17% for the only UV; on the other hand, it is increased to 73% with the combination of UV/ozone.

Franke et al. [73] researched the removal of PFASs via heterogeneously catalyzed ozonation. 98% PFAS removal efficiency achieved for all functional groups.

Li et al. [11] investigated PFOA degradation via photocatalysis, ozonation, and electrocatalysis by using r60/Boil nanocomposites as catalysts. After 3 hours 95,4% PFOA removal efficiency was achieved. In the case of photocatalytic ozonation and photo electro-peroxone process removal efficiencies are limited as 80,5% and 56,1% respectively.

Wu et al. [74] used ZnO nanorods as a catalyst for PFOA degradation. With just ozonation or UV254 irradiation removal efficiencies of PFOS were achieved as 9,5% and 18,2% respectively. In contrast with $ZnO/UV/O_3$ system 70,5% removal efficiency was achieved.

Thomas et al. [75] used alkali ozonation for PFAS removal from old production facilities groundwaters in Michigan. At acidic conditions after a pretreatment PFAS removal efficiency ranged between 75–97% by using alkali ozonation.

Results and Conclusion

At present, there are few analytical methods for PFCs, and these methods are not applicable for most water samples. Thus, most of the researchers are trying to create their own methods for analyses and this creates conflicts over results since there is not a generally accepted method. To prevent conflicts new methods must be created for each specific water type.

PFCs can be observed within all water samples across the world with high amounts of concentrations. Furthermore, these concentrations can also be seen in living tissues from wildlife and it is well known that PFCs are bioaccumulative.

PFCs concentrations may likely be associated with dense urban and industrial areas. This suggests that human and industrial activities may play a major role in the contribution of these materials.

Although there are lots of PFCs researched and found across the world, PFOS and PFOA are the most observed PFCs of all the PFCs. Furthermore, the highest concentrations of PFCs mostly measured for them. Since they are present highly in water sources, most of the studies for the removal of PFCs also conducted with these two PFCs.

PFCs can be formed by intermediate products as well. As a result, effluents (especially in wastewater) could contain more PFCs according to influents. This situation can also be explained by the sediment-water partition of PFCs. It is crucial to conduct further studies to illuminate the fate of PFCs.

PFCs have highly resistant characteristics, which makes their removal very difficult. These materials can't be removed via conventional treatment methods. Thus, advanced techniques must be utilized.

As can be seen from the literature PFCs removal can be achieved via adsorption, filtration, and advanced oxidation processes. The main factors affecting adsorption capacities must be further observed to find optimum conditions for removal processes.

By using a combination of techniques removal efficiencies can be increased to even higher levels. Thus, further experiments and researches must be conducted to find more efficient, feasible, cheap, and environmentally unharmful techniques.

Literature

[1] Giesy, J.P. and K. Kannan, *Global Distribution of Perfluorooctane Sulfonate in Wildlife.* Environ. Sci. Technol., 2001. 35: p. 1339–1342.

[2] Paul, A.G., K.C. Jones, and A.J. Sweetman, *A First Global Production, Emission, And Environmental Inventory For PFerfluorooctane Sulfonate.* Environ. Sci. Technol., 2009. 43: p. 386–392.

[3] Dinglasan, M.J.A., et al., *Fluorotelomer AlcoholBiodegradation Yields Poly- and Perfluorinated Acids.* Environ. Sci. Technol., 2004. 38: p. 2857–2864.

[4] Giesy, J.P. and K. Kannan, *Peer Reviewed: Perfluorochemical Surfactants in the Environment.* Environmental Science & Technology, 2002. 36(7): p. 146A–152A.

[5] Kissa, E. and E. Kissa, *Fluorinated surfactants and repellents.* 2001.

[6] Giesy, J.P., et al., *Aquatic toxicology of perfluorinated chemicals.* Rev Environ Contam Toxicol, 2010. 202: p. 1–52.

[7] Ahrens, L., *Polyfluoroalkyl compounds in the aquatic environment: a review of their occurrence and fate.* J Environ Monit, 2011. 13(1): p. 20–31.

[8] Yamashita, N., et al., *Analysis of Perfluorinated Acids at Parts-Per-Quadrillion Levels in Seawater Using Liquid Chromatography-Tandem Mass Spectrometry.* Environ. Sci. Technol., 2004. 38: p. 5522–5528.

[9] Hansen, K.J., et al., *Quantitative Characterization of Trace Levels of PFOS and PFOA in Tennessee River.* Environ. Sci. Technol., 2002. 36: p. 1681–1685.

[10] Monteleone, M., et al., *A rapid and sensitive assay of perfluorocarboxylic acids in aqueous matrices by headspace solid phase microextraction-gas chromatography-triple quadrupole mass spectrometry.* J Chromatogr A, 2012. 1251: p. 160–168.

[11] Li, Z., et al., *Highly efficient degradation of perfluorooctanoic acid: An integrated photo-electrocatalytic ozonation and mechanism study.* Chemical Engineering Journal, 2020. 391.

[12] Hu, Z., et al., *Determination of perfluoroalkyl carboxylic acids in environmental water samples by dispersive liquid–liquid microextraction with GC-MS analysis.* Journal of Liquid Chromatography & Related Technologies, 2020. 43(7–8): p. 282–290.

[13] Ji, Y., et al., *Simultaneous determination of seven perfluoroalkyl carboxylic acids in water samples by 2,3,4,5,6-pentafluorobenzyl bromide derivatization and gas chromatography-mass spectrometry.* Environ Pollut, 2020. 266(Pt 3): p. 115043.

[14] Saito, N., et al., *Perfluorooctane sulfonate concentrations in surface water in Japan.* Arch Environ Contam Toxicol, 2003. 45(2): p. 149–58.

[15] Taniyasu, S., et al., *A Survey of Perfluorooctane Sulfonate and Related Perfluorinated Organic Compounds in Water, Fish, Birds, and Human from Japan.* Environ. Sci. Technol., 2003. 37: p. 2634–2639.

[16] Naile, J.E., et al., *Perfluorinated compounds in water, sediment, soil and biota from estuarine and coastal areas of Korea.* Environ Pollut, 2010. 158(5): p. 1237–44.

[17] Rostkowski, P., et al., *Perfluorinated Compounds in Streams of the Shihwa Industrial Zone and Lake Shihwa, South Korea.* Environmental Toxicology and Chemistry, 2006. 25(9): p. 2374–2380.

[18] Boulanger, B., et al., *Detection of Perfluoroctane Surfactants in Great Lakes Water.* Environ. Sci. Technol., 2004. 38: p. 4064–4070.

[19] Moody, C.A., et al., *Monitoring Perfluorinated Surfactants in Biota and Surface Water Samples Following an Accidental Release of Fire-Fighting Foam into Etobicoke Creek. pdf>.* Environ. Sci. Technol., 2001. 36: p. 545–551.

[20] So, M.K., et al., *Perfluorinated Compounds in Coastal Waters of Hong Kong, South Chine and Korea.* Environmental Science & Technology, 2004. 38(15): p. 4056–4063.

[21] So, M.K., et al., *Perfluorinated compounds in the Pearl River and Yangtze River of China.* Chemosphere, 2007. 68(11): p. 2085–95.

[22] Senthilkumar, K., et al., *Perfluorinated compounds in river water, river sediment, market fish, and wildlife samples from Japan.* Bull Environ Contam Toxicol, 2007. 79(4): p. 427–31.

[23] Lein, N.P.H., et al., *Contamination of perfluorooctane sulfonate (PFOS) and perfluorooctanoate (PFOA) in surface water of the Yodo River basin (Japan).* Desalination, 2008. 226(1–3): p. 338–347.

[24] Schultz, M.M., D.F. Barofsky, and J.A. Field, *Quantitative Determination of Fluorotelomer Sulfonates in Groundwater by LC MS/MS.* Environ. Sci. Technol., 2004. 38: p. 1828–1835.

[25] Murakami, M., et al., *Occurence and Sources of Perfluorinated Surfactants in Rivers in Japan.* Environ. Sci. Technol., 2008. 42: p. 6566–6572.

[26] Ju, X., et al., *Perfluorinated Surfactants in Surface, Subsurface Water and Microlayer from Dalian Coastal Wasters in China.* Environ. Sci. Technol., 2008. 42: p. 3538–3542.

[27] Yamashita, N., et al., *A global survey of perfluorinated acids in oceans.* Mar Pollut Bull, 2005. 51(8–12): p. 658–68.

[28] Zhang, Q., et al., *Removal of perfluorooctane sulfonate from aqueous solution by crosslinked chitosan beads: sorption kinetics and uptake mechanism.* Bioresour Technol, 2011. 102(3): p. 2265–71.

[29] Mak, Y.L., et al., *Perfluorinated Compounds in Tap Water from China and Several Other Countries.* Environ. Sci. Technol., 2009. 43: p. 4824–4829.

[30] Ullah, S., T. Alsberg, and U. Berger, *Simultaneous determination of perfluoroalkyl phosphonates, carboxylates, and sulfonates in drinking water.* J Chromatogr A, 2011. 1218(37): p. 6388–95.

[31] Zafeiraki, E., et al., *Determination of perfluoroalkylated substances (PFASs) in drinking water from the Netherlands and Greece.* Food Addit Contam Part A Chem Anal Control Expo Risk Assess, 2015. 32(12): p. 2048–57.

[32] Brandsma, S.H., et al., *The PFOA substitute GenX detected in the environment near a fluoropolymer manufacturing plant in the Netherlands.* Chemosphere, 2019. 220: p. 493–500.

[33] Dasu, K., et al., *An ultra-sensitive method for the analysis of perfluorinated alkyl acids in drinking water using a column switching high-performance liquid chromatography tandem mass spectrometry.* Journal of Chromatography A, 2017. 1494: p. 46–54.

[34] Ünlü Endirlik, B., et al., *Assessment of perfluoroalkyl substances levels in tap and bottled water samples from Turkey.* Chemosphere, 2019. 235: p. 1162–1171.

[35] Ericson, I., et al., *Levels of perfluorochemicals in water samples from Catalonia, Spain: is drinking water a significant contribution to human exposure?* Environmental Science and Pollution Research, 2008. 15(7): p. 614–619.

[36] Ericson, I., et al., *Levels of Perfluorinated Chemicals in Municipal Drinking Water from Catalonia, Spain: Public Health Implications.* Archives of Environmental Contamination and Toxicology, 2009. 57(4): p. 631–638.

[37] Eriksson, U., et al., *Perfluoroalkyl substances (PFASs) in food and water from Faroe Islands.* Environmental Science and Pollution Research, 2013. 20(11): p. 7940–7948.

[38] Essumang, D.K., et al., *Perfluoroalkyl acids (PFAAs) in the Pra and Kakum River basins and associated tap water in Ghana.* Science of The Total Environment, 2017. 579: p. 729–735.

[39] Filipovic, M. and U. Berger, *Are perfluoroalkyl acids in waste water treatment plant effluents the result of primary emissions from the technosphere or of environmental recirculation?* Chemosphere, 2015. 129: p. 74–80.

[40] Skutlarek, D., M. Exner, and H. Farber, *Perfluorinated surfactants in surface and drinking waters.* Environ Sci Pollut Res Int, 2006. 13(5): p. 299–307.

[41] Gellrich, V., H. Brunn, and T. Stahl, *Perfluoroalkyl and polyfluoroalkyl substances (PFASs) in mineral water and tap water.* Journal of Environmental Science and Health, Part A, 2013. 48(2): p. 129–135.

[42] Jin, Y.H., et al., *PFOS and PFOA in environmental and tap water in China.* Chemosphere, 2009. 77(5): p. 605–611.

[43] Kaboré, H.A., et al., *Worldwide drinking water occurrence and levels of newly-identified perfluoroalkyl and polyfluoroalkyl substances.* Science of The Total Environment, 2018. 616–617: p. 1089–1100.

[44] Loos, R., et al., *Polar herbicides, pharmaceutical products, perfluorooctanesulfonate (PFOS), perfluorooctanoate (PFOA), and nonylphenol and its carboxylates and ethoxylates in surface and tap waters around Lake Maggiore in Northern Italy.* Analytical and Bioanalytical Chemistry, 2007. 387(4): p. 1469–1478.

[45] Lu, G.-H., et al., *Perfluoroalkyl acids in surface waters and tapwater in the Qiantang River watershed—Influences from paper, textile, and leather industries.* Chemosphere, 2017. 185: p. 610–617.

[46] Park, H., et al., *Evaluation of the current contamination status of PFASs and OPFRs in South Korean tap water associated with its origin.* Science of The Total Environment, 2018. 634: p. 1505–1512.

[47] Shafique, U., et al., *Perfluoroalkyl acids in aqueous samples from Germany and Kenya.* Environmental Science and Pollution Research, 2017. 24(12): p. 11031–11043.

[48] Schwanz, T.G., et al., *Perfluoroalkyl substances assessment in drinking waters from Brazil, France and Spain.* Science of The Total Environment, 2016. 539: p. 143–152.

[49] Shiwaku, Y., et al., *Spatial and temporal trends in perfluorooctanoic and perfluorohexanoic acid in well, surface, and tap water around a fluoropolymer plant in Osaka, Japan.* Chemosphere, 2016. 164: p. 603–610.

[50] Takagi, S., et al., *Perfluorooctanesulfonate and perfluorooctanoate in raw and treated tap water from Osaka, Japan.* Chemosphere, 2008. 72(10): p. 1409–1412.

[51] Thompson, J., G. Eaglesham, and J. Mueller, *Concentrations of PFOS, PFOA and other perfluorinated alkyl acids in Australian drinking water.* Chemosphere, 2011. 83(10): p. 1320–1325.

[52] Castiglioni, S., et al., *Sources and fate of perfluorinated compounds in the aqueous environment and in drinking water of a highly urbanized and industrialized area in Italy.* Journal of Hazardous Materials, 2015. 282: p. 51–60.

[53] Liu, W., et al., *Perfluorosulfonates and perfluorocarboxylates in snow and rain in Dalian, China.* Environ Int, 2009. 35(4): p. 737–42.

[54] Liang, X., et al., *Facile preparation of magnetic separable powdered-activated-carbon/ Ni adsorbent and its application in removal of perfluorooctane sulfonate (PFOS) from aqueous solution.* J Environ Sci Health A Tox Hazard Subst Environ Eng, 2011. 46(13): p. 1482–90.

[55] Qu, Y., et al., *Equilibrium and kinetics study on the adsorption of perfluorooctanoic acid from aqueous solution onto powdered activated carbon.* J Hazard Mater, 2009. 169(1–3): p. 146–52.

[56] Ochoa-Herrera, V. and R. Sierra-Alvarez, *Removal of perfluorinated surfactants by sorption onto granular activated carbon, zeolite and sludge.* Chemosphere, 2008. 72(10): p. 1588–1593.

[57] Hansen, M.C., et al., *Sorption of perfluorinated compounds from contaminated water to activated carbon.* Journal of Soils and Sediments, 2010. 10(2): p. 179–185.

[58] Yu, Q., et al., *Sorption of perfluorooctane sulfonate and perfluorooctanoate on activated carbons and resin: Kinetic and isotherm study.* Water Res, 2009. 43(4): p. 1150–8.

[59] Deng, S., et al., *Removal of perfluorooctane sulfonate from wastewater by anion exchange resins: effects of resin properties and solution chemistry.* Water Res, 2010. 44(18): p. 5188–95.

[60] Senevirathna, S.T., et al., *A comparative study of adsorption of perfluorooctane sulfonate (PFOS) onto granular activated carbon, ion-exchange polymers and non-ion-exchange polymers.* Chemosphere, 2010. 80(6): p. 647–51.

[61] Chen, X., et al., *A comparative study on sorption of perfluorooctane sulfonate (PFOS) by chars, ash and carbon nanotubes.* Chemosphere, 2011. 83(10): p. 1313–9.

[62] Wang, F. and K. Shih, *Adsorption of perfluorooctanesulfonate (PFOS) and perfluorooctanoate (PFOA) on alumina: influence of solution pH and cations.* Water Res, 2011. 45(9): p. 2925–30.

[63] Yu, J. and J. Hu, *Adsorption of Perfluorinated Compounds onto Activated Carbon and Activated Sludge.* Journal of Environmental Engineering, 2011. 137(10): p. 945–951.

[64] Rattanaoudom, R., C. Visvanathan, and S.K. Boontanon, *Removal of Concentrated PFOS and PFOA in Synthetic Industrial Wastewater by Powder Activated Carbon and Hydrotalcite.* Journal of Water Sustainability, 2012. 2(4): p. 245–258.

[65] Appleman, T.D., et al., *Nanofiltration and granular activated carbon treatment of perfluoroalkyl acids.* Journal of Hazardous Materials, 2013. 260: p. 740–746.

[66] Steinle-Darling, E. and M. Reinhard, *Nanofiltration for Trace Organic Contaminant Removal: Structure, Solution, and Membrane Fouling Effects on the Rejection of Perfluorochemicals.* Environ. Sci. Technol., 2008. 42: p. 5292–5297.

[67] Tang, C.Y., et al., *Effect of solution chemistry on the adsorption of perfluorooctane sulfonate onto mineral surfaces.* Water Res, 2010. 44(8): p. 2654–62.

[68] Schroder, H.F., et al., *Biological wastewater treatment followed by physicochemical treatment for the removal of fluorinated surfactants.* Water Sci Technol, 2010. 61(12): p. 3208–15.

[69] Mahyar, A., et al., *Development and Application of Different Non-thermal Plasma Reactors for the Removal of Perfluorosurfactants in Water: A Comparative Study.* Plasma Chemistry and Plasma Processing, 2019. 39(3): p. 531–544.

[70] Huang, J., et al., *Efficient degradation of perfluorooctanoic acid (PFOA) by photocatalytic ozonation.* Chemical Engineering Journal, 2016. 296: p. 329–334.

[71] Lin, A.Y., et al., *Removal of perfluorooctanoic acid and perfluorooctane sulfonate via ozonation under alkaline condition.* J Hazard Mater, 2012. 243: p. 272–7.

[72] Dai, X., et al., *Comparative study of PFAS treatment by UV, UV/ozone, and fractionations with air and ozonated air.* Environmental Science: Water Research & Technology, 2019. 5(11): p. 1897–1907.

[73] Franke, V., et al., *Removal of per- and polyfluoroalkyl substances (PFASs) from tap water using heterogeneously catalyzed ozonation.* Environmental Science: Water Research & Technology, 2019. 5(11): p. 1887–1896.

[74] Wu, D., et al., *Mechanism insight of PFOA degradation by ZnO assisted-photocatalytic ozonation: Efficiency and intermediates.* Chemosphere, 2017. 180: p. 247–252.

[75] Thomas, R., et al., *Evaluation of PFAS treatment technology: Alkaline ozonation.* Remediation Journal, 2020. 30(3): p. 27–37.

Comparison of Energy Performance of existing building with adoption of Nearly Zero Energy Building concept in Rural area of Bhutan

Abstract: Climate is changing very fast today and this is not natural. We are experiencing the impact of the climate change in many aspects. It is also expected to impact the performance of buildings badly in due course of time. In the recent years, many countries started investing to evaluate energy performances of the buildings and opting for the best suited energy-saving measures. However, this concept may be new in the context of Bhutan. But the expectation of author is that this new concept may revolutionize the building construction sectors in Bhutan.

Many studies shows that Buildings are one of the world's largest consumer of energy and on the other hand strategies are available to reduce the energy consumption. The strategies can be applied right from the design phases for the new buildings and retrofits for the old buildings. In-order to apply the best strategies of energy consumption reduction and to understand building energy consumption pattern, needs to carry out energy performance of the buildings.

Therefore, one of the single-story residential building located in Dewathang is chosen as model building for study purpose. The simulation is carried out using OpenStudio and support by sketchup and the results are discussed under result discussion.

Introduction

Bhutan is a small country located between two giant countries, China to the North and India to East, South and West. With the rapid economic growth in the recent years, the living standards of people in Bhutan also keeps increasing. The higher standards of living have resulted in a significant increase in energy consumption from the residential sector, and this trend is expected to continue into the future. Many new buildings being constructed in this era do not perform well as they could be with today's technology in energy efficiency.
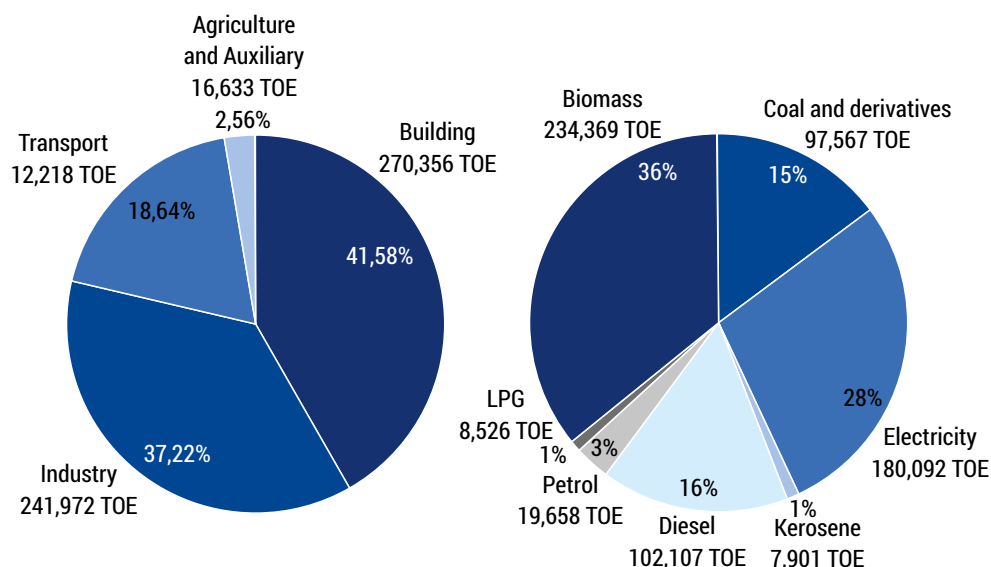

FIGURE 1: **Energy consumption and Sectoral break-up and fuel mix (source: Bhutan energy data directory 2015)**

The building sector contributes to 42% of the total energy consumption (Power data 2014). Bhutan's population is 62.2% rural and 37.8% urban (Kuensel, June 26, 2018) and 100% household in the country have access to electricity. The electricity is the main source of energy next to fuel wood. Electricity is solely produced from hydro power plants and as of now no fossil fuel powered generating power station in Bhutan. Energy consumption in the building sector amounts to 270,356 TOE in 2014 with the Residential segment consuming 213,422 TOE of energy and Commercial & Institutional segment consuming 56,934 TOE of energy. While the thermal energy consumption in buildings stands at 242,916 TOE, the electrical energy consumption is 27,440 TOE for the year 2014 [9] and also shown in Figure 1. The main contributing factor for consumption of energy in building/residential sector is space heating in colder regions and space cooling in warmer regions of the country. The daily

electricity load curve of Thimphu (capital city) and Phuentsholing located in colder and warmer regions respectively as shown in the Figure 2 and 3 clearly depicts the energy consumption based on winter and summer seasons [5].
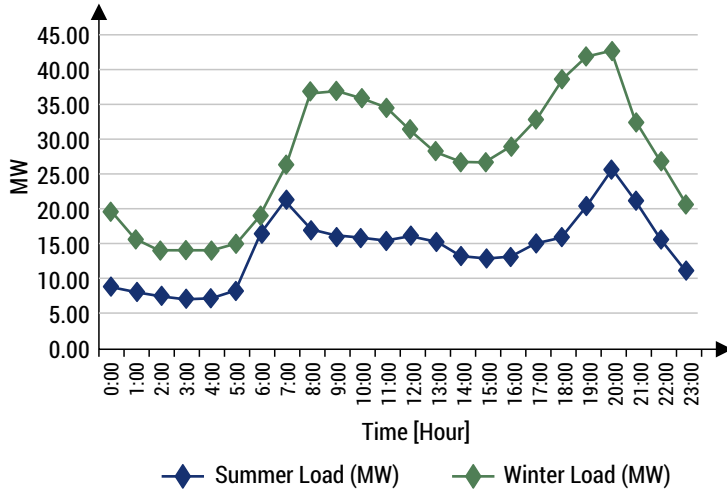
FIGURE 2: **Thimphu daily load curve (source BPC Power data 2014)**
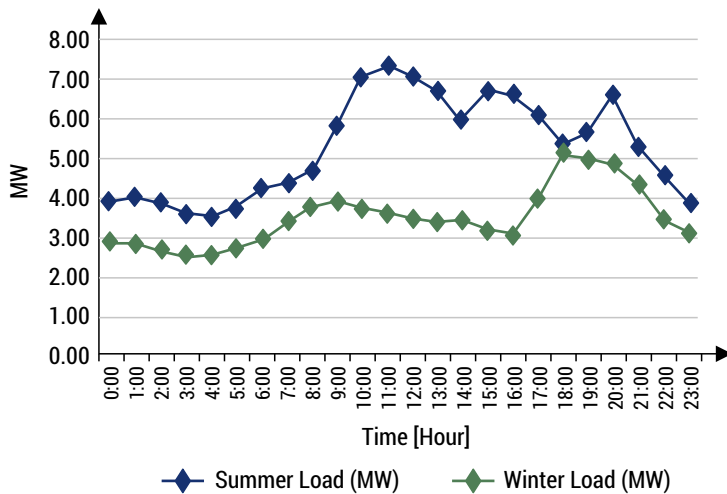
FIGURE 3: **Phuentsholing daily load curve (source BPC power data 2014)**

The known fact is that urban areas are the major contributors to consumption of energy while comparing to rural areas. Fortunately, 100% households in Bhutan are connected to grid and there is drastic increase in domestic consumption. In-order to reduce the domestic consumption, one of the best possible solution could be to have

an energy efficient building even in rural areas. The implementation of energy efficient building concepts even in rural areas may help in reducing the peak demand pressure on the power grid. Moreover, very limited literatures on energy efficiency buildings in Bhutan are available. Therefore, the main intend of this research is to understand the nZEB concept and apply the concept to improve the building thermal conditions for dwellers in the rural areas.

Materials and Methods

The main intend of this research is to start realization of nZEB concept in rural areas, since the college where the author is employed is also located in one of the remote areas of Bhutan.

Location and climatic conditions

Dewathang is a small town located under Samdrup Jongkhar district with GPS coordinates of 26.8541° N, 91.4580° E at an altitude of 1000 m above the msl.

TABLE 1: climatic information of Dewathang

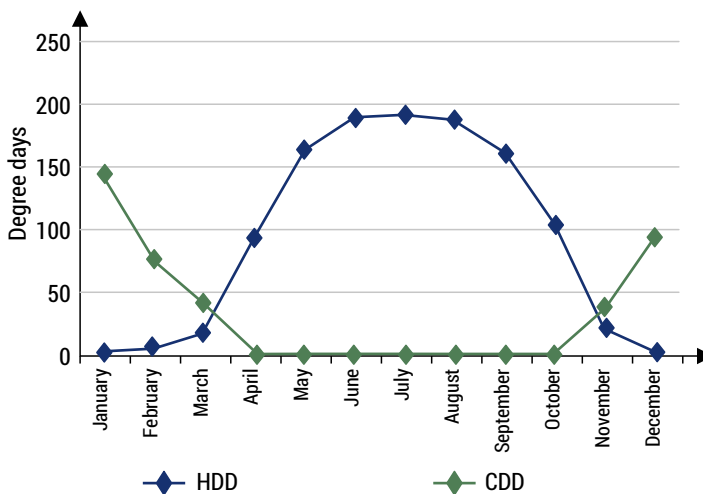| Altitude (m)	Mean Temperature (°C)	Global horizontal radiation (kJ/hr. m²)	Direct normal radiation (kJ/hr. m²)	Diffuse radiation (kJ/hr. m²)	Wind speed (m/s)	Relative humidity (%)
1000	22.03	633.43	574.57	283.47	1.86	82.38

FIGURE 4: Heating degree days and cooling degree days

The temperature varies from 15^{0}C to 34^{0}C with hot humid climate and it falls under subtropical climatic zone as mention in the Bhutan Building energy efficiency study report. The climatic information of the location as shown in table 1 and figure 4.

Model Building descriptions

The building used as model for the energy simulation is located inside Jigme Namgyel Engineering college campus under Dewathang municipality. It is a single-story residential building with the floor area of 130 m^2 and floor to roof height of 3.5 m. The indoor layout as follow: 3 bed rooms, 1 living room, 1 kitchen, 1 study room and 2 toilets as shown in the figure 5 and 6.

Building has a fairly standard construction with light weight 100–150 mm concrete floor slabs and enclosed by burnt clay brick wall of 250 mm. All the wall surfaces are plastered on both sides. The internal partition erected with brick wall of 125 mm. The building is of frame structure with reinforced concrete beams and columns. The 4 mm single clear glass is used on all the windows. No mechanical equipment was found in the building except electrical fan for cooling.
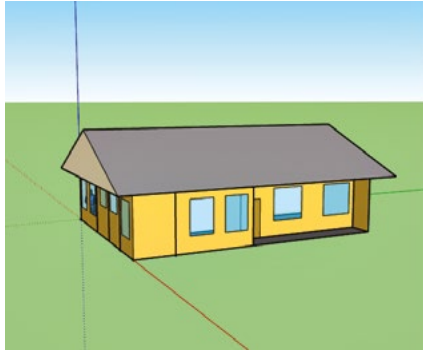
FIGURE 5: **Model building**
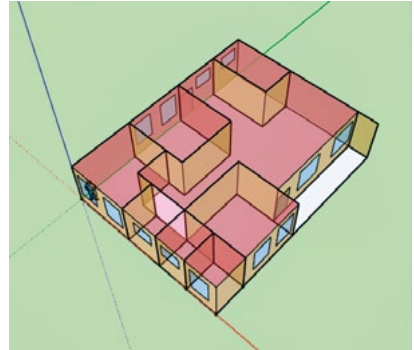
Figure 6: Internal layout

The details of building envelop, windows and glazing are provided in tables 2 and 3.

TABLE 2. **Construction materials and specifications**

Components	Thickness (m)	Density (kg/m^3)	Specific heat (J/kg.K)	Conductivity (W/m.K)	U-value (W/m^2.K)
Wall (Clay bricks)	0.25	1992	837	0.727	6.7
Cement plaster	0.025	1860	800	0.60	12.5
Concrete (floor)	0.10	1282	837	0.6	3.9
Plywood	0.127	560	2500	0.15	1.6

TABLE 3. Glazing

Glazing type	Thickness (mm)	Total Solar Transmission (SHGC)	U-value (W/m².K)
Single clear	5	0.83	5.88

Results and Discussion

The results obtained from the simulation are presented in the subsequence sections. The discussion will mainly focus on the energy required for cooling, since the energy required for cooling is almost 80% of the total energy required by the building. From figure 4, one can also understand the energy demanded by the building is mainly for cooling.

Simulation result of the existing building

From the simulation result as shown in figure 6, the maximum energy required for cooling is 1047.87 kWh in the month of August, where as minimum is 2.47 kWh in the month of January. For heating, maximum energy required is 961.62 kWh in the month of January and zero during summer months. The simulation is carried out purely based on the existing model building conditions.
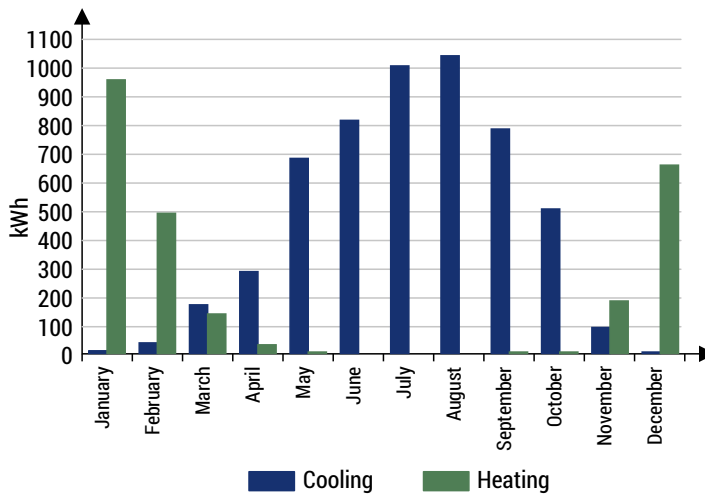
FIGURE 6: cooling & heating energy demand(simulation result)

The main supply of energy to the building is only electricity and the figure 7 shows the monthly electricity bill. The monthly electricity bill is the average of year 2017–2020. The maximum electrical energy consumed is 325.67 kWh and minimum is 230.67 kWh.
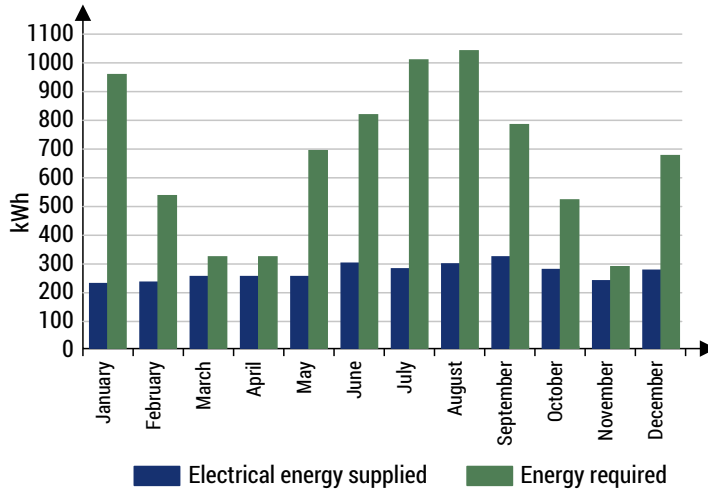
FIGURE 8: **Total energy required and electrical energy supplied/consumed**

Performance evaluation

The simulation was carried out to evaluate the performances of the building by adopting few methods and technologies in reducing the energy requried by the building. The focus is on the reduction of cooling energy, since almost 80% of energy required for the building is for cooling during summer. The simulation result as shown in figure 9.
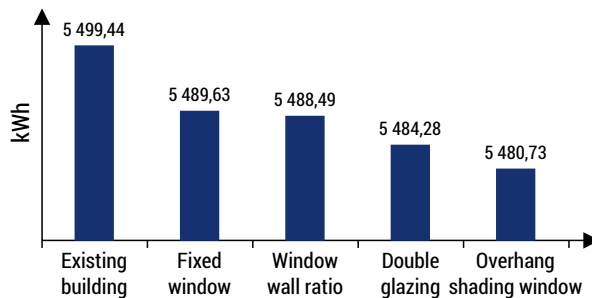
FIGURE 9: **Energy performance summery**

Figure 9 shows that there is reduction of energy required by building for cooling from 10–19 kWh by a adopting few energy saving measures like Fixed window, window wall ratio, double glazing and overhang shading window. The maximum energy saving can be achieved by having overhaing shading in the Dewathang location.

Conclusion

Globally residential sectors are characterized by highest consumption of energy. Though the contribution from rural communities on total energy consumption may not be noticable. This research also spins over the building energy modeling and energy consumption in rural area. Therefore, from this research the way forward is that there should be a policy for adopting energy saving measures in the rural communities. Since rural communities will have distinct in their energy use, econimic drivers and demographics. May be for Bhutan, it is on time to deliver high-quality efficiency programs to rural people on energy saving meaures. As a finding from this research, there is huge scope in reducing the energy consumption in rural communities by adopting simple energy saving measures. With the add on simple energy saving measures will not scal up the construction cost but definitely save the energy consumption as well as improve the living thermal comfort and may enjoy the benefit from enery saving in long run.

Finally, to achieve global sustainable future, the policy maker and governmental organization should focus more public attention on behavioral changes in addition to other investment measures of energy efficiency.

Literature

[1]   Ascione, F. (brak daty). *Energy Performance of Buildings: Low Energy Heating and Cooling in European Climates*. Università degli Studi di Napoli Federico II, Scuola di Dottorato in Ingegneria Industriale.

[2]   Change, D. o. (June 2013). *National Energy Efficiency data – Framework*.

[3]   Department of Energy, B. (2009). *Overview of Energy policies of Bhutan*.

[4]   Department of Engineering Services, M. (2013). *Bhutan Green Building Guidelines*.

[5]   Energy, D. o. (2015). *Bhutan Energy data directory*. Thimphu.

[6]   Laustsen, M. J. (2008). *Energy Efficiency Requirements in Building Codes, Energy Efficiency Policies for New Buildings*. International Energy Agency (IEA).

[7]   Lhendup, S. L. (2017). Performance simulation of Residential Building envelope with real environment in Thimphu, The capital city of Bhutan. *International Journal of Science and Research* (IJSR), 391–395.

[8]   Paul Gilman, C. (2009). *Potential for Development of Solar and Wind Resource in Bhutan*. National Renewable Energy Laboratory.

[9]   Power Corporation of Bhutan. (2014). *Power data book*.

[10]   Tshewang Lhendup* and Pema Lhamo, m. I. (2015). System Design and Performance Analysis of a Grid-Tied Solar PV Power System in Bhutan. *2015 IEEE International Conference on Computational Intelligence & Communication Technology.*

[11]   Tshewang Lhendup*, S. L. (2010). Domestic energy consumption patterns in urban Bhutan. *Energy for Sustainable Development.*

Smoke parameters obtained from the cone calorimeter method and the single-Chamber test

Abstract: Smoke generated in the combustion process of plastics reduces the visibility and contains toxic products causing severe health problems for society. It may be hazardous to both people and the environment. Therefore, the awareness of smoke specification is important. This paper presents two most common small-scale methods for measuring smoke parameters. The cone calorimeter method and single-chamber test respectively standardized by ISO 5660 and PN-EN ISO 5659-2 were reviewed. Fundamentals of these methods and measurement techniques were described. Diverse smoke parameters obtained from these methods were collected and specified. Attention was also drawn to the relevance of these parameters to standard requirements for various industry fields such as rail transport or shipbuilding.

Introduction

Plastics are very common and versatile materials. Their global production reaches 300 million tons annually. Plastics have many advantages such as longevity, degradation resistance, inertness, ease of forming and low production cost therefore they play an important role in everyday use [1].

Unfortunately, plastics are readily combustible in fire conditions and their combustion process generates smoke and toxic products which may have a negative impact on people and the environment [2].

Smoke consists of gases, vapors and particulates specifically microdroplets formed from condensed organic vapors as well as soot from carbonaceous agglomerated structures [3]. Beside generating toxic gases smoke shows an incapacitating effect by reducing visibility which cause failures in escaping from fire [4].

Thereupon analysis of smoke parameters is crucial for providing fire safety. This paper describes two most common small-scale methods for measuring smoke parameters: cone calorimeter method and single-chamber test. Smoke parameters obtained from these methods have been specified and their usage in rail transport and shipbuilding have been presented.

Cone calorimeter method

This method is very common in the field on fire testing. It can be conducted in accordance with ISO 5660 or ASTM E1354. Cone calorimeter measures mass loss rate, emissions and heat release rate (HRR) at the same time. The measurement of HRR is based on the principle that a gram of oxygen consumed during combustion generates 13,1 MJ of heat released [5]. The Thornton's rule is true for most organic gas, liquid and solid fuels. It constitutes the basis for Oxygen Consumption Calorimetry [6]. Smoke measurement is based on the Bouguer's law, which describes the attenuation of a beam light in combustion products [7]. The equation is given below.

$$\frac{I}{I_0} = \exp(-k \cdot L)$$

where $I[-]$ and $I_0[-]$ are respectively overall light intensity and initial overall light intensity, $k[\mathrm{m}^{-1}]$ is the extinction coefficient and $L[\mathrm{m}]$ is the length of the light beam [8].

The measuring device is presented in Figure 1.

The earliest devices were developed in the 1950's. Their structure was slightly different, for example there were burners instead of electrical heaters, which caused more problems. In the 1970's the original calorimeter from National Bureau of Standards (NBS) was assembled [9].

Cone calorimeter tests provide data about combustion and pyrolysis conditions and behavior of materials burned under well-ventilated conditions. The specimen size is 100 mm x 100 mm and it is a small sample in fire engineering, but it is one of the biggest in polymer analysis. Thereupon cone calorimeter is a linking device between these fields of study [10].
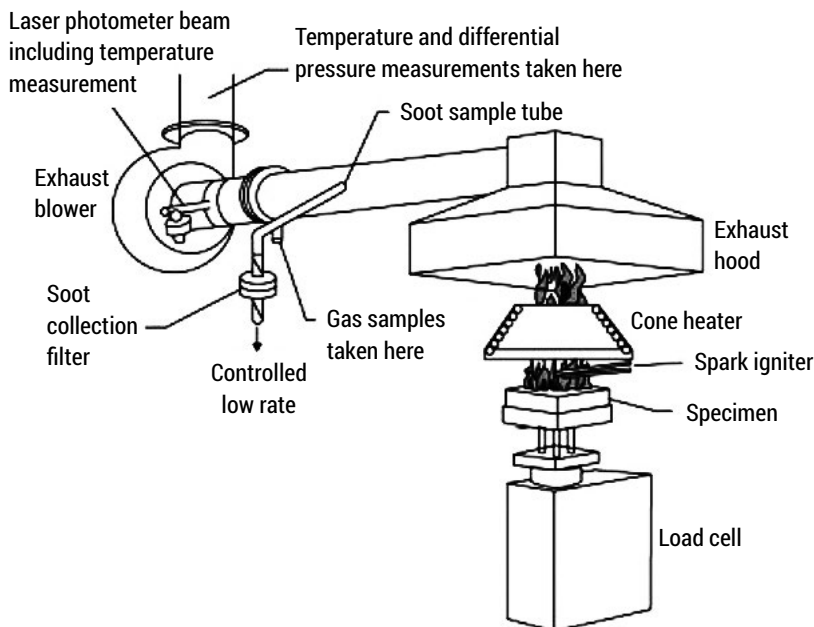
FIG. 1. A scheme of a cone calorimeter
SOURCE: [6]

Sample thickness cannot exceed 50 mm. Before tests specimens must be conditioned to constant weight at temperature of 23±2°C and relative humidity of 50±5%.

Metal sample holders with open or close edges can be used, whereby the second type is used mostly. A sample holder after putting in a specimen is placed on the load cell. Above there is a cone heater in the shape of truncated cone. Between them there is placed a spark igniter, which ignites flammable combustion products. To protect sample area and give an extra time to operator before the test, shutter mechanisms are used. They are linked by lever with the igniter, which is moved away after ignition.

Exhaust hood located above the heater collects gaseous combustion products. The flow rate is set by an exhaust blower mounted in the flue gas duct. Before the fan there are also a smoke measurement system based on absorption of a laser beam and a gas sampling ring transferring samples through two filters, a cold trap and a drying agent to gas analysis unit [9, 11].

The measurement can be held at various irradiance levels up to 75 kW/m². The heat flux is important because it has a significant impact on test results. Research show longer ignition times, lower HRR and THR (Total Heat Released) for higher irradiance for most materials [12].

The most significant factor in predicting fire hazard is HRR. It is used in simple risk assessments as well as in advanced numerical modelling. In the cone calorimeter HRR is measured by means of oxygen consumption, but it is possible to use temperature rise, mass loss or species production also [13]. The equation for calculating HRR is as follows:

$$\dot{q}(t) = \left(\frac{\Delta h_c}{r_0}\right)(1,10)C\sqrt{\frac{\Delta p}{T_e}}\left(\frac{x_{O_2}^0 - x_{O_2}}{1,105 - 1,5x_{O_2}}\right)$$

where $\dot{q}(t)$ is the heat release rate, Δh_c the net heat of combustion, r_0 is the stechiometric oxygen to fuel mass ratio, C is constant related to calibration, Δp is the orifice flow meter pressure differential, T_e is the absolute temperature of gas at the orifice flow meter and the x_{O_2} and $x_{O_2}^0$ are the oxygen analyzer readings, where 0 refers to initial conditions [14].

Some indices like FIGRA (FIre Growth RAte) or MARHE (Maximum Average Rate of Heat Emission) simplifying the interpretation of cone calorimeter data base on the maximum HRR [15]. Equations for average heat of emission $ARHE\left[\dfrac{\text{kW}}{\text{m}^2}\right]$ and $FIGRA\left[\dfrac{\text{kW}}{\text{m}^2\text{s}}\right]$ are as follows [16]:

$$ARHE(t) = \frac{\sum_{t_i}^{t_{end}}\dfrac{\left(HRR(t) + HRR(t-1)\right)}{2}}{t - t_i} \cdot \Delta t$$

$$FIGRA = max\frac{\dfrac{HRR(t-1) + HRR(t) + HRR(t+1)}{3}}{t - t_i}$$

where $\Delta t\,[\text{s}]$ is the smallest time interval, $t\,[\text{s}]$ is time, $t_i\,[\text{s}]$ is the ignition time, $HRR(t-1), HRR(t), HRR(t+1)\left[\dfrac{\text{kW}}{\text{m}^2}\right]$ are HRR values measured at different interval time.

Smoke production rate (SPR) and total smoke production (TSP) are the basic smoke parameters measured by cone calorimeter. $SPR\left[\dfrac{\text{m}^2}{\text{s}}\right]$ may be expressed as:

$$SPR = k \cdot V_f$$

where $k\left[\mathrm{m^{-1}}\right]$ is an extinction coefficient and $V_f\left[\dfrac{\mathrm{m^3}}{\mathrm{s}}\right]$ is the volume flow rate through the duct. This measurement is not related to specimen's mass. SPR may also be conducted with exposed specimen area if it is known. Then $\left[\dfrac{\mathrm{m^3}}{\mathrm{m^2/s}}\right]$ or $\left[\dfrac{1}{\mathrm{s}}\right]$ units are used [17]. An index dependent on SPR is $SMOGRA\left[\dfrac{\mathrm{m^2}}{\mathrm{s^2}}\right]$ defined as the maximum value of the ratio of SPR to time when it was measured [18].

SPR varies in periods of time. Thus the $TSP\left[\mathrm{m^2}\right]$ or $\left[\dfrac{\mathrm{m^3}}{\mathrm{m}}\right]$ is also an important parameter for comparison of materials. Total smoke production may be expressed as:

$$TSP = \int SPR(t)\,dt$$

where t is time. Summation is carried out until the end of the test. TSP may also be expressed per exposed specimen area as SPR.

A smoke parameter dependent on mass loss is the specific extinction area (SEA) $\sigma_f\left[\dfrac{\mathrm{m^2}}{\mathrm{kg}}\right]$, which may be expressed as:

$$\sigma_f = \dfrac{k \cdot V_f}{\dot{m}}$$

where $\dot{m}\left[\dfrac{\mathrm{kg}}{\mathrm{s}}\right]$ is the fuel's mass loss rate. The SEA describes the amount of smoke generated per 1 kg of fuel during combustion. It is obtained not only in small but also large scale tests [17].

Other important parameters are CO and CO_2 yields which describe the mass of particular gas per mass loss of fuel. They may be expressed in $\left[\dfrac{\mathrm{g}}{\mathrm{kg}}\right]$ or $\left[\dfrac{\mathrm{kg}}{\mathrm{kg}}\right]$ [19].

Examples of values of smoke parameters for different materials are shown in Table 1.

TABLE 1. **Smoke parameters for different fuels obtained from the cone calorimeter at irradiance level 35 kW/m^2**

Material	TSP [m^2]	SEA [m^2/kg]	Yield CO [kg/kg]	Yield CO$_2$ [kg/kg]
Polypropylene [20]	153	6842	0,045	2,70
Polypropylene modified with macromolecular intumescent flame retardant[20]	18	921	0,092	1,59
Polycarbonate [21]	19	680	0,148	1,652
Polycarbonate modified with flame retardant containing sulfonamide [21]	18	580	0,096	1,781
Flexible PVC [22]	41	1263	0,085	0,98
Flexible PVC modified with melamine [22]	25	808	0,088	1,36
Glass-fiber reinforced poly(1,4-butylene terephthalate) [23]	354	520	0,052	1,64
Glass-fiber reinforced poly(1,4-butylene terephthalate) modified with aluminum hypophosphite [23]	222	388	0,144	1,15

Single-chamber test

Smoke density chamber is also common in fire testing. It can be conducted in accordance with ISO 5659-2 or ASTM E662. The original NBS test method was adopted in 1979 [24]. As distinct from the cone calorimeter, the smoke density chamber is made specifically for smoke measurements. It is used for monitoring smoke generation from burning materials and quantifying smoke obscuration [25]. The measuring device is presented in Figure 2.

Square specimens of side 75 mm and thickness smaller than 25 mm are used. All the specimens should be conditioned in accordance with ISO 291 as in the cone calorimeter method.

A specimen set in the sample holder is placed on the load cell. Above there is a radiator cone. Specimens may be exposed to an irradiance of 25 or 50 kW/m^2 in the presence or absence of a pilot flame. As in the cone calorimeter method removing the radiation shield is required before starting the measurement [27].
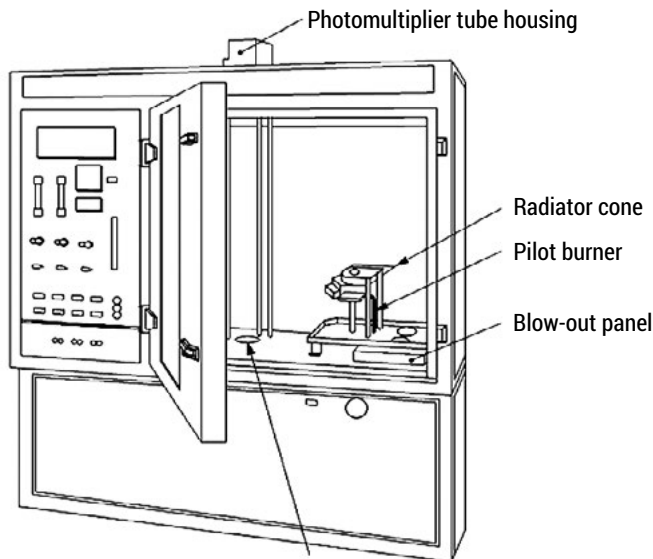
FIG. 2. A scheme of a smoke density chamber

SOURCE: [26]

During sample decomposition smoke is accumulated in the chamber. The attenuation of the light beam is measured according to Bouguer's law (1). Smoke density $D[-]$ is calculated according to equation [28]:

$$D = log\frac{I_0}{I}$$

This parameter is dependent on the sample geometry. Therefore specific optical density $D_s[-]$ is used more often. The equation is as follows:

$$D_s = log\left(\frac{I_0}{I}\right)\frac{V}{A \cdot L}$$

where $V[\text{m}^3]$ is the chamber volume, $A[\text{m}^2]]$ is the exposed area of the specimen, $L[\text{m}]$ is the path length of the light beam, $I_0[-]$ and $I[-]$ are the intensities of the light beam respectively before and during the test [29].

There are two important values of specific optical density D_s measured during the test: the maximum value of specific optical density D_{smax} and specific optical density at 4th minute of measurement $D_s(4)$. They are used for comparison of materials [30]. Another parameter related to D_s is $VOF(4)[\text{min}]$ which is defined as the area under curve of specific optical density during the first 4 minutes of measurement. The equation is as follows [31]:

$$V_{OF4} = \int_0^4 D_S \cdot dt$$

where $t\,[\mathrm{min}]$ is time.

The parameter related with specimen mass loss during the test is mass optical density $MOD\,[\mathrm{m^2/g}]$ which may be given by equation:

$$MOD = \frac{D \cdot V}{L \cdot \Delta m}$$

where $\Delta m\,[\mathrm{g}]$ is the mass loss [27].

A value of the Conventional Index of Toxicity CIT_G [–] may be obtained by connecting the FTIR analyzer to the smoke chamber. The concentration of eight toxic gases such as CO_2, CO, HF, HCl, HCN, NO_x, SO_2 and HBr is measured during the test. CIT_G [–] provides information's about overall toxicity of analyzed gases. It may be calculated as follows:

$$CIT_G = 0{,}0805 \sum_{i=1}^{i=8} \frac{c_i}{C_i}$$

where $c_i\,[\mathrm{mg/m^3}]$ is the concentration of the gas in the chamber after 4 or 8 minute and $C_i\,[\mathrm{mg/m^3}]$ is the reference concentration of the gas [32].

Examples of values of smoke parameters for different materials is shown in Table 2.

TABLE 2. **Smoke parameters for different fuels obtained from the smoke density chamber at irradiance level 25 kW/m² without the burner flame**

Material	$D_{s\,max}$ [–]	$D_s(4)$ [–]	VOF(4) [min]
Polypropylene [33]	569,2	304,8	401,8
Polycarbonate [34]	–	1070,1	1720
PVC floor panel [35]	>699,74	355,44	559,02
Glass-vinyl ester resin laminate [34]	–	629,17	955,4

Relevance of smoke parameters to standard requirements

The presented smoke parameters obtained from the cone calorimeter and smoke density chamber may be used for classifying materials in terms of fire protection. They are used in some industry fields such as rail transport or shipbuilding.

An European standard relevant to rolling stock is EN 45545-2:2020 Railway applications – Fire protection on railway vehicles. In part 2 requirements for fire behavior of materials and components are specified.

Vehicles may vary by design category:

- N – standard vehicles,
- A – vehicles forming part of an automatic train having no emergency trained staff on board,
- D – double decked vehicle,
- S – sleeping and couchette vehicles.

There are also defined operational categories from 1 to 4, where 1 is for trains that would be easiest to escape and 4 for the hardest. Basing on these informations hazard level classification have been proposed described in Table 3.

TABLE 3. **Hazard level classification for rolling stock according to EN 45545-2**

Operation category	Design category			
	N	**A**	**D**	**S**
1	HL1	HL1	HL2	HL2
2	HL2	HL2	HL2	HL2
3	HL2	HL2	HL2	HL3
4	HL3	HL3	HL3	HL3

SOURCE: **[36]**

For different products and components used in vehicles, for example interior vertical surfaces, floor composites or walls of external body shell, there are defined sets of requirements from R1 to R28. EN ISO 5659-2 and ISO 5660-1 test methods appear single or both in sets R1-R3, R5-R12, R17, R19-R23 and R28. Examples of sets and values of parameters are shown in Table 4.

TABLE 4. **Examples of material requirements sets according to EN 45545-2**

Requirement set	Test method	Parameter	HL1	HL2	HL3
R1	ISO 5660-1: 50 kW/m^2	MARHE [kW/m^2]	–	90	60
	ISO 5659-2: 50 kW/m^2	$D_s(4)$ [–]	600	300	150
		VOF(4) [–]	1200	600	300
	EN 17084 50 kW/m^2	CIT_G [–]	1,2	0,9	0,75

Requirement set	Test method	Parameter	HL1	HL2	HL3
R3	ISO 5659-2: 50 kW/m^2	$D_s(4)$ [−]	−	480	240
		VOF(4) [−]	−	960	480
	EN 17084 50 kW/m^2	CIT_G [−]	1,2	0,9	0,75
R5	ISO 5660-1: 25 kW/m^2	MARHE [kW/m^2]	50	50	50
	ISO 5659-2: 25 kW/m^2	$D_{s\,max}$ [−]	300	250	200
	EN 17084 50 kW/m^2	CIT_G [−]	1,2	0,9	0,75

SOURCE: **[36]**

Smoke parameters obtained from the cone calorimeter are not mentioned in rolling stock requirements. The only used parameter is $MARHE$. The measurement conditions depend on the requirement set, heat flux may be set on 25 or 50 kW/m^2.

Single chamber test is more usable and provide parameters such as D_{smax}, $D_s(4)$ and $VOF(4)$. Tests may be conducted with pilot flame for the first parameter or without for others. Measurements are mainly taken under heat flux of 50 kW/m^2, except test with pilot flame where 25 kW/m^2 heat flux is used.

The European standard EN 17084:2018 Railway applications – Fire protection on railway vehicles – Toxicity of materials and components describes a method for obtaining CIT_G parameter by gas analysis in the smoke chamber EN ISO 5659-2 using FTIR technique thus it is included in the comparison in Table 4 [36].

International Maritime Organization (*IMO*) adopted International Convention for the Safety of Life at Sea (*SOLAS*) after few amendments in 1974. It focuses on enhancing safety of human life during shipping activities. Chapter II-2 of the convention contains measures to mitigate the risk of fire. SOLAS makes mandatory meeting the requirements of International Code for Application of Fire Test Procedures (*FTP*) adopted by the IMO's Maritime Safety Committee (*MSC*) [37].

The 2010 FTP Code contains fire test procedures, including smoke and toxicity and heat release, smoke production and mass loss rate tests. A reference for the smoke generation test is a method described in ISO 5659-2. Tests must be taken under exposure of 25 kW/m^2 heat flux (with and without a pilot flame) and 50 kW/m^2 heat flux (without pilot flame).

A classifying criterion for smoke generation test is D_m [−] which is an average value of the D_{smax} of each of three tests. Values of D_m for different materials are shown in Table 5.

TABLE 5. Examples of material requirements according to 2010 FTP Code

Material	Test method	Max value of D_m [−]
Surface of bulkhead, lining, ceiling	ISO 5659-2:	200
Primary deck covering	• 25 kW/m², with pilot flame	400
Floor covering	• 25 kW/m², without pilot flame	500
Plastic pipe	• 50 kW/m², with pilot flame	400

SOURCE: [38]

A criterion for toxicity is an average value of the maximum value of the gas concentration measured at each test condition. Limits for different gases are presented in Table 6.

TABLE 6. Limits of gases concentration according to 2010 FTP Code

Gas	Test method	Max value of gas concentration [ppm]
CO	ISO 19702 and ISO 5659-2:	1,450
HCl	• 25 kW/m², with pilot flame	600
HF	• 25 kW/m², without pilot flame	600
NO$_x$	• 50 kW/m², with pilot flame	350
HBr		600
HCN		140
SO$_2$		120/200*

*for floor coverings

SOURCE: [38]

Gas measurements by FTIR according to ISO 19702 Guidance for sampling and analysis of toxic gases and vapours in fire effluents using Fourier Transform Infrared (FTIR) spectroscopy have to be carried out when D_{smax} occurs.

Heat release, smoke production and mass loss rate for furniture and other components materials of high-speed craft are measured in accordance with ISO 5660-1 Reaction-to-fire tests – Heat release, smoke production and mass loss rate – Part 1: Hear release rate (cone calorimeter method) and ISO 5660-2 – Part 2: Smoke production rate (dynamic measurement). The irradiance level has to be set on 50 kW/m².

Time to ignition (*TTI*) for fire-restricting materials have to be greater than 20 s, the maximum 30-second sliding average heat release rate (*HRR30,max*) cannot exceed 60 kW/m², the total heat release (*THR*) cannot exceed 20 MJ/m² and the time average SPR cannot exceed 0,005 m²/s [38].

Summary

Despite smoke and toxicity hazard of plastics in fire their global production raises every year. Plastics are commonly used in various industry fields as construction or transport due to their significant advantages. Enhancing fire safety is related to the necessity of meeting standard requirements for materials.

The most common small scale tests for measuring smoke generated from plastics are the cone calorimeter method and the single-chamber test. In Europe these tests are made according to respectively ISO 5660 and EN ISO 5659-2. Materials used in rail transport or shipbuilding have to positively pass the assessment of diverse parameters, including these associated with smoke generation.

In rail transport the cone calorimeter method provides information's only about *MARHE* which relates to heat emission. Smoke parameters are measured by single-chamber test. Depending on the requirement set $D_s(4)$, *VOF(4) or $D_{s\,max}$* are used. Toxicity of smoke is represented by CIT_G obtained also from the smoke chamber.

The main smoke parameter crucial in shipbuilding is D_m dependent on $D_{s\,max}$. The analysis of toxic gases and vapours may be held with the additional usage of FTIR module. The cone calorimeter method is used in high-speed crafts and besides heat parameters there is only *SPR* related to smoke generation.

Thus there are more smoke parameters obtained from smoke density chamber than from the cone calorimeter in standard requirements.

References

[1]   Bajt O., *From plastics to microplastics and organisms*, Febs Open Bio 2020, 4(4), p. 1–28.

[2]   Simoneit B.R.T., Medeiros P.M., Didyk B.M., *Combustion Products of Plastics as Indicators for Refuse Burning in the Atmosphere*, Environmental Science and Technology 2005, 39(18), p. 6961–6970.

[3]   Butler K.M., Mulholland G.W., *Generation and Transport of Smoke Components*, Fire Technology 2004, 40, p. 149–176.

[4]   Stec A.A., *Fire Toxicity – the Elephant in the Room?*, Fire Safety Journal 2017, 91, p. 79–90.

[5]   Brohez S., Delvosalle C., Marlair G., Tewarson A., *The Measurement of Heat Release from Oxygen Consumption in Sooty Fires*, Journal of Fire Sciences 2000, 18(5), p. 327–353.

[6]   McCoy C.G., Tilles J.L., Stoliarov S. I., *Empirical Model of flame heat feedback for simulation of cone* calorimetry, Fire Safety Journal 2019, 103, p. 38–48.

[7]   ISO 5660-1 Reaction to fire tests – Heat release, smoke production and mass loss rate – Part 1: Heat release rate (cone calorimeter method) and smoke production rate (dynamic measurement), 2015.

[8] Tissot J., Talbaut M., Yon J., Coppalle A., Bescond A., *Spectral study of the smoke optical density in non-flaming condition*, The 9th Asia-Oceania Symposium on Fire Science and Technology, Proceedia Engineering 2013, 62, p. 821–828.

[9] Lindholm J., Brink A., Hupa M., *Cone Calorimeter – a Tool for Measuring Heat Release Rate*, Materials Science/Åbo Akademi Process Chemistry Centre 2009, p. 2–5.

[10] Marquis D., Guillaume E., Lesenechal D., *Accuracy (trueness and precision) of cone calorimeter tests with and without a vitiated air enclosure*, Proceedia Engineering 2013, 62, p. 103–119.

[11] Bryn J., *Sampling-Window Based Approach for Fire Gas Analysis or Rigid foams*, Master Thesis 2013, Canada, p. 34–36.

[12] Urbas J., *Effects of retainer frame, irradiance level and specimen thickness on cone calorimeter test results*, Fire and Materials 2005, 29, p. 1–13.

[13] Biteau H., Steinhaus T., Schemel C., Simeoni A., Marlair G., Bal N., Torero J.L., *Calculation Methods for the Heat Release Rate of Materials of Unknown Composition*, Fire Safety Science – Proceedings of the ninth international symposium 2008, p. 1165–1176.

[14] Enright P.A., Fleischmann C.M., *Uncertainty of Heat Release Rate Calculation of the ISO 5660-1 Cone Calorimeter Standard Test Method*, Fire Technology 1999, 35(2), p. 155–156.

[15] Schartel B., Hull T.R., *Development of fire-retarded materials – Interpretation of cone calorimeter data*, Fire and Materials 2007, 31, p. 327–354.

[16] Martinka J., Dibidiakova J., *Materials for Safety and Security: Materials for Shielding, Protective Suits, Electrical Insulation and Fire Protection* [in:] Rehak D., Bernatik A., Dvorak Z., Hromada M., *Safety and Security Issues in Technical Infrastructures 2020, IGI Global, p. 303.*

[17] Birgit A., Östman L., *Smoke and Soot* [in:] Babrauskas V., Grayson S.J., *Heat Release in Fires*, Elsevier Science Publishers 1992, Great Britain, p. 236–245.

[18] Hansen A. E. S., *No fire without smoke. Prediction models for heat release and smoke production in the SBI test and the Room Corner test based on Cone Calorimeter test results.* April, 2002.

[19] Martinka J., Rantuch P., Wachter I., *Impact of Water Content on Energy Potential and Combustion Characteristics of Methanol and Ethanol Fuels*, Energies 2019, 12, 3491, p. 1–16.

[20] Yang R., Ma B., Zhang B., Li J., *Fire retardance and smoke suppression of polypropylene with a macromolecular flame retardant containing caged bicyclic phosphate and piperazine*, Journal of Applied Polymer Science 2019, 136, 47593, p. 1–9.

[21] Yang H., Yue H., Zhao X., Song M., Guo J., Cui Y., Fernandez-Blazquez J.P., Wang D., *Polycarbonate/Sulfonamide Composites with Ultralow Contents of Halogen-Free Flame Retardant and Desirable Compatibility*, Materials 2020, 13, 3656, p. 1–13.

[22] Wu W.H., Wu H.J., Liu W.H., Wang Y.E., Liu N., Yang X.M., Li Y.M., Qu H. Q., *Two Series of Inorganic Melamine Salts as Flame Retardants and Smoke Suppressants for Flexible PVC*, Polymer Composites 2018, 39(2), p. 529–536.

[23] Yang W., Song L., Hu Y., *Comparative Study on Thermal Decomposition and Combustion Behavior of Glass-Fiber Reinforced Poly(1,4-butylene terephthalate) Composites Containing Trivalent Metal (Al, La, Ce) Hypophosphite*, Polymer Composites 2013, 34, p. 1832–1839.

[24] Lawson J.R., *A History of Fire Testing*, NIST Technical Note 1628 2009, p. 25.

[25] Stec A.A., Rhodes J., *Bench Scale Generation of Smoke Particulates and Hydrocarbons from Burning Polymers*, Fire Safety Science – Proceedings of the tenth international symposium 2008, p. 629–640.

[26] Olimat A.N., Awad A.S., Al-Ghathaian F.M., *Effect of Fire Retardant Painting Product on Smoke Optical Density of Burning Natural Wood Samples*, International Journal of Energy and Power Engineering 2017, 11(9), p. 1028–1037.

[27] ISO 5659-2 Plastics – Smoke generation. Part 2: Determination of optical density by a single-chamber test, 2017.

[28] Kolbrecki A., *O dymotwórczości wyrobów budowlanych w czasie pożaru*, Prace Instytutu Techniki Budowlanej – Kwartalnik 2000, 4(116), p. 50.

[29] Peacock R.D., Cleary T.G., Reneke P.A., Murphy D.C., *A Literature Review of the Effects of Smoke from a Fire on Electrical Equipment*, National Institute of Standards and Technology, 2012, p. 26–28.

[30] Gregory S., Grayson S.J., Kumar S., *Test Methods and Instrumentation for Assessing Reaction to Fire Properties of Railway Rolling Stock*, Problemy Kolejnictwa 2013, 160, p. 35–43.

[31] Półka M., Szajewska A., *Smoke Emission Properties of Floor Covering Materials of Furnished Apartments in a Building*, International Journal of Environmental Research and Public Health 2020, 17, 9019, p. 1–11.

[32] Marset D., Dolza C., Fages E., Gonga E., Gutierrez O., Gomez-Caturla J., Ivorra-Martinez J., Sanchez-Nacher L., Quiles-Carillo J., *The Effect of Halloysite Nanotubes on the Fire Retardancy Properties of Partially Biobased Polyamide 610*, Polymers 2020, 12, 3050, p. 1–21.

[33] Zubek Ł., *The smoke emission properties of selected elements of passenger car interior design*, E3S Web of Conferences 2018, 45, 00107, p. 1–8.

[34] Radziszewska-Wolińska J.M., Tarka I., *The Influence of Reinforcing Layers and Varnish Coatings on the Smoke Properties of Laminates Based on Selectec Vinyl Ester and Polyester Resins*, Materials Research Proceedings 2018, 5, p. 210–215.

[35] Półka M., Białek J., *The smoke emission properties of selected elements of furnishing apartments in the building*, Modern Building Materials, Structures and Techniques, 13th International Conference 2019, Vilnius, Lithuania, p. 657–662.

[36] EN 45545-2:2020 Railway applications – Fire protection on railway vehicles. In part 2 requirements for fire behavior of materials and components.

[37] Joseph A., Dalaklis D., *The international convention for the safety of life at sea: highlighting interrelations of measures towards effective risk mitigation*, Journal of International Maritime Safety, Environmental Affairs and Shipping 2021, 5(1), p. 1–11.

[38] International Code for Application of Fire Test Procedures, 2010 (2010 FTP Code).

Energy consumption, thermal comfort and indoor air quality assessment in a school building using three air-cooling systems

Abstract: Efficient air-cooling systems for hot climatic conditions, such as southern Europe, are required in the context of Nearly Zero Energy Buildings. Regenerative indirect evaporative coolers, RIEC, and desiccant regenerative indirect evaporative coolers, DRIEC, could be considered an innovative alternative to direct expansion conventional systems, DX. The main objective of this work was to evaluate the seasonal performance of three air-cooling systems in terms of thermal comfort, air quality and energy consumption in a standard classroom. Several energy simulations were carried out to evaluate these indexes in the climate zone of Lampedusa, in Mediterranean area, by using European Standards. The simulations were based on experimentally validated models.

DRIEC system was the recommended system to serve a standard classroom in terms of thermal comfort and RIEC system in terms of air quality and energy consumption. DX system achieved similar comfort favourable conditions to DRIEC system. However, it always worked in III unfavourable category of air quality and consumed three times more than RIEC and DRIEC systems.

Introduction

According to the Energy Performance of Building Directive, sustainable development and the achievement of competitive HVAC systems were established as main objectives [1]. The final energy consumption in buildings account for 40% of the total

energy consumption and the 36% of the total CO_2 emissions in Europe [2]. HVAC systems represent a significant percentage of this energy consumption. Then, several research works analysed the energy behaviour of different hybrid HVAC systems [3–5].

Other authors carried out comparative studies between conventional and hybrid HVAC systems in terms of thermal comfort [6, 7]. A recent work concluded that adaptative setpoint temperature for the cooling season could achieve thermal comfort conditions and reduce energy consumption of buildings, in selected zones of the Mediterranean area [8].

A research of ventilation in classrooms showed that insufficient ventilation affects learning and health's students [9]. This study concluded that ventilation rates in school buildings were often below the minimum required by building standards. Other work determined that several factors such as climate zone, characteristics of the building and its use and thermal envelope were decisive in the choice of the ventilation technology [10].

The main objective of this work was to evaluate the seasonal performance of three air-cooling systems in terms of thermal comfort, air quality and energy consumption in school buildings of Mediterranean area. Several annual energy simulations were carried out during the warmest period of the year, by using European Standards.

## Systems and building description

Three air-cooling systems were studied in the present work: (i) a conventional air-cooling system based on a direct expansion unit, DX; (ii) an air-cooling system based on a regenerative indirect evaporative cooler, RIEC; (iii) a hybrid air-cooling system based on a desiccant regenerative indirect evaporative cooler, DRIEC. Figure 1 shows a schematic of these three air-cooling systems.

The DX system was mainly composed of an air-mixing box and a vapor-compression cycle, where the evaporator, EV, and the condenser, CO, were installed in a parallel arrangement.

The RIEC system works with a single inlet air stream, outdoor air, OA, which is divided into two air streams, exhaust air, EA, and supply air, SA. The outdoor air flow was cooled and supplied to the room without increasing its humidity ratio and the exhaust air flow was humidified and heated and the exhausted outside.

The DRIEC system was mainly composed of a desiccant wheel, DW, and a heating coil, HC, to dehumidify the supply air and a RIEC equipment to cool this stream.

The control system of the DX and the RIEC systems were based on indoor air temperature and indoor air CO_2 concentration controls, in that order. The air humidity ratio was no controlled in these air-cooling systems. The control system of the DRIEC system was based on control by air temperature, air humidity and air CO_2 concentration. The control strategies used had as priority to achieve thermal comfort conditions, reducing energy consumption.
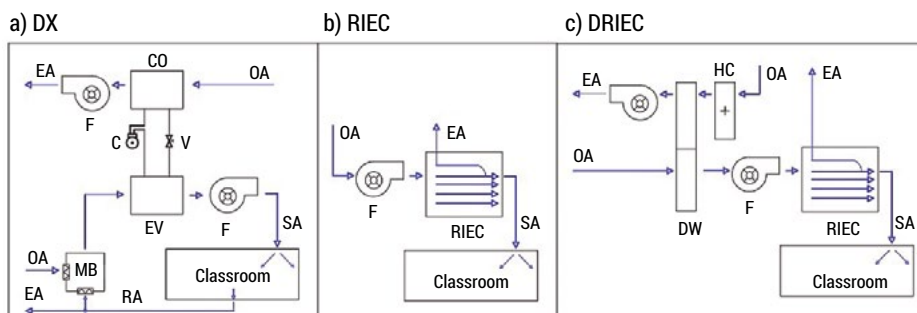
Nomenclature:
OA – Outdoor air, SA – Supply air, RA – Return air, EA – Exhaust air, CO – Condenser, EV – Evaporator, C – Compressor, V – Expansion valve, MB – Mixing box, F – Fan, HC – Heating coil, DW – Dessicant wheel, DX – Direct expansion, RIEC – Regenerative indirect evaporative cooler, DRIEC – Dessicant regenerative evaporative cooler

FIG. 1. Schematics of a) DX; b) RIEC; and c) DRIEC systems

Detailed energy simulations were carried out with the assumption that the three air-cooling systems served a standard classroom in Lampedusa, with the typical conditions of the Mediterranean area. All the air-cooling systems elements were modeled from experimental data and integrated into TRNSYS17 software [11]. The main characteristics of the building model are shown in Table 1.

TABLE 1. Characteristics of the standard classroom

Building	Floor area	55.8 m^2
	Height	3 m
Heat gain	People	20
	Sensible	60 W person^{-1}
	Latent	60 W person^{-1}
Daily Schedule	09:00 to 15:00 pm	

Systems evaluation

The behaviour of three air-cooling systems was analysed regarding thermal comfort, air quality and energy consumption. Each evaluation method is described below.
- Thermal comfort. This index was evaluated according to predict mean vote, PMV, and predicted percentage dissatisfied, PPD. Both parameters were calculated according to European Standard 16798–2 [12]. Four categories of thermal comfort were differentiated in relation to PPD values. Categories I, II, III and IV for PPD values less than 6%, 10%, 15% and 25%, respectively. The weighing factor calculated to determine the percentage of occupancy hours in each category was the ratio between the current PPD and the PPD limit.

- Air quality. This indicator was determined analogously to thermal comfort evaluation method. Four categories of air quality corresponding to ΔCO_2 difference between indoor and outdoor concentration (420 ppm) were considered. Categories I, II, III and IV for ΔCO_2 values less than 550 ppm, 800 ppm, 1350 ppm and more than 1350 ppm, respectively. In this case, the weighing factor values for each category were obtained with the real ΔCO_2 value and the limit ΔCO_2 value.
- Energy consumption. Each air-cooling system consumption was calculated as the sum of energy consumption of each air-cooling system element, such as compressor, fans, pumps.

Results and Discussion

The annual results of the thermal comfort for the three air-cooling systems are shown in Figure 2. The bars show the percentage of occupancy hours for each air-cooling system working in each thermal comfort category. In the present work, favourable comfort conditions were assumed when the indoor conditions were within categories I and II. It can be observed that the DX and the DRIEC systems achieved similar favourable conditions. However, a significant reduction was obtained with the RIEC system, mainly due to the high humidity in the supply air.
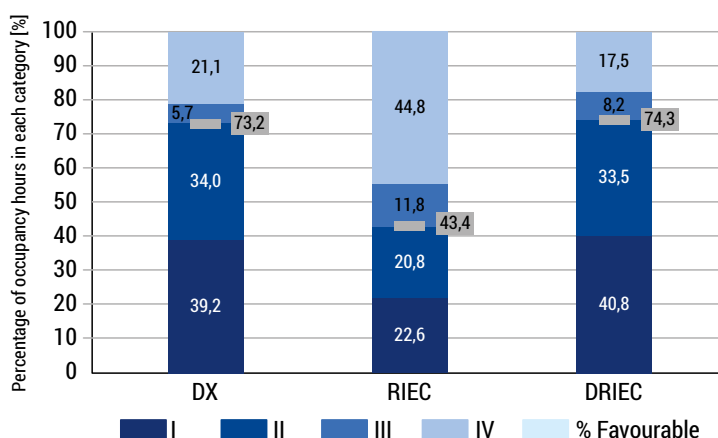
FIG. 2. Thermal comfort results. Percentage of occupancy hours in each category

Figure 3 shows the annual air quality results for the three air-cooling systems. The bars show the percentage of occupancy hours for each air-cooling system working in each air quality category, and the categories I and II were considered favourable, as well as for the thermal comfort. It can be observed that the DX system was

in unfavourable category throughout occupation period, since only a low percentage of supply air came from outside. The RIEC and DRIEC systems achieved similar favourable conditions because they were all outside air systems.
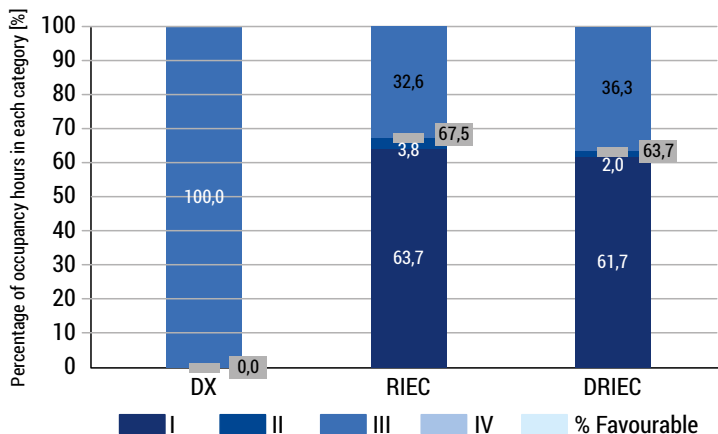
FIG. 3. Air quality results. Percentage of occupancy hours in each category

The annual energy consumption results for the three air-cooling systems are shown in Figure 4. It can be observed that the RIEC and the DRIEC systems had similar consumes during the occupation period. However, the DX system consumed three times more than the DRIEC system, mainly due to compressor consumption.
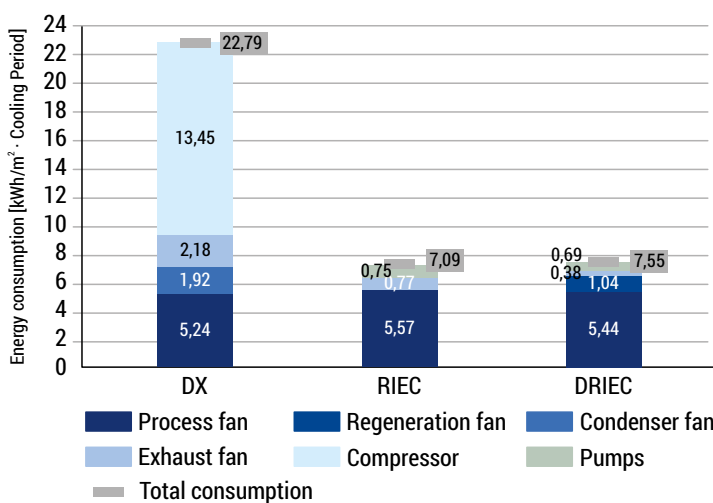
FIG. 4. Energy consumption results. Percentage of occupancy hours in each category

Summary

The present work showed the results of a comparative analysis between three air-cooling systems in terms of thermal comfort, air quality and energy consumption in school buildings of Mediterranean area.

Based on the results obtained, the following conclusions can be drawn:

- Thermal comfort. The most favourable comfort conditions were obtained with the DX and DRIEC systems. However, the RIEC system achieved more unfavourable thermal comfort conditions since the supply air humidity was no controlled.
- Air quality. The air-cooling system with the longest period in favourable air quality conditions was the RIEC system, 67.5%. The DRIEC system reached 4% less than the RIEC system. The DX system always worked in category III, unfavourable category.
- Energy consumption. The systems with the lowest energy consumption were the RIEC and the DRIEC systems, up to three times less than the DX system.

Literature

[1] Directive 2010/31/EU, "European parliament and of the council of 19 May 2010 on the energy performance of buildings (recast). Off J Eur Union 2010," pp. 13–35.

[2] P. M. Congedo, C. Baglivo, D. D'Agostino, and I. Zacà, *Cost-optimal design for nearly zero energy office buildings located in warm climates* Energy, 2015, vol. 91, no. 244, pp. 967–982.

[3] F. Comino, J. Castillo González, F. J. Navas-Martos, and M. Ruiz de Adana, *Experimental energy performance assessment of a solar desiccant cooling system in Southern Europe climates*, Appl. Therm. Eng., 2020, vol. 165, no. September 2019, p. 114579.

[4] A. Franco and F. Leccese, *Measurement of CO2 concentration for occupancy estimation in educational buildings with energy efficiency purposes*, J. Build. Eng., 2020, vol. 32, no. July, p. 101714.

[5] P. M. Congedo, D. D'Agostino, C. Baglivo, G. Tornese, and I. Zacà, *Efficient solutions and cost-optimal analysis for existing school buildings*, Energies, 2016, vol. 9, no. 10, pp. 1–24.

[6]   D. Mumovic et al., "*A comparative analysis of the indoor air quality and thermal comfort in schools with natural, hybrid and mechanical ventilation strategies*, Proc. Clima 2007 WellBeing Indoors, 2007, no. c, p. 8.

[7]   H. Breesch, B. Merema, and A. Versele, *Ventilative cooling in a school building: Evaluation of the measured performances*, Fluids, 2018, vol. 3, no. 68.

[8]   C. Munonye and Y. Ji, *Evaluating the perception of thermal environment in naturally ventilated schools in a warm and humid climate in Nigeria*, Build. Serv. Eng. Res. Technol., 2021, vol. 42, no. 1, pp. 5–25.

[9]   W. J. Fisk, *The ventilation problem in schools: literature review.*, Indoor Air, 2017, vol. 27, no. 6, pp. 1039–1051.

[10]   A. Andriamamonjy and R. Klein, *A modular, open system for testing ventilation and cooling strategies in extremely low energy lecture rooms*, 36th AIVC- 5th TightVent- 3rd Vent. 2015, 2015.

[11]   S.A. Klein, "TRNSYS 17: A Transient System Simulation Program." University of Wisconsin, Madison USA, SEL, 2006.

[12]   CEN/TR 16798-2:2019, "Energy performance of buildings – Ventilation for buildings – Part 2: Interpretation of the requirements in EN 16798–1 – Indoor environmental input parameters for design and assessment of energy performance of buildings addressing indoor air quality, ther," p. 88, 2019.

Microbiological air monitoring and long-term evaluations of selected urban areas in the city of Tirana

Abstract: The described experimental study, performed over the years, includes the quantitative and qualitative monitoring of the presence of microorganisms of air in outdoor and indoor environments of the Albanian Capital, Tirana, during a time when large demographic movements, accompanied by critical urban interventions and infrastructural changes have been part of our lives. A project, part of the National Program in Biotechnology (R&D – the year 2000), was the first support to obtain a database on microbiological air pollution in selected urban areas in Tirana and isolate and identify specific air microbial pollutants. The results obtained were an incentive to continue further with additional scientific evaluation monitoring research that included 2011 to 2015 and then those of 2016-2020.

Over the years, there has been a significant reduction in pollutant microbial loads (for example, some outdoor areas of the center of Tirana), together with substantial fluctuations in indoor microbial loads, which were observed in many cases. Also, a prominent presence of typical environmental fungi pollutants was identified, such as Aspergillus niger, Aspergillus flavus, Aspergillus terreus, and bacterial pollutants, cocci and bacilli (typical Bacillus megaterium), during Total Viable Count (TVC) and other microbiological tests of identification.

Introduction

Atmospheric changes over the centuries have also been associated with an increase in the number of particles present in the air and microbiological loads. This is related to the activities of the growing population as industrial activities and others, responsible for increasing microbiological and physicochemical air pollution.

Microorganisms are present in the air in different layers of the Troposphere. They pass into the air from various sources. Dust, plants, animals, excrements of human bodies, waste materials, new constructions, changes of urban infrastructure, etc., are primarily responsible for increasing the number of microorganisms in the air outside and indoor environments [1, 2, 3]. Airborne particles that originate from biological sources: animals, plants, fungi, bacteria, protozoa, and viruses can form bioaerosols, possibly to be isolated from indoor and outdoor environments [4, 5].

Assessment of air microbiological loads is essential to ensure a clean environment for a healthy life and control the cleanliness of raw materials, food & pharmaceutical products, as polluted air can be a common source of infections. Various bacilli, various micrococci, and fungi (molds and yeasts) are determined in air particles [2, 3, 6]. Air pathogens are responsible for critical human pathologies, such as *Streptococcal Respiratory Infections, Tuberculosis, Pneumonia, Aspergillosis*, and other viral diseases [3, 7, 8, 9].

The research work was performed through a collaboration between the University of Medicine of Tirana, Faculty of Medicine, Department of Pharmacy and University of Tirana, Faculty of Natural Sciences, Department of Industrial Chemistry.

Evaluation of air microflora and its impact on health and well being

The air acts as a carrier of microorganisms and is not favorable for their growth. Air microorganisms are transported by dust particles considered "large particles", that stay suspended for a short time. Microorganisms through the particles can be transported from several meters to even several kilometers. Their survival (from few seconds to few months or more) and destination depend on the species, the ability to form spores, particle size, humidity, temperature, sunlight, etc. Pathogenic microorganisms are also spread through the air, which poses a significant risk to the health of human being. [8, 9, 11].

The composition of the air microflora is highly related to the surrounding environment. Bacteria and fungi are found in the air of hospital environments. Yeasts are found in vineyard areas. In the air that surrounds streams, rivers, and lakes, there

is an aquatic microflora. Different types of microorganisms can be found in the air of cities and other inhabited areas. Particles in the air are a primary cause of respiratory diseases, such as asthma, respiratory tract infections, allergies, etc.

Particle size plays an important role. Particles up to 5 μm are transported deep to the lungs. Particles 2–4 μm make an alveolar deposition. Such are the spores of *Penicillium spp.* and *Aspergillus spp.* Smaller particles, like spores 1 μm of *Ascomycetes* are less able to deposit in the alveoli.

The Brownian movement randomly brings bacteria into the lungs. The source of diseases are also fungi, including toxin producers as *Aspergillus flavus, Aspergillus fumigatus,* etc. Living in humid areas is often associated with headaches, fatigue, sore throats, flu, diarrhea, etc. Fungi are considered potential causes of S.B.S. (Sick Building Syndrome), which often appear indoors. Yeasts with an abundant concentration in the air can cause allergies in allergic people. Positive skin allergy tests have been observed in some of them [5, 8, 11]. Table 1 presents diseases caused by bacterial strains found in cities, residential and industrial areas, and human activities.

TAB. 1. Some of bacterial strains responsible for human diseases

Bacterial strains	Negative effects on human body
Cocci (Gr+)	
Staphylococcus aureus	bacteremia, toxic shock, skin and soft tissue infections, arthritis, osteomyelitis
Streptococcus pneumonia	meningitis, pneumonia, endocarditis, peritonitis
Enterococcus spp.	infectious endocarditis, urinary tract infections, renal abscess
Bacilli (Gr+)	
Bacillus anthracis	anthrax
Corynebacterium diphtheriae	diphtheria
Bacilli (Gr-)	
Brucella	brucellosis
Escherichia coli	acute enteritis, urinary tract infections, renal abscess, prostate, diarrhea, respiratory illness
Klebsiella	urinary tract infections, renal abscess, prostate
Proteus	urinary tract infections, renal abscess
Salmonella typhi	typhoid fever, acute enteritis
Shigella	shigellosis, bloody diarrhea, fever, stomach cramps, acute enteritis, reactive arthritis
Vibrio cholerae	cholera disease

SOURCE: [7, 8, 11].

Study of the presence of air microorganisms in the capital of Albania, Tirana

After the 1990-s throughout Albania, there were large-scale changes in infrastructure and demographic movements. The changes extended over the years and reconfigured the structure of the capital of Albania. They brought a concentration of population in Tirana and an increase in industrial and construction activities. Tirana, from a city in central Albania with 200.000 inhabitants, quickly changed to a metropolis with about 500.000 people today. In addition, the number of those who visit Tirana every day for work, activities, healthcare, or tourism, is increasing day by day, including visitors from other countries. This situation significantly affected the increase of physicochemical and microbiological pollution of the environment and set as a primary study objective to evaluate pollution levels, prevention, risk assessment and management.

The presented experimental work, performed over the years, includes the quantitative and qualitative monitoring of the air microorganisms, in outdoor and indoor environments of Tirana, at a time when large demographic movements, accompanied by urban interventions and infrastructural changes, mentioned above, have been part of our lives.

The study was conducted in two main time periods:

- **2002–2009** The study was performed by the Research Group of Industrial Microbiology and Food Sciences (Department of Industrial Chemistry) Faculty of Natural Sciences, Tirana University. The conclusions of two-year results were made public in 2004 [11]. From 2004–2009 the monitoring of microbiological air contamination continued by expanding the sampling areas.
- **2010–2020** The study was carried out based on the experience of the years 2002–2009, with excellent cooperation between the Research Group of the Department of Industrial Chemistry, Faculty of Natural Sciences, University of Tirana & Research Group of the Department of Pharmacy, Faculty of Medicine, University of Medicine, Tirana. The second period of monitoring also included evaluating of microbial pollutants in outdoor environments of healthcare and education institutions, where the presence of microbial pollutants can have an extensive direct impact on the population's health.

General information for the data network and experience of the research activity for 2002–2009 and 2009–2015

Below, there is a brief and general description of the first period of research. The experimental work was planned to be carried out in some well-known and populated areas of Tirana. At that time, in these areas were many infrastructural interventions, which

affected the increase of physicochemical pollution and potentially also the microbiological one. While physicochemical pollution had become part of the research studies in Albanian Universities and Environmental Protection Institutions, there were no data on microbial pollution.

Initially, air samples were taken from 20 geographical locations in Tirana (10 of them analyzed in 2002 and 10 others in 2003). In addition, six geographical areas of the capital were monitored in both years for comparative studies.

Some of the analysed locations were:

- CC – City Center
- BZ – Boulevard ZOG 1
- BL – Boulevard at the Lana river bridge
- HTI – Hotel Tirana International Area
- BA – Bank of Albania
- P – Pyramid Building Area
- UT – University of Tirana
- NL – National Library, etc.

After the first results, new locations were selected, analyzed, and monitored over the years: "Scanderbeg" square, "Myslym Shyri" street, University Hospital Center, "Mother Teresa" square, Zoo, Botanical Garden, "Lapraka" area, etc.

Areas with innumerable loads of bacteria were identified, especially the very frequented areas of the city center. In some zones, the determination of molds showed a load of order 10^4–10^5. During the monitoring, the loads varied significantly in the same area, and this was mainly related to the periodic interventions and constructions in streets and squares.

The identified molds belonged to the classes *Phycomycetes*, *Ascomycetes* and *Fungi imperfecti*. The dominant mold genera were *Rhizopus* (*Rhizopus nigricans*); *Mucor (Mucor hiemalis); Aspergillus (Aspergillus niger, Aspergillus terreus, Aspergillus glaucus, Aspergillus flavus); Penicillium (Penicillium spp.); Cladosporium (Cladosporium herbarum); Alternaria (Alternaria radicina).*

The detailed experimental work was published, supported by the projects of National Research Programs of that time. A project in the framework of the National Program (R&D) in Biotechnology (the year 2000) was the first support to obtain a database on microbiological air pollution and to isolate and identify some specific air microbial pollutants. The project also supported creating a work collection of air microorganisms in the Department of Industrial Chemistry in the Faculty of Natural Sciences [11].

The results achieved during the years 2002–2009 were an incentive to increase cooperation and continue further with additional scientific evaluations, including the years 2009–2015 and 2016–2020.

In the monitoring period 2009–2015, the air of 20 outdoor environments, in the city and suburbs, was monitored during two periods of 6 years (now the monitored suburbs are part of the city due to expansion toward peripherals, the creation of large urban areas and the increasingly large number of population living there).

The responsibility was of many institutions in charge of environmental protection and companies that carried out infrastructure interventions with a low level of protection against pollution. Many microorganisms were also related to the combination of physicochemical and microbiological pollutants and the transmission of microbial loads through dust, wind, and rain. A negative impact came from low awareness of specific categories of populations about environmental pollution and their problems in health and quality of life.

The results obtained for average loads (CFU/m^2) in 10 outdoor samples in the monitoring period 2011–2015 (4 to 5 logarithmic scales) are presented in Table 2 and Figure 1.

TAB. 2. Average loads of microorganisms (CFU/m^2) in 10 outdoor samples in the monitoring period 2011–2015 (4 to 5 logarithmic scales)

Nr.	Sampling areas	Average loads of microorganisms (CFU/m^2)
1	Center of the city	123125
2	Boulevard „ZOG 1"	216406
3	Boulevard „ZOG 1" after the rain	124843
4	Train Station	90781
5	Tirana International Hotel-outdoor	97500
6	Tirana Lake Park	27500
7	University Campus	40312
8	„Durres" Street	66718
9	„Luigj Gurakuqi" Street	46406
10	„Kavaja" Street	47031

SOURCE: **own study**

The results above show a large number of microorganisms in Tirana air. However, after the rain, on the central Boulevard of Tirana, the number of microorganisms decreased by about 43%. Approximate results were also obtained from monitoring before and after the rain in other streets of Tirana. The lowest load was observed in Tirana Lake Park. At that time, it was an area with extensive vegetation, fewer constructions, fewer visitors.
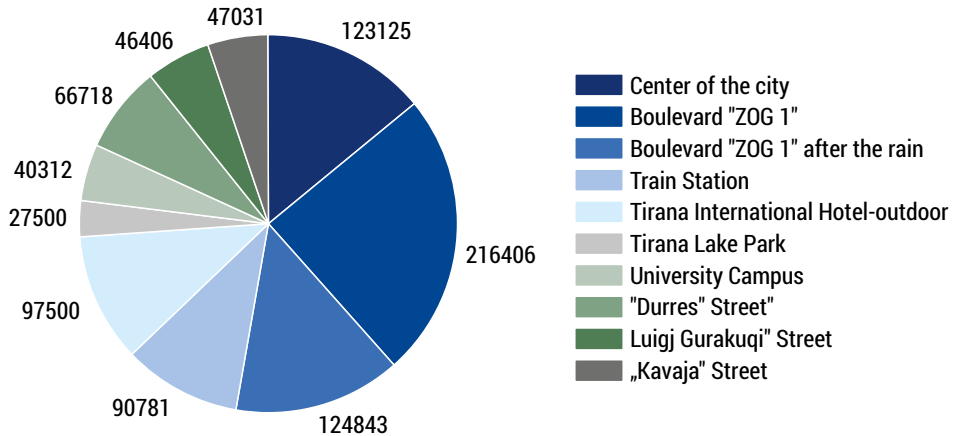
FIG. 1. Comparison of average loads of microorganisms (CFU/m^2) in 10 outdoor samples in the monitoring period 2011–2015

SOURCE: own study

The most present microorganisms were *Cocci Gr.+, Bacillus megaterium, Aspergillus niger, Aspergillus terreus, Aspergillus fumigatus, Aspergillus versicolor, Penicillium cyclopium, Trichoderma spp., Geotrichum spp., etc.*

Detailed information for the data network and experience of the research activity of the period 2016–2020

The results summarized from now on belong to the period 2016–2020 and serve as a comparison with data obtained before 2015.

25 outdoor and indoor environments were selected [1, 10, 11]. In this paper are described the results taken from 5 of them, coded as follows:

- OGH – University Hospital Center
- FNS – University Institution
- NM – Museum Center
- MTS – Mother Teresa Square
- TLP – Tirana Lake Park

For each area under monitoring, samples were taken outdoors and indoors belonging to each outdoor environment mentioned above [8, 12].

Passive sampling was carried out with settle plates, using the settling plate technique. The principle of this simple method is the gravitational force. Open Petri dishes with 20 ml of solid culture media were placed 1 m distant from the ground level. An air volume with the dust particles and microorganisms was settled onto each plate's

selected solid medium. Plate Count Agar-PCA was used to determine the total number of microorganisms. Meat Peptone Agar-MPA was used for bacteria and Sabouroauds Dextrose Agar-SDA for yeasts and molds. The microbial load was evaluated as CFU/ m^2 hour. The plates were incubated for total mesophilic microorganisms at 28°C, for weak pathogens at 37°C, for molds &yeasts at 25–28°C [3, 5, 10]. The Total Viable Count (TVC) and qualitative analysis were performed every year in the same period (April, around 12 o'clock), to prevent significant effects of temperature and climate on final results. Total Viable Count is presented in Table 3:

TAB. 3. Total Viable Count (CFU/ m^2 hour) of outdoor and indoor samples in years

Nr.	Samples	TVC-2016	TVC-2017	TVC-2018	TVC-2019	TVC-2020
1	OGH-outdoor	$3.65x10^4$	$1.51x10^4$	$4.04x10^3$	$6.49x10^3$	$3.52x10^2$
1-1	OGH-indoor	$2.31x10^1$	$2.22x10^2$	$5.71x10^2$	$2.78x10^2$	$2.70x10^1$
2	FNS-outdoor	$7.23x10^5$	$8.85x10^4$	$4.44x10^3$	$5.59x10^3$	$4.55x10^2$
2-1	FNS-indoor	$1.22x10^3$	$7.41x10^4$	$3.02 x10^3$	$3.26 x10^2$	$2.20 x10^1$
3	NM-outdoor	$1.41x10^2$	$2.91x10^2$	$4.34x10^4$	$11.43x10^2$	$1.42x10^2$
3-1	NM-indoor environment	$2.45x10^1$	$2.90x10^2$	$9.10x10^3$	$3.33x10^3$	$2.53 x10^1$
4	MTS-outdoor	$1.39x10^2$	$2.78x10^2$	$6.71x10^3$	$6.71x10^3$	$5.67x10^3$
4-1	MTS-indoor	$1.25x10^2$	$3.44x10^2$	$7.39 x10^3$	$1.56 x10^3$	$2.30x10^1$
5	TLP-outdoor	$5.30x10^1$	$6.52x10^2$	$9.91 x10^2$	$4.98 x10^2$	$2.35x10^2$
5-1	TLP-indoor	$6.00x10^1$	$8.51x10^2$	$7.26 x10^2$	$7.36 x10^2$	$4.59x10^2$

SOURCE: **own study**

As can be seen from the table, the year 2019 marks a significant decrease in loads due to the monitored areas' infrastructural systematization. Increased loads in some outdoor and indoor environments can be associated with a higher number of people circulating there (MTS &TLP outdoors). In some indoor environments, ventilation was sufficient for microbial decontamination. In April 2020, there was a drastic decrease in air contamination due to local Covid-19 lockdown.

The percentage in years of the most critical microbial contaminants identified during qualitative tests are in Figures as follows:
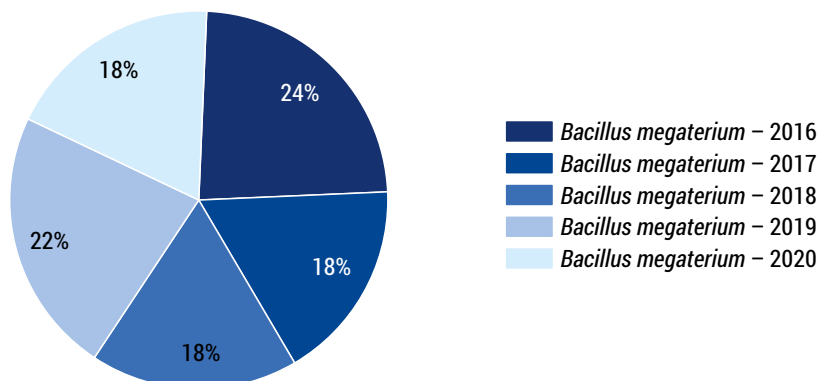
FIG. 2. Presence of Bacillus megaterium through years

SOURCE: own study

Figure 2 shows a decrease in the presence of *Bacillus megaterium* from 24% to 18%. It is a weak environmental pathogen. The reduction of the number of colonies of *Bacillus megaterium* is a reduction of the pollution in analyzed areas.
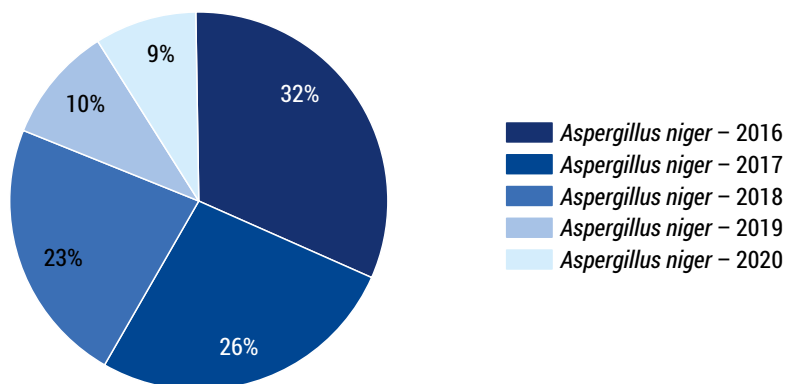
FIG. 3. Presence of *Aspergillus niger* through years

SOURCE: own study

Figure 3 shows a decrease in the presence of *Aspergillus niger* from 32% to 9%. It is a common environmental pollutant, that comes from soils, fruits, vegetables and other organic substances.

A comparison of results was made for some genera and species of fungi with significant presence, including pre-2015 evaluations. The total mold loads of *Aspergillus flavus*, *Aspergillus fumigatus*, *Rhizopus nigricans*, and *Cladospora spp.*, identified in years were calculated. Their reduction in years is shown in Figures 4, 5, 6 and 7.
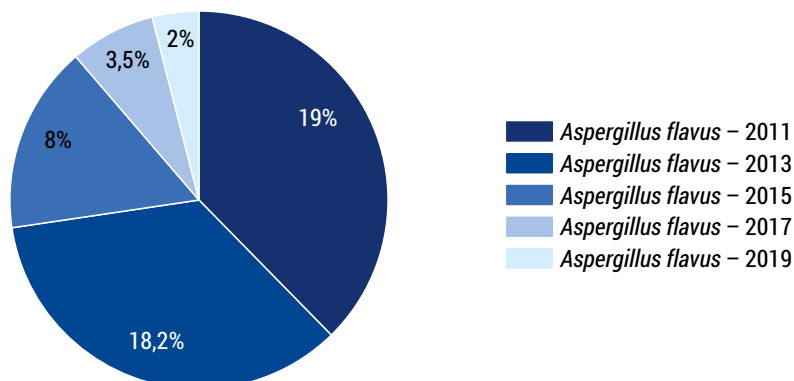
FIGE. 4. The reduction of the presence of pathogen *Aspergillus flavus* from 2011 until 2019

SOURCE: own study
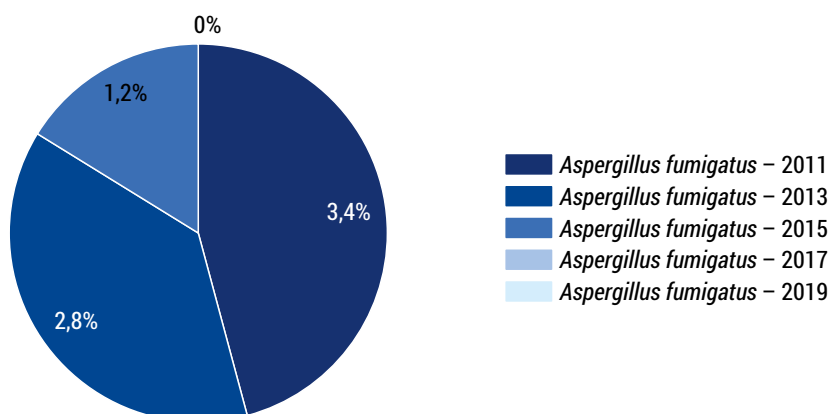
FIGURE. 5. The reduction of the presence of pathogen *Aspergillus fumigatus* from 2011 until 2019 (0.00% in 2017 & 2019)
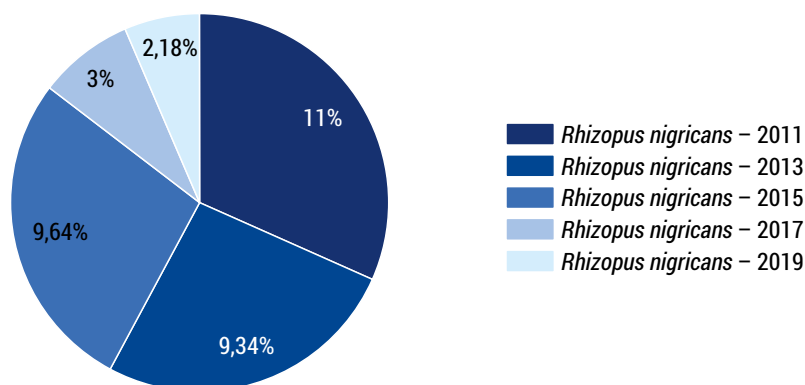
FIGURE. 6. The reduction of the presence of *Rhizopus nigricans* from 2011 until 2019
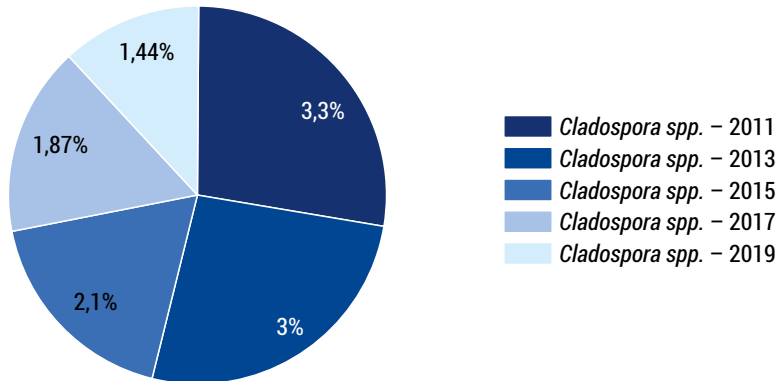
FIGURE. 7. The reduction of the presence of *Cladospora spp.* from 2011 until 2019

The above results testify to a positive environmental change over the years, but again there are opportunities for improvement and increased care.

Summary

In all cases, decontamination in years is evident. There has also been a decrease of Bacillus cereus (from 24% to 8%), *Aspergillus flavus* (source of an aflatoxin production), 11% to 3%, and a decrease in the presence of *micrococci, diplococci*, and streptococci.

Yeasts were observed rarely, such as *Saccharomyces spp.*, *Rhodotorula spp.* (no contaminants, the first, fermented yeasts and the second, important for the biomolecules production), *Aureobasidium pullulans*, and others.

Over the years, only 0.2% of yeasts were detected, among them *Candida albicans,* a pathogen, and source of human infections. In assessing microbiological air pollution during 2016 and 2017, a considerable presence of *Fungi imperfecti*, *Cladosporium spp.* and *Alternaria spp.* were observed onto the MTS and TLP outdoor samples.

Many factors have contributed the last years to the improvement of the microbial pollution situation in a developing and growing city such as Tirana:
- Improving the legal framework for pollution control and prevention.
- The implement of legal measures in practice, coordinating them with increasing community awareness.
- Obligation of construction companies to apply techniques for dust protection during constructions.
- Obtaining information in schools for the protection of the environment, air, soil, and water.
- Organization of different activities (scientific or not) with the community and specialists for the damages from all pollutants, including microbial ones.
- Vegetation growth, etc.

Our research contibute to the description and better understanding of micro-biological air quality, in urban enviroments, based on long-term collected data. It is important to know more about recent trends (positive or negative ones), in order to choose and suggest correctly the next interventional steps.

Literature

[1] Bekkari. H.; Benchemsi N.; Touijer. H.; Berrada. S.; Maniar S.; Ettayebi. M.; El Ouali Lalam. A.; "Microbial Analysis of Air in a Public Hospital in the City of Fez, Morocco", International Journal of Pharmaceutical and Clinical Research 2016; 8(6), pp. 533–537, ISSN- 0975 1556.

[2] Pepper. I.L.; Gerba. Ch. P.; Gentry. T. J.; *"Environmental Microbiology, 3rd Edition"*, Academic Press, 2014, pp.1–728, ISBN: *9780123946263*.

[3] Frashëri. M.; Prifti.D.; *"Practicum of Technical Microbiology"*, Publishing House "University Books", Tirana, Albania, 1997, pp. 145–149.

[4] Sattar. A.S; Richard J. Kibbee. R.J.; Zargar.B.; Wright.K.E.; Rubino. J.R. Khalid. M.I.; *"Decontamination of indoor air to reduce the risk of airborne infections: Studies on survival and inactivation of airborne pathogens using an aerobiology chamber". American Journal of Infection Control*, 2016, V.44, Issue 10, pp. 177–182, DOI: 10.1016/j.ajic.2016.03.067.

[5] Stetzenbach. L.D.; Buttner. M.P.; Cruz. P.; *"Detection and Enumeration of Airborn Biocontaminants"*, Current Opinion in Biotechnology, Elsevier 2004, Vol.15, Issue 3, pp. 170–174.

[6] Back. W.; *"Color Atlas and Handbook of Beverage Biology"*, Fachverlag Hans Carl, Nurnberg, Germany, 2006, pp. 1–309, ISBN 3-418-00799-6.

[7] Haleem. A.A.; Karuppayil. K.S.M.; *"Fungal Pollution of Indoor Environments and its Management"*, 2012, Vol.19, Issue 4, pp. 405–426.

[8] Pascuarella. C.; Pitzurra. O.; Savino. A.; *"Index of Microbial Contamination (IMA)"*. J.Hosp. Infect.2000, 46 (4), pp. 241–256, DOI: 10.1053/jhin.2000.0820.

[9] William. G. L.; Brett. J. G.; Francoise. M.; Blachere F. M.; Stephen B. M.; Brandon. F. L.; Jensen. P. A.; Schafer. M, P.; *"Sampling and Characterization of Bioaerosols"*, *"Manual of Analytical Methods"* (NMAM), 5th Edition, Department of Health and Human Services Centers for Disease Control and Prevention. National Institute for Occupational Safety and Health-NIOSH, USA, 2017, pp.1–115.

[10] Napoli. Ch.; Marcotrigiano. V.; Montagna M.T.; *"Air Sampling Procedures to Evaluate Microbial Contamination: A Comparison Between Active and Passive Methods in Operating Theatres"*, Biomed Central, BMC Public Health *2012(1) pp. 594, DOI:* 10.1186/1471-2458-12-594.

[11] Prifti. D.; Troja. R.; Shabani. L.; Xhangolli. L.; Petre. A.; *"Air Microflora in Tirana Environments"*, Publishing House "Mihal Duri e Re", Tirana, Albania, 2004, pp. 1-100.

[12] Grisoli. P.; Albertoni. M.; Rodolfi. M.; *"Application of Airborne Microorganism Indexes in Offices, Gyms and Libraries"*, Applied Sciences, 2019, 9(6), 1101; DOI: 10.3390/app9061101.

European experience of waste management and implementation of best practices in Ukraine

Abstract: Development of waste management system in the European Union is studied. The waste management practice in a range of the EU countries is analyzed. Main principles of solving the problem of managing waste in the EU are revealed. Comparison of indicators for waste management in the EU and Ukraine is provided. The dominant European trends among other areas of waste – "zero waste" and "circular economy" – are identified. The regulatory framework for waste management developed in Ukraine as a step towards international environmental safety standards is discussed.

Introduction

Our generation is responsible for solving the environmental problems facing the world. Improving living conditions (public health) and productivity of natural resources depend on the quality of waste utilization, so the issues of reducing the environmental hazards caused by waste accumulation are actively discussed in the scientific community. In Ukraine, the main attention is paid to the assessment of the polluting impact of waste storage sites. To a lesser extent, general issues of waste management, in particular environmentally sound management, have been addressed. To ensure their effectiveness, it is necessary to study the experience of other countries, especially the European Union (hereinafter – EU), for which, regardless of the level of economic development, a common policy in the field of waste management is developed. The proposed ways to solve this problem can be useful for study and implementation in Ukraine.

The aim of the study is to analyze the development of the waste management system that has been developed in the EU and to illustrate it by the practice of the most developed countries in this regard (within the execution of the Jean Monnet Module "An interdisciplinary approach to waste management study: implementing the EU practices" (621029-EPP-1-2020-1-UA-EPPJMO-MODULE).

Legislative aspects of waste management in the EU

The main ways for waste management for the world community were identified at the International Conference on Sustainable Development in Johannesburg in 2002 [1]. These include waste prevention, maximum reuse and recycling, and the use of alternative environmentally friendly materials. Implementation of the planned ways will minimize the negative impact of waste on humans and the environment and increase the efficiency of secondary resources.

In the EU countries, along with national measures, the development of general strategies makes a great contribution to waste management. The processes of generation, accounting, processing and disposal of waste are regulated by a number of documents, which can be divided into two major groups – programme and regulatory. Programme (Action Programmes) ones – have a framework character, define the main goals for the EU countries in the medium or long term (usually from 3–5 to 10 years or more). Normative documents (agreements, directives, rules, regulations, etc.) are the ones required for execution. They can be of a framework nature (for example, the Waste Framework Directive) or relate to specific tasks (for example, regulation of emission limit values for waste incineration, landfill technology). The EU Action Programmes are strategic documents that set specific targets to be achieved in the long or medium term.

For example, in developing an EU Sustainable Development Strategy, it was decided that the link between production growth and waste generation should be broken. General waste management issues are covered in the Waste Framework Directive (2006) [2]. The document provides a list of substances that can be classified as waste, individuals or organizations are required to bear the costs of waste disposal (the polluter pays principle), establishes a hierarchy of desired methods of waste management: "Prevention of generation or minimization of sources → reuse → processing into raw materials and products → composting → incineration or burial with energy → burial without energy → incineration without energy". It took 20 years for Poland to reduce the share of municipal waste disposal from 98% to 42%. The EU financial support has been one of the determinants of this shift. It took the Czech Republic the same amount of time to reduce this figure from 93% to 49%. Financial support from businesses through the Extended Producer Responsibility (hereinafter – EPR) policy approach has been one of the main drivers of such progress. In addition, in 4

years, the Czech Republic will have a complete ban on the disposal of unsorted mixed municipal waste, which has been in force in many EU countries since the early 2000s. The development of waste management systems in some countries will be discussed later in the paper.

The Environment Action Programme for 2002–2012, adopted by the European Parliament and the European Council [3], reflected a gradual reduction in the amount of waste destined for disposal: by 20% in the period of 2000–2010 and by 50% by 2050. Therefore, waste generation should grow 15% slower than the gross national product of the EU. The Waste Incineration Directive [4] sets emission limit values for incinerators and cogeneration units. It lists the fractions of municipal waste that must be collected separately and are not subject to incineration. The Landfill Directive [5] sets out measures to reduce the risk to human health. It regulates the treatment of waste before burial, separation and separate processing of hazardous and safe waste, control over landfills during their operation and after closure.

In the United Kingdom (hereinafter – UK), a project on the distribution of biodegradable packaging materials is being implemented on the basis of a voluntary agreement between supermarkets and the Waste and Resources Action Programme [6]. The agreement was signed by 35 large retail chains and distributors, representing 92% of the country's grocery market. At the same time, the country is developing a project to "halve landfills", aimed at reducing waste generated during construction or demolition. In France, Eco-Emballages [7] provides training and advice to anyone, but mostly engineering students, on packaging waste minimization. Belgium is implementing a regional program (Flanders) [8] to significantly reduce household waste, while part of the waste after grinding is used for energy. In Ireland, the so-called Green Business Initiative operates under the auspices of the National Waste Prevention Committee, which provides assistance to businesses and organizations in three areas – waste, water and energy [9].

"*It's smart with less waste*" programme is being implemented in Finland. It works with private entrepreneurs, municipalities and households. In Hungary, the re-use of building materials and their exchange between construction companies is becoming more common: exchange items cover 12 categories – brick, tile, wooden components of construction, window frames and others. In Austria, the Act on Waste Management (2002) regulates the initial ecodesign of products, the appropriate organization of production and distribution processes and work with consumers [10].

Waste reduction is one of the key reforms of the Grenelle Environment Round Table [11], which proposed legislation aimed at increasing recycling to 35% in 2012 and 45% by 2015. This has been successfully implemented. The annual recycling of waste, mainly household waste (28 MT), municipal waste (14 MT) and industrial waste (90 MT), which together account for 132 MT, represents only 16% of the total amount of waste generated (849 MT), including waste from agricultural and construction activities (717 MT). However, France offers a better solution for the recycling

process: in this country, 38.7 million tons of material is recovered from the waste stream and converted into 31.9 million tons of raw materials. This sector is represented by 2,400 companies employing 31,500 people.

Since 1992, eco-packaging has played a key role in the organization of selective processing, in the work of organizations specializing in specific materials, such as Aliapur (rubber tires), Valorplast (plastic / household packaging), Ecopse (polystyrene), Recyfilm (plastic films), Ecofut (plastic containers), Motus-Véolia (paper and documents) and Adivalor (agricultural waste). These companies have set tariffs for the repurchase of waste from collectors and purchase prices for processing plants. This sector is particularly attractive to international investors.

The legal regulation of hazardous waste disposal in England and Wales is almost entirely based on the EU legislation. One of the most important documents in the field of waste disposal regulation in the EU legislation today is the Waste Directive 2008/98 / EC3 [12]. British legislation on the disposal of hazardous waste is based on two regulations adopted in accordance with the EU law. These are The Waste (England and Wales) Regulations (2011) [13], and the List of Wastes (England) Regulations (20 05) [14] which implements into the English law the European Waste Catalog approved by the above Decision of the European Commission 2000/532/EC6 [15]. The main principle of The Waste Regulations is the need for strict accountability of enterprises engaged in the processing and disposal of hazardous waste.

The most important document regulating the waste incineration process in the EU is the Industrial Emissions Directive 2010/75/ EU8 [16]. This document sets out the specific technical requirements that waste incineration plants must meet, including those aimed at generating electricity. In 2013, this Directive was implemented in English legislation by amendments to the Environmental Permitting Regulations in 2010. The public policy program can be reduced to the six theses, which were previously formulated in the Strategy for Hazardous Waste Management in England 2010 published by the Department of Environment, Food and Rural Affairs of Great Britain [17].

"Economy of recycling" is being paid attention nowadays: recycling turns waste into a resource and prevents the costs that would occur if they were disposed of at the landfill. This type of waste treatment also creates additional jobs. It is established that the removal of 10 tons of waste to the landfill creates 6 jobs, and the recycling of the same 10 tons – 361 jobs. Additional economic effect is achieved when recycled waste is used "on site", eliminating the need to import this category of materials from other places or other countries. A country may not produce paper, but receives it by recycling waste: this is the strategy that increasingly is being implemented in the EU. Recycling, like no other waste management method, paves the way for significant resource savings. In the production of aluminum, it saves up to 95% of energy, copper – 85%, steel – 74, lead – 65% [18]. Glass can be recycled any number of times without loss of quality or purity, while acquiring a variety of shapes; at the same time for each ton of recycled glass a ton of natural raw materials is saved. An important and not always easy to solve problem is the processing of construction

waste and demolition of buildings (hereinafter – construction waste). Construction waste accounts for a third of all EU-controlled waste: concrete, brick, tile, wood, glass, plastic, gypsum, bituminous mixtures and resins, metals (ferrous and non-ferrous), stones, insulating materials, chemicals, packaging materials etc. The main task in this direction is to reduce this class of waste by 70% (by weight) by methods of reuse and / or recycling: today in the EU countries reuse ranges from 10 to 90% [19].

Due to the rapid development of organic agriculture and methods of production of alternative fuels, the recycling of biowaste is becoming increasingly important. This category includes: 1) food waste; 2) organic waste ("any waste of vegetable or animal origin"); 3) biodegradable waste ("any waste that decomposes anaerobically or aerobically, such as food or garden waste as well as paper and cardboard"); 4) biowaste ("green mass of gardens and parks, food and kitchen waste from households, restaurants, cafes and food enterprises") [20]. Composting is an ideal way to recycle organic kitchen, garden and agricultural waste. Large composter plants are covered by the European Compost Network, which has 72 associate members from the 27 EU countries and serves more than 3,000 companies [21]. A network of "eco-volunteers" has been created in Italy. They have conducted trainings among the population on "selective" collection of food waste, which later began to be used by up to 80% of households in the communes; 90% of households, as the analysis testified, have mastered the methods of home composting "at the appropriate level"; fee for the removal of household waste has been reduced everywhere. In the county of Kent (UK), in a similar project 95 thousand households were involved.

The next level of the "waste management hierarchy" is "other uses". In the EU documents, this is covered by the term "waste-to-energy". The physical basis of the technologies used in this area is the incineration of waste in special plants. In some EU countries (Germany, Belgium, Sweden, the Netherlands, Austria, Denmark) the percentage of waste sent to landfills today is in the range of 1–2%; while 35–50% of waste is incinerated in different ways and 50–60% is recycled and composted. In all these countries, landfilling without prior treatment is prohibited by law [22].

In this regard, special attention is drawn to the concept of "energy balance", proposed by the working group of the World Energy Council: the energy obtained should cover the energy costs of waste recycling. Another promising way to recycle waste for energy purposes is the biogas production. Directive 2009/28/EC, known as the Renewable Energy Directive, set a goal for Member States to achieve 20% renewable energy consumption by 2020 "in all sectors" and at least 10% in the transport sector [23]. In the future, it is estimated that biomass will provide up to two-thirds of renewable energy in Western Europe. The share of biogas as a transport fuel is growing systematically in Germany, France, Sweden and Switzerland and the "green transport" appears.

With regard to landfills, it should be noted that the EU documents define this method as the "least desirable option", which should be kept to a minimum. According to the European directive it is forbidden to place the following types of waste

on landfills: 1) liquid; 2) flammable; 3) explosive or oxidizable; 4) medical (because there is a risk of infection); 5) car tires; 6) some other species. The directive also stipulates that landfills are only permitted for pre-treated waste.

In 2015, the European Commission adopted the program "Closing the loop – An EU action plan for the Circular Economy" [24]. The central idea of the programme is "everything that is possible should be recycled": "the transition to a more circular economy, where the value of products, materials and resources is maintained in the economy for as long as possible, and the generation of waste minimised, is an essential contribution to the EU's efforts to develop a sustainable, low carbon, resource efficient and competitive economy". Nowadays sustainable development is shaped with the principle of using fewer resources per unit of output and the concept of circular economy is being developed as a fundamental component of the "green economy" [18; 25].

According to the estimations of the Ellen MacArthur Foundation [26], the EU companies which produce durable goods will be able to save up to 630 billion dollars annually in 2025 due to the emphasis on the circular economy. At the level of households, transport, housing and food industry costs may decrease by 25% in 2030. The financial platform of the circular economy in recent years has focused mainly on the following three tasks: promotion of best practices in order to attract potential investors and other stakeholders; analysis of specific projects and their financial needs; financial consulting; coordination of the activities of enterprises operating in the circular economy; promotion of circular economy projects and organization of their financial support; lending to business organizations engaged in the circular economy, especially for medium- and long-term projects. In 2020, 40 billion euros were spent on municipal solid waste management by the European Investment Bank [25].

Waste management practice in the selected EU countries

It should be noted that the most active environmental policies are implemented in Sweden, Denmark, Germany, and the Netherlands.

Sweden has a system for sharing responsibility for waste collection and treatment. Households (municipalities) are responsible for the separate collection and disposal of waste in appropriate containers; collection points are usually within 300 m of any household. Homeowners pay an average of SEK 2,000 a year for waste collection. The number of fractions (different factions are taken out on different days of the week) varies from municipality to municipality and can reach a number of 10–15. Garbage collection on the roadsides is also organized.

Depending on the profile of their activities, Swedish manufacturers are responsible for the organization of systems and the order of collection of their waste; at the same time, they must provide consumers with relevant information. There

is the responsibility of all kinds of business structures: they collect everything else that is not collected by households and producers. According to established practice, the manufacturer can either organize the collection and export of their packaging and containers (which is burdensome and almost impossible), or on certain contractual terms to transfer this responsibility to companies that are part of the "dual system". In the latter case, under the terms of the license, such manufacturer receives a "Green Dot" (der Grune Punkt) – a special sign (icon), which means that the manufacturer has covered in advance all the costs of processing their waste and guarantees the receipt and recycling of labeled packaging material. Subsequently, the "dual system" along with paper and cardboard packaging covered a range of waste – plastics, glass, aluminum and composite materials.

Today, the level of landfills in Sweden has dropped to less than 1%. Approximately 6,000 recycling stations operate separately, collecting packaging, newspapers, all other waste paper and other types of waste: the network is built on the principle of EPR, which ultimately finances this work. The upper level of this system is thermal power plants (unless the waste is sent to biogas production): today in Sweden there are more than 30 powerful incinerators. Their combined capacity is such that they lack their own fuel to ensure smooth operation, and Sweden imports significant amounts of waste, mainly from Norway, the UK and Ireland: more than 1.5 million tonnes a year [27]. Around 20% of domestic demand for domestic heat today is covered by waste incineration.

Today, two-thirds of the country's bus fleet runs on renewable fuels. Transport biomethane is produced in a dozen of cities in Sweden – in Örebro, Uppsala, Västerås, the provinces of Södermanland and Östergötland, around Stockholm and elsewhere.

The Danish model of waste management [28] is shaped with a clear division of roles, responsibilities and competencies between members of the system – state, regional and local authorities, waste generators and waste management companies. The structure of all waste management activities: the system covers all types of waste (domestic, industrial and hazardous); the full responsibility lies with the local government, which determines the methods of waste collection and further treatment – the rules that are strictly guided by waste generators; strict adherence to the "polluter pays" principle; the whole process is based on the principle of separate collection. The national goal set out in the Energy Agreement is to ensure full independence of Denmark from fossil fuels by 2050, in connection with which a sharp increase in funding for bioenergy projects is expected.

Kalundborg is a city in Denmark, which created the world's first industrial symbiosis with the concept of a circular economy. The interaction of the participating companies is based on the principle that the balances from the production of one company become a resource for another, and at the same time all reduce economic costs and reduce CO_2 emissions. In addition to the environmental impact, the consortium members save € 24 million on operating processes each year.

According to its technical level, the waste management system in Germany is one of the most developed in the world where level of various waste streams treatment had significantly exceeded the average European level. Thus, more than 90% of household waste is recycled, while for Europe as a whole this figure (in average) accounts for 37%. The overall recycling rate of various materials in Germany exceeded 80%; more than 70% of paper, 94% of glass and 45% of steel are being made from "secondary" materials [29]. Recycling plastic bottles saves such an amount of energy that would supply heat to almost 2 million Berliners in 130 days. Data on German experience in waste disposal, waste incineration and recycling are shown in Fig. 1.

	1998	1999	2000	2001	2002	2003	2004	2005	2006	2007	2008	2009	2010	2011	2012	2013	2014	2015	2016	2017	2018	2019	2020
■ waste disposal	34	29	27	26	22	19	18	1	1	1	0	0	1	0	0	0	0	0	0	0	0	0	0
▫ waste incineration	20	20	21	22	22	23	25	34	34	34	34	34	34	33	34	33	32	32	32	32	32	32	32
■ recycling	46	51	52	52	56	58	57	65	65	65	66	66	65	67	66	67	68	68	68	68	68	68	68
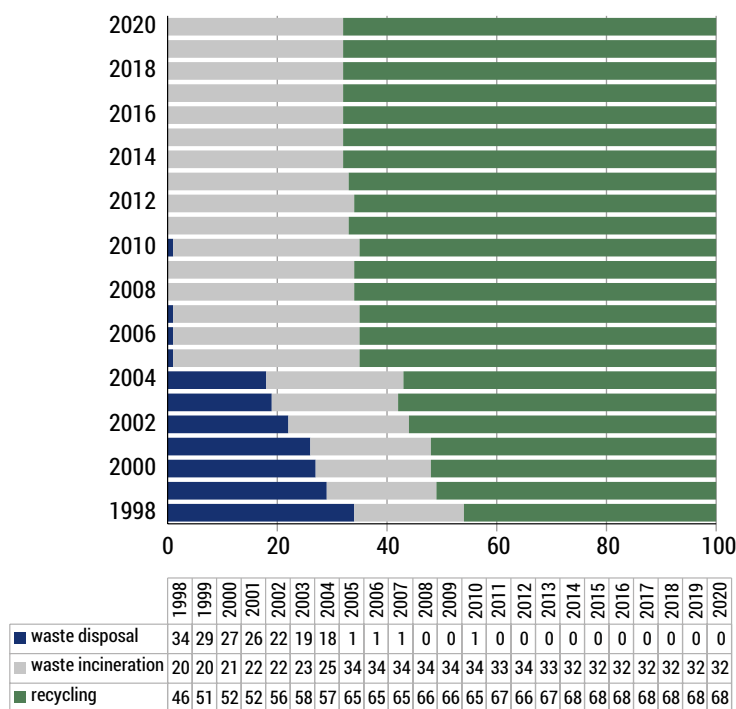
FIG.1. German experience in waste disposal, waste incineration and recycling in 1998–2020, %

Back in the 1960s, there were more than 50,000 existing landfills in Germany, no significant security measures were envisaged at the landfills. Most of them have been closed since 1980, and about 150 large and well-organized landfills have continued to operate. In 2005, the disposal of household waste at landfills without intensive pre-treatment has been prohibited. Today, household waste that cannot be recycled is incinerated or undergoes intensive mechanical and biological processing. All valuable materials, in particular metals, must be removed and put back into circulation, and elements with high heat capacity must be used as fuel substitutes. The remaining waste is fermented and decomposed, i.e. treated biologically so that when placing

humus on the landfill no gases are released and there is no risk of subsidence. Separate collection of recyclable waste has been identified as a necessary component for an efficient waste management system and has become mandatory for major recyclables. Today most of the waste can be handed over directly to the area adjacent to the house.

That is why today in Ukraine inside residential areas there are separate containers for residual waste (gray container), paper (blue container), packaging (yellow bag or basket) and organic waste (green or brown container). Glass is mainly collected in separate containers, usually divided by the color of the glass (white, green, brown or multicolored). In addition, you can recycle large waste, including electrical equipment. Many types of waste, such as batteries, fluorescent lamps, etc. can be handed over at the place of purchase of these goods. The obligation of the point of sale to accept this waste is regulated by the relevant laws [30].

In the Netherlands, the task of gradual progress to the circular economy is approved at the state level and is the national priority. In 2014, a special program, RACE – "The Realization of Acceleration of a Circular Economy" [31], has been developed. Since 2016, the so-called "government-wide" program "Circular Netherlands until 2050" has been initiated. Since 2016, the "government-wide" programme "Circular Dutch Economy by 2050" was initiated. The programme provides two time periods, where for the first one until 2030 – an (interim) objective of a 50% reduction in the use of primary raw materials (minerals, fossil and metals). There are five priority sectors (programmes) that need priority attention in terms of expanding the "circular economy": biomass and food, plastics, the manufacturing industry, construction sector and consumer goods.

Dutch experts identify nine levels of the "circular economy" – the so-called 9 Re: refusal to overuse raw materials (Refuse); reduction of raw material use (Reduce); Reuse; maintenance and repair (Repair); Refurbish; production of new products from elements of the old (Remanufacture); use of the product for other purposes (Repurpose); recycling and reuse of materials (Recycle); energy production from materials (Recover).

Increasingly, "circular" methods are used in urban construction. In circular Amsterdam, as the Dutch experts write, "the emphasis is on "reasonable demolition" (structural elements and materials are preserved that can still be used in new construction). Houses are built in a "modular and flexible" way, which provides for the possibility of remodeling houses without radical reconstruction [32].

Poland, on the basis of the EU directives, has adopted the Act on Maintaining Cleanliness and Order in Municipalities (1996), the Act on packaging and packaging waste management (2013) and other laws which define the terms and basic principles of waste management, as well as methods of processing, utilization and disposal of waste. The permit for waste generation is issued by the voivodship (regional council) or county (district council). This permit applies only to waste generation by enterprises. The commune (gmina, local government) does not receive a permit for waste generation. Legislation in the field of waste management in Poland regulates the development of waste management plans at two levels: national and voivodship (regional). The plans should apply two basic principles of waste management: self-sufficiency and proximity of location.

The dynamics of changes in the structure of solid waste management in Poland over the period of 1998–2018 is shown in Fig. 2. The situation with landfills in Poland began to change after the country joined the EU. Poland has agreed with the EU on a transitional period for landfills. An important stage in solving the problem of waste was the so-called "waste revolution" during 2012–2013, when the state fully transferred the issue of municipal waste to local governments. Since then, it is the local authorities in Poland that set the prices for the residents of the houses for garbage removal, and are also responsible for the implementation of the EU directives in this area, including waste sorting and recycling. In order to minimize the possibility of fires in landfills, Poland has banned the storage of flammable and explosive substances on them. Many Polish landfills have been modernized and technically equipped with the EU funds. In 2015–2016, six new waste incineration plants were opened in Białystok, Bydgoszcz, Kopin, Kraków, Poznań and Szczecin and in 2018 – in Rzeszów. The European Commission has approved the allocation of 100 million euros for the construction of two new incinerators in Poland.

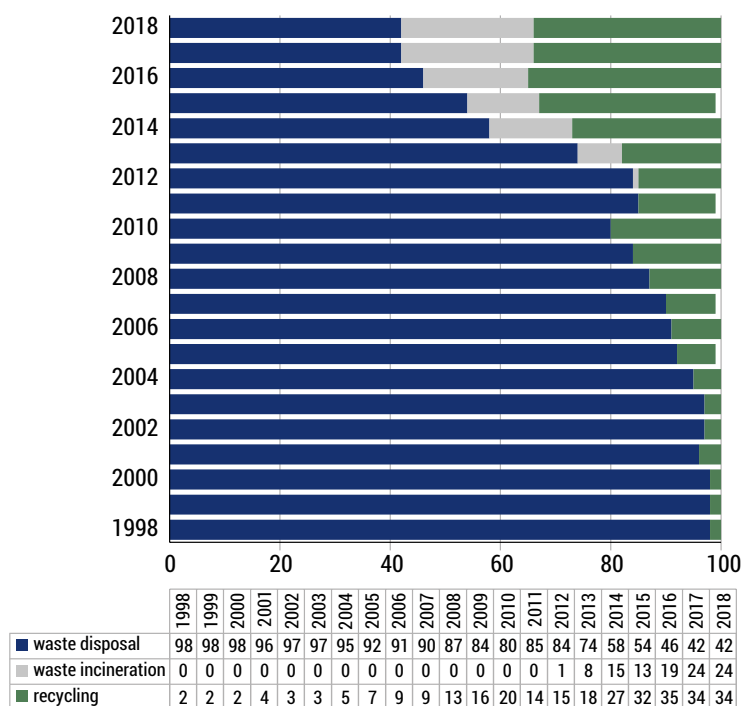|	1998	1999	2000	2001	2002	2003	2004	2005	2006	2007	2008	2009	2010	2011	2012	2013	2014	2015	2016	2017	2018
■ waste disposal	98	98	98	96	97	97	95	92	91	90	87	84	80	85	84	74	58	54	46	42	42
▦ waste incineration	0	0	0	0	0	0	0	0	0	0	0	0	0	1	8	15	13	19	24	24
■ recycling	2	2	2	4	3	3	5	7	9	9	13	16	20	14	15	18	27	32	35	34	34

FIG. 2. **Polish experience and dynamics of change in the structure of solid household waste treatment in 1998−2018, %**

SOURCE: **[33−35]**

In the early 2000s, Poland was similar to Ukraine as it is now, both in the volume and morphology of solid waste and in the state of waste management infrastructure.

In 15 years, the country has managed to reduce waste disposal from 97% to 42%. First, the recycling industry has been developed successfully, due to work with the publics to encourage sorting in particular. Secondly, there was a real boom in the construction of incinerators in the country. By moving from the lowest level of the waste management hierarchy (disposal) to the penultimate (recovery), Poland has strengthened its energy independence through the use of waste-to-energy technology. The requirement for the treatment of used oils is not to burn, but to regenerate. Legislation also regulates the management of biodegradable waste (greens and food), as well as the obligation to collect and compost it separately. There are two areas of waste management that are subject to biodegradation: composting, with the resulting methane emitted into the atmosphere and anaerobic fermentation with its subsequent combustion and generation of electricity. According to the waste management plan, municipal waste cannot be taken out of the region. This requirement does not apply to certain hazardous wastes, the recycling facilities of which are not available in the region. GOAP [36] and waste collection companies control the movement of machines and the accuracy of the declared number of persons in the submitted declaration. In Poland, the law regulates the issuance of a mandatory waste transfer card, which is issued by the waste-generating company in triplicate. The waste generator is responsible for what happens in future with the waste.

The experience of Slovenia is also worth of attention. Residents of the city of Ljubljana pay up to 10 Euros per month from one household, which has a conditional 2.2 people. Residents have the opportunity to sort waste in five different containers: mixed waste, organic waste, packaging, glass, paper. All waste is taken by the municipal company. However, residents pay only for mixed and organic waste. Exemption of the rest waste is covered by the sale of this waste as a secondary raw material and due to the operation of EPR systems (for packaging), which was proposed by the EU Directive. Access to public containers for displacement is created using an electronic resident card. Residents of individual houses have their own waste containers and float for waste depending on the volume of the containers. Significant role in Ljubljana in measures to prevent waste generation is given to municipalities and the local waste prevention programme is adapted and designed to involve all stakeholders. Individual composting and design changes for certain products (such as coffee capsules), access to drinking water in public places (to minimize the number of plastic bottles), the opening of repair shops, collection points for used products which can be reused, introduction of a green procurement system for municipalities, approval of rules and standards for public events by the municipality, development of a food waste management programme etc. can help prevent the waste generation.

The public company Snaga Ljubljana [37] is the largest Slovenian municipal waste management company. Snaga also manages municipal public and green areas, public toilets etc. The company supports Ljubljana's regional parks. It created an expert

group for the care and maintenance of urban trees. Snaga sees itself as a leader in developing and implementing sound waste management solutions that can be delivered in an environmentally conscious and cost-effective way. The main focus of the company is on waste prevention, in particular through cooperation with the municipality and encouraging the transition of Ljubljana to a closed-cycle economy, waste reuse and recycling. Thirteen years ago, Snaga Ljubljana started collecting biowaste separately. From them pure and qualitative compost by anaerobic fermentation is made. Such compost is sold to residents or farmers. During the production of such compost, biogas is formed, which is burned to produce electricity.

The path of the Czech Republic can be characterized in several stages. The data on waste disposal, waste incineration and recycling in this country is shown in Fig. 3. The first steps were taken in 1986–1989 when the old incinerators in Brno (248 thousand tons of waste per year) and in Prague (310 thousand tons of waste per year), which were built in 1905 and 1930 respectively, were reconstructed. The first Waste Act 1991 was adopted in 1991.

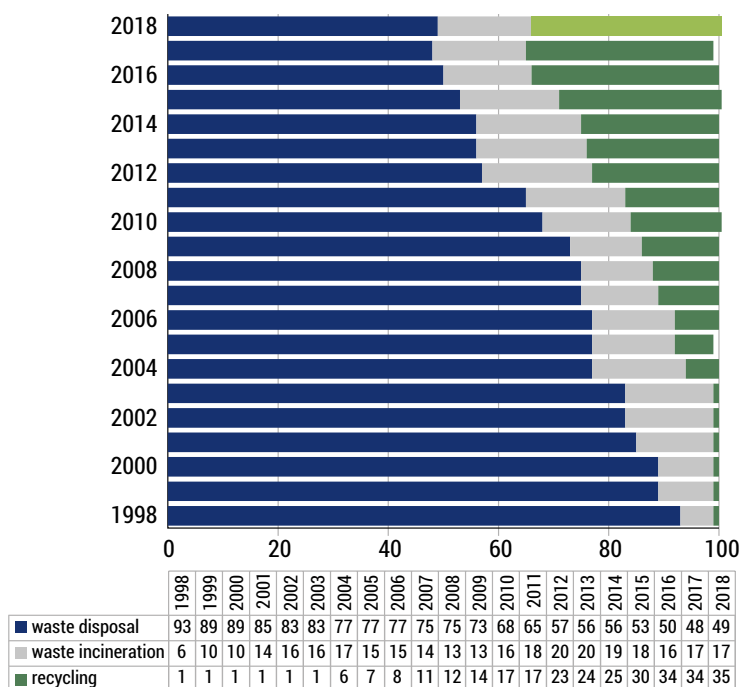|	1998	1999	2000	2001	2002	2003	2004	2005	2006	2007	2008	2009	2010	2011	2012	2013	2014	2015	2016	2017	2018
waste disposal	93	89	89	85	83	83	77	77	77	75	75	73	68	65	57	56	56	53	50	48	49
waste incineration	6	10	10	14	16	16	17	15	15	14	13	13	16	18	20	20	19	18	16	17	17
recycling	1	1	1	1	1	1	6	7	8	11	12	14	17	17	23	24	25	30	34	34	35

FIG. 3. **The Czech Republic experience in waste disposal, waste incineration and recycling in 1998–2018, %**

In 1992 a tax on waste disposal (up to 1 euro per ton) was introduced and the State Environmental Fund was established. In 1999, a waste incineration plant was built in Liberec (96 thousand tons of waste per year), and in 2001 the waste hierarchy

was determined, the foundations of EPR were laid, and tariffs for waste management, including waste disposal, have been determined (Waste Act 2001). In 2002 the extended principles of the EPR of packing (Waste Act 2001) have been fixed, in 2003 Waste Management Plan until 2014 (2003–2014 Waste Management Plan) has been approved. In 2004, the Czech Republic joined the EU and in 2007 an amount of 776 million euros became available to the Czech Republic under the EU Waste Management Program (2007–2014). In 2009, the landfill tax was increased to 19 euros per tonne (in 2007 it used to be 15 euros, in 2002 – 7 euros). In 2014, a ban on the disposal of unsorted mixed municipal waste from 2024 has been introduced. The next step was to approve a program to prevent waste generation by 2024 in various sectors of the economy, including: dissemination of quality information among businesses and households, inclusion of lessons in schools, research etc. (2015–2024 Waste Prevention Program). The waste management plan until 2024 focusing on waste prevention, recycling, reuse, transition to a circular economy (2015–2024 Waste Management Plan) has also been approved.

Since 2015, mandatory separate collection of biowaste has been introduced in all municipalities. The main priorities from 2019 remain: increasing the landfill tax, avoiding the construction of an excessive number of incinerators and mechanical and biological plants, increasing the level of recycling, including biowaste, using the principle of "pay-as-you-throw". The Ministry of the Environment of the Czech Republic has drafted a law on waste. One of the innovations is new garbage cans. It is assumed that black tanks should be filled the slowest and garbage from them will have to be removed less often than from others. By 2030, the Ministry plans to raise the fee for waste disposal by more than three times. In addition, due to the new tracking system, City Hall will be able to calculate the unauthorized release of waste and remove it. From 2025, textile sorting will be introduced. By 2026, all the EU member states are obliged to reduce the consumption of plastic tableware.

The Lithuanian experience in waste management is also worth of being studied. Regulation of the waste management system in Lithuania began in 1998 (with the adoption of the Law on Waste Management). Waste management in Lithuania is coordinated by 10 regional centers in 10 waste management regions. Self-governments are the main institutions that organize the management of waste generated on their territory. The main goal of self-government is to create an effective solid waste management system. The tasks of local governments are: to ensure the availability and high quality of services in the field of solid waste management; equip places for separate collection of secondary raw materials (paper / cardboard, glass, plastics, metals), large and hazardous waste; to ensure the collection and treatment of municipal waste that can be biodegradable; perform tasks to reduce waste at landfills. Since 2013, 75% of municipal waste has been collected, recycled or otherwise used separately; only treated solid waste is deposited at landfills.The share of solid waste processing in Lithuania is shown in Fig. 4 (government data). Today in Lithuania more than 800 old landfills are already closed and rehabilitated.
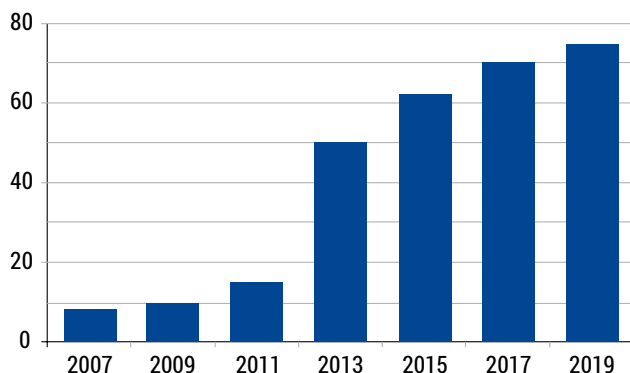
FIG.4. The share of solid waste processing in Lithuania in 2007–2019, %

Eleven regional modern landfills for solid waste have been opened and operated. Currently, there are 70 sites for the collection of bulky waste in Lithuania and 13 sites for composting green waste (capacity ≈ 34,000 tons / year).

In the city of Klaipeda there is a thermal power plant that uses solid waste (after pre-sorting) as fuel together with biomass. In Lithuania, there are: one nationwide hazardous waste landfill with an area of 7880 m^2 near the city of Siauliai, 32 additional sites for composting green waste, 7 additional sites for bulky waste, 9 mechanical and biological treatment plants, 2 "waste to energy" stations in Vilnius and Kaunas, the system of using the high-calorie fraction of solid waste at the cement plant. Data on biodegradable solid waste disposal in Lithuania in the period of 2007–2020 is given in Fig. 5.

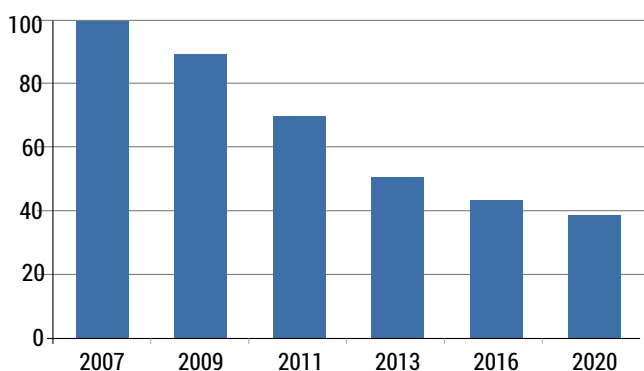FIG.5. Disposal of solid household waste in Lithuania, 2007–2020, in %

Thus, today the European trends of "zero waste" and "circular economy" among other areas of waste are dominant and aimed at benefiting the environment, rather than polluting it.

Ukraine's performance in the area of waste management

For several years, within the requirements of the Association Agreement between Ukraine and the EU, the regulatory framework for waste management in Ukraine has been developed. In particular, the National Waste Management Strategy until 2030, the Law of Ukraine "On Housing and Communal Services" and the draft Law of Ukraine "On Waste Management" 2207–1d, which passed the first reading in the Verkhovna Rada, are aimed at accelerating the country's movement towards international environmental safety standards. The comparison of some indicators for waste management in Ukraine and the EU is given in Table 1.

It should be noted that despite the smaller volume, the indicators of waste management efficiency in Ukraine, unfortunately, are not in favor of Ukrainians. And this applies not only to the areas of separate collection and processing, but also to basic indicators. For example, 22% of the Ukraine's population does not have access by household waste removal services at all. And even where there is an adequate infrastructure, there are other problems, such as unauthorized landfills. In 2019, about 27,000 such illegal dumps were discovered.

TABLE 1. Indicators for waste management

Indicators	Municipal recyclable waste, including composting	Municipal waste buried in landfills	Separate waste collection	Penalty for separate waste collection
EU countries	48%	23%	89%	€ 5000
Ukraine	3%	94%	5%	€45

SOURCE: **[38; 39]**

The National Waste Management Strategy until 2030, approved by the Cabinet of Ministers of Ukraine in 2017, has many goals for Ukraine. For example, the level of municipal waste disposal should decrease from 94% to 35% by 2030 (Fig. 6).
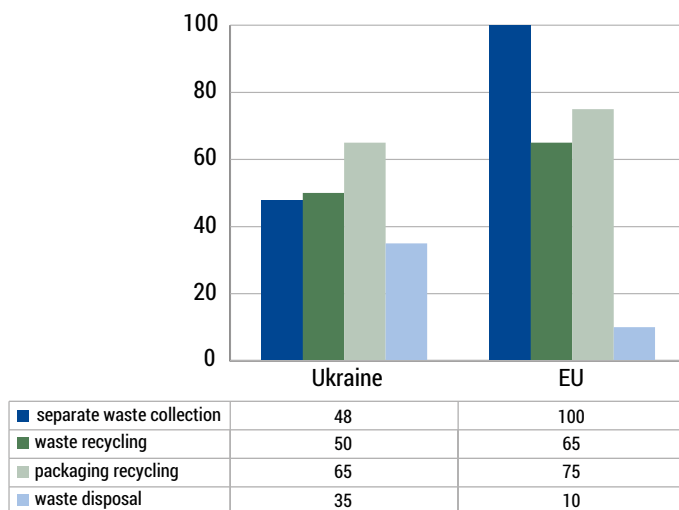
	Ukraine	EU
■ separate waste collection	48	100
■ waste recycling	50	65
■ packaging recycling	65	75
■ waste disposal	35	10

FIG. 6. **Waste management indicators until 2030 in Ukraine and the EU**

That is, in 13 years Ukraine needs to go the way that other countries took almost twice as long. Achieving the indicators set out in the National Waste Management Strategy and the National Waste Management Plan requires effective joint work of all stakeholders: central and local authorities, business, the publics, international partners and volunteers. The main tasks facing Ukraine in the light of the implementation of the EU practices are analyzed and comparison with the best European practice is given (Fig. 7).

	The Czech Republic	Ukraine	Poland	Germany
■ other	17	22	28	22
■ plastic	2	7	12	13
■ glass	2	5	10	10
■ metal	8	4	2	1
■ paper cardboard	9	25	11	24
■ organic food waste	62	37	37	30

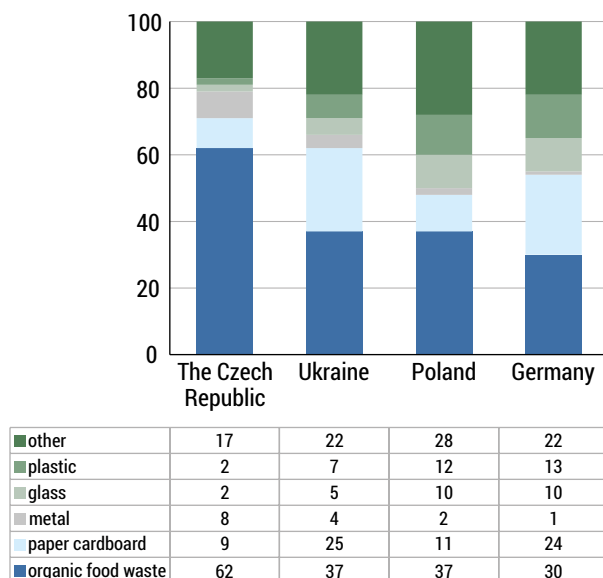FIG. 7. **Composition of solid waste in the Czech Republic, Ukraine, Poland and Germany, %**
SOURCE: **[40]**

One of the priority tasks is the introduction of mandatory separate collection of household waste. Organic food waste in Ukraine accounts for 37% of total solid waste, so the issue of sorting and further management of biowaste is of great importance. The EU experience also testifies that the inclusion in the system of separate collection of biowaste significantly increases the quality of dry household waste sorting.

The main fractions into which household waste can be divided are: plastic, paper/cardboard, glass, metal, biowaste, clothing/footwear, mixed waste (residual waste that does not belong to the previous fractions). Hazardous waste should also be collected separately.

The development of waste management infrastructure remains an important issue and the situation in Ukraine is to be discussed. In 2019, the Kyiv city authorities initiated a pilot project to develop a separate solid waste collection system. During the year, 3.5 thousand tanks were installed in the city. In 2019, about 4.5% of the collected waste went to processing plants. This is 1% more than in 2018. However, according to "Kyivkomunservis", in the first months of the project only about 15–20% of waste collected separately was suitable for recycling due to the low quality of sorting by the population.

The public project "Ukraine without garbage" (creates sorting stations and raises the level of citizens' consciousness) has been working since 2015 and aims to improve the environment by involving communities in waste sorting.

In Ukraine, there are 17 enterprises for the processing of waste paper, 39 – for the processing of polymers, 19 – for the processing of PET raw materials, 16 – for the processing of cullet.

It is important to work in this direction at all levels of government. In particular, the central authorities: enshrine at the legislative level the mechanism of separate waste collection; approve methods of calculating targets for preparation for reuse and recycling of household waste; approve the procedure for setting tariffs for household waste management services in compliance with the principle of "pay-as-you-throw", except for payment for waste; develop universal instructions for labeling products, waste from which is subject to separate collection; develop and approve general requirements for the design of containers for separate collection, in particular, ease of use, information support and general rules for the use of colors for the collection of various types of waste. Local authorities are responsible for: organization of separate collection of household waste, including creation of municipal waste collection points; ensuring the implementation of target indicators and quality parameters for biowaste recycling and treatment of other household waste products. On the business side, it is advisable to: ensure simple labeling of products, waste from which is subject to separate collection in accordance with the approved instructions; inclusion of separate collection in waste management plans at the enterprise level. The population is obliged to sort waste and treat it if wished.

The introduction of the EPR System [41] is one of the target areas for the implementation of the European waste management experience. In 30 years, the number of EPR systems in the world has reached 400. The legal framework for the development of EPR at the EU level consists of both framework legislation on waste and sectoral directives aimed at regulating the waste of certain types of products, including packaging, waste from electrical and electronic equipment (WEEE), end-of-life vehicles (ELV), batteries and accumulators (B&A). There is no strict obligation in the EU to introduce EPR systems for packaging manufacturers. Despite this, at least for household waste, the most EU member states (25 out of 28) have chosen the EPR path. In the case of the introduction of the EPR packaging system in Ukraine, there will be potential for the development of the domestic market of secondary raw materials. Currently, due to the high cost of materials, processing companies are forced to import secondary raw materials from abroad.

One more direction for the implementation of the European waste management experience is raising public awareness and educational activities. The experience of countries that have made significant progress in the field of waste management testifies that raising public awareness is a prerequisite for creating sustainable waste management systems. The results of educational initiatives can be observed in 5, 10 or even more years, but without proper training of the population, the waste management system will not be able to function. In many countries, environmental education begins in kindergarten and primary school. Some countries 15–20 years ago have conducted educational campaigns at the state level and managed to form the mentality of the nation in relation to the environment. Among such initiatives the following ones can be mentioned: introduction of waste sorting with the participation of children in kindergartens and schools, environmental lectures, integration of waste management in children's daily lives through cartoons, books, toys, involving children in special environmental projects. In addition to educating children, informational and educational activities among the adult population are mandatory. Communication must be sustainable and carried out at the national level. It should be borne in mind that the media space on waste management is quite active. However, the focus of the discussion is blurred and does not always stimulate action and change the behavior of the population. In addition, there is no reliable and transparent source of comprehensive data on the sector's work, which does not make it possible for interested citizens to explore issues and get involved in solving problems or implement public control where appropriate.

In order to implement the European experience, the infrastructure for separate collection and the quality of waste sorting must be improved. Today the current state of infrastructure in Ukraine is as follows: 34 waste sorting lines for household waste, 1 waste incineration plant "Energy" for municipal waste, ≈5 thousand landfills for municipal waste, 3 incinerators for municipal waste, > 27 thousand unauthorized landfills, the need to build 384 new landfills.

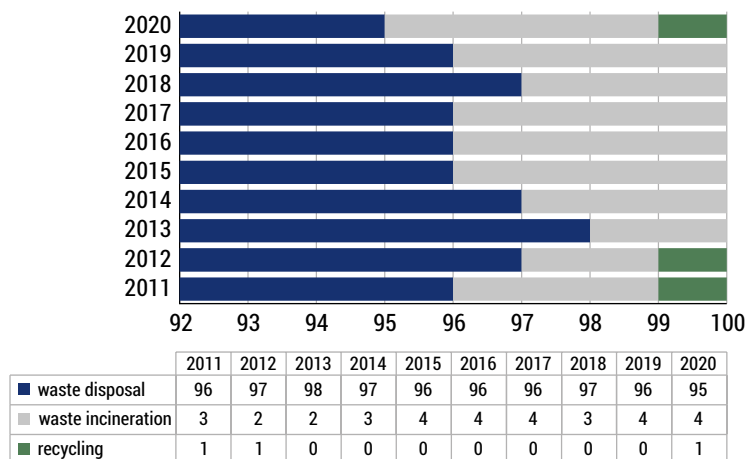Data on waste management in Ukraine in 2011–2020 is shown in Fig. 8.

	2011	2012	2013	2014	2015	2016	2017	2018	2019	2020
■ waste disposal	96	97	98	97	96	96	96	97	96	95
■ waste incineration	3	2	2	3	4	4	4	3	4	4
■ recycling	1	1	0	0	0	0	0	0	0	1

FIG. 8. **Waste management in Ukraine in 2011−2020, %**

It should be noted that the level of waste disposal in Ukraine compared to European countries remains insufficient, which is primarily due to the limited amount of organized collection of municipal waste and this contributes to uncontrolled waste disposal. The lack of technical capacity to recycle or dispose of certain categories of waste is a prerequisite for uncontrolled emissions and disposal. Many existing waste disposal facilities, such as landfills and incinerators, do not meet legal requirements and modern technical standards. In addition, the syndrome "my house is on the edge" further complicates the construction of new facilities and structures for recycling. It is also affected by the continued operation of some facilities etc., which are directly related to the danger to the environment.

In this regard, Ukraine, based on the experience of the European countries, has adopted the main strategic goals to be achieved by 2030.

Summary

The implementation of the EU's best waste management practices is of great importance for Ukraine. The stated objectives are general and can be applied to the waste management strategy based on the European experience as a whole. Among the important priorities of the strategy are:
- reducing the risk of adverse effects on human health and the environment in Ukraine in the early stages, improving waste management practices based on hierarchy principles and assumption criteria;
- optimizing opportunities for new generation and minimizing existing waste, increasing the amount of waste destined for recycling, re-utilization and restoration, where it is economically viable and financially feasible;

- increasing the volume and improving the quality of waste collection;
- development of waste management facilities, restoration and disposal in accordance with the latest technical standards;
- reducing the risks to human health and the environment from the spread of landfills;
- strengthening the influence of institutions responsible for waste management at the national, regional and local levels;
- providing comprehensive and reliable data on waste production, management and disposal;
- increasing sectoral investment and expanding the application of the principles of "extended producer responsibility" and "polluter pays";
- raising public awareness and involvement, increasing efforts to address the waste management issues within the country.

Among the quantitative tasks that must be performed in Ukraine the following ones should be named:
- dissemination of the municipal waste collection service;
- reuse and recycling of household and similar waste into paper, cardboard, plastic, glass and metal;
- reuse and recycling of construction and demolition waste;
- specific tasks for certain types of waste, including packaging waste, disposal of waste electrical and electronic equipment, batteries and accumulators, end-of-life vehicles, and the use of waste petroleum products must also be ensured.

Literature

[1] Sustainable Development Goals Knowledge Platform. Available online: URL https://sustainabledevelopment.un.org/milesstones/wssd (accessed on 21 April 2021).

[2] Directive 2006/12/EC of the European Parliament and of the Council on waste. Official Journal of the European Union L 114/9. Available online: URL eur-lex.europa.eu/LexUriServ/LexUriServ.do?uri=OJ:L:2006:114:0009:0021:EN:PDF (accessed on 23 January 2021).

[3] European Commission. The Sixth Environment Action Programme of the European Community 2002–2012. Available online: URL https://ec.europa.eu/environment/archives/action-programme/ (accessed on 01 February 2021).

[4] European Environment Agency. Waste Incineration Directive (2000/76/EC). Directive 2000/76/EC of the European Parliament and of the Council of 4 December 2000 on the incineration of waste. Available online: URL https://www.eea.europa.eu/themes/waste/links/waste-incineration-directive-2000-76-ec (accessed on 04 February 2021).

[5]   EUR-Lex Access to European Union Law. Directive (EU) 2018/850 of the European Parliament and of the Council of 30 May 2018 amending Directive 1999/31/EC on the landfill of waste (Text with EEA relevance) PE/10/2018/REV/2 OJ L 150, 14.6.2018, p. 100–108 (BG, ES, CS, DA, DE, ET, EL, EN, FR, GA, HR, IT, LV, LT, HU, MT, NL, PL, PT, RO, SK, SL, FI, SV). Available online: URL https://eur-lex.europa.eu/eli/dir/2018/850/oj (accessed on 22 February 2021).

[6]   Designing Buildings Wiki. Available online: URL https://www.designingbuildings.co.uk/wiki/Waste_and_Resources_Action_Programme_WRAP (accessed on 20 February 2021).

[7]   Eco Emballages. Available online: URL http://www.ecoemballages.fr/ (accessed on 25 March 2021).

[8]   European Comission. Operational Programme ESF Flanders 2014–2020. Belgium. Available online: URL https://ec.europa.eu/regional_policy/en/atlas/programmes/2014-2020/belgium/2014be05sfop002 (accessed on 28 March 2021).

[9]   Environmental Protection Agency. Available online: URL https://www.epa.ie/our-services/compliance--enforcement/waste/ (accessed on 27 February 2021).

[10]   European Environment Agency. Austria municipal waste management. Available online: URL https://www.eea.europa.eu/api/SITE/publications/managing-municipal-solid--waste/austria-country-paper-on-municipal/view (accessed on 05 February 2021).

[11]   Grenelle Environment Roundtable. Available online: URL https://sustainabledevelopment.un.org/index.php?page=view&type=99&nr=17&menu=1449 (accessed on 17 March 2021).

[12]   Directive 2008/98/EC of the European Parliament and of the Council of 19 November 2008 on waste and repealing certain Directives. Available online: URL https://eur-lex.europa.eu/LexUriServ/LexUriServ.do?uri=OJ:L:2008:312:0003:0030:en:PDF (accessed on 10 April 2021).

[13]   The Waste (England and Wales) Regulations 2011. UK Statutory Instruments. No. 988, 2011. Available online: https://www.legislation.gov.uk/uksi/2011/988/contents/made (accessed on 17 April 2021).

[14]   The List of Wastes (England) Regulations 2005. UK Statutory Instruments. No. 895, 2005. Available online: https://www.legislation.gov.uk/uksi/2005/895/contents/made (accessed on 18 April 2021).

[15]   Notices from European Union Institutions, Bodies, Offices and Agencies European commission, Commission notice on technical guidance on the classification of waste (2018/C 124/01). Official Journal of the European Union, 2018, 134 p. Available online: URL https://eur-lex.europa.eu/legal-content/EN/TXT/PDF/?uri=CELEX:52018XC0409(01)&from=EN (accessed on 19 April 2021).

[16]   EUR-Lex Access to European Union Law. Directive 2010/75/EU of the European Parliament and of the Council of 24 November 2010 on industrial emissions (integrated pollution prevention and control) Text with EEA relevance OJ L 334, 17.12.2010, p. 17–119 (BG, ES, CS, DA, DE, ET, EL, EN, FR, IT, LV, LT, HU, MT, NL, PL, PT, RO, SK, SL, FI, SV). Available online: URL https://eur-lex.europa.eu/legal-content/EN/TXT/?uri=CELEX%3A32010L0075 (accessed on 08 April 2021).

[17] Thomson Reuters Practical Law. Defra: A Strategy for Hazardous Waste Management in England (March 2010). Available online: URL https://uk.practicallaw.thomsonreuters.com/9-501-8934?transitionType=Default&contextData=(sc.Default)&firstPage=true (accessed on 01 May 2021).

[18] Beatriz Ferreira, Javier Monedero, Juan Luís Martí, César Aliaga, Mercedes Hortal and Antonio Dobón López (May 23rd 2012). The Economic Aspects of Recycling, Post-Consumer Waste Recycling and Optimal Production, Enri Damanhuri, IntechOpen, DOI: 10.5772/34133. Available online: URL https://www.intechopen.com/books/post--consumer-waste-recycling-and-optimal-production/the-economic-aspects-of-recycling (accessed on 10 February 2021).

[19] European Commission. Construction and demolition waste. Available online: URL http://ec.europa.eu/environment/waste/construction_demolition.htm (accessed on 12 April 2021).

[20] European Commission. Cordis. Final Report Summary – PLASCARB (Innovative plasma based transformation of food waste into high value graphitic carbon and renewable hydrogen). Available online: URL https://cordis.europa.eu/project/id/603488/reporting/pl (accessed on 15 April 2021).

[21] Inventory of good practices regarding (bio-)waste minimization in Europe. Available online: URL https://www.acrplus.org/images/project/Miniwaste/Miniwaste-inventory-of-prevention-good-practices.pdf (accessed on 21 April 2021).

[22] Waste-to-Energy in the Circular Economy: CEWEP. Available online: URL https://www.cewep.eu/stengler-wte-communication/ (accessed on 03 March 2021).

[23] The European Commision's Renewable Energy Proposal for 2030. Policy Update. International Council on Clean Transportation. 2017, 8 p. Available online: URL https://theicct.org/sites/default/files/publications/RED%20II_ICCT_Policy-Update_vF_jan2017.pdf (accessed on 10 April 2021).

[24] European Environment Agency. Closing the loop – An EU action plan for the Circular Economy COM/2015/0614 final. Available online: URL https://www.eea.europa.eu/policy-documents/com-2015-0614-final (accessed on 26 March 2021).

[25] The EIB in the circular economy. Available online: URL https://www.eib.org/en/about/initiatives/circular-economy/index.htm (accessed on 12 February 2021).

[26] Towards the circular economy. Economic and business rationale for an accelerated transition. 2013. Available online: URL https://www.ellenmacarthurfoundation.org/assets/downloads/publications/Ellen-MacArthur-Foundation-Towards-the-Circular-Economy-vol.1.pdf. (accessed on 15 February 2021).

[27] Avfall Sverige – the Swedish Waste Management Association. Available online: URL https://www.avfallsverige.se/in-english/ (accessed on 09 March 2021).

[28] Rene Rosendal. Danish Policy on Waste Management – Denmark without waste. Proc. of Linnaeus Eco-Tech, Linnaeus University, Denmark, November 2014. Available online: https://www.researchgate.net/publication/287210935_DANISH_POLICY_ON_WASTE_MANAGEMENT_-_DENMARK_WITHOUT_WASTE (accessed on 10.06.2021).

[29] ALBA Group the recycling company. Available online: URL www.alba.info/en/alba--group/press/press-kit/figures-and-facts-on-the (accessed on 10 May 2021).

[30] National Strategy of Waste Management. SEC ECOLOGY, Kyiv, December 2016. Available online: URL https://eco.kiev.ua/assets/files/Osnovna-chastina.pdf (accessed on 05 May 2021).

[31] European Commission. Eco-Innovation at the heart of European policies. Netherlands. Available online: URL https://ec.europa.eu/environment/ecoap/about-eco-innovation/policies-matters/netherlands/netherlands-pulls-ahead-in-circular-economy-race_en. (accessed on 29 April 2021).

[32] European Circular Economy Stakeholder Platform. Available online: URL https://circulareconomy.europa.eu/platform/en/strategies/circular-economy-netherlands-2050. (accessed on 16 May 2021).

[33] Mohamed Alwaeli. An overview of municipal solid waste management in Poland. The current situation, problems and challenges, Environment Protection Engineering, Vol. 41, 2015, No. 4, pp. 181–193.

[34] Statistics Poland. Available online: URL https://stat.gov.pl/en/ (accessed on 07 May 2021).

[35] Mohamed Alwaeli. The impact of product charges and EU directives on the level of packaging waste recycling in Poland, Resources Conservation and Recycling, 2010, 54 (10):609–614. DOI: https://doi.org/10.1016/j.resconrec.2009.11.011 (accessed on 07 May 2021).

[36] GOAP. Available online: URL https://www.goap.org.pl (accessed on 20 April 2021).

[37] ISSUU. Snaga Ljubljana, the biggest Slovenian waste management company. Available online: URL https://issuu.com/snaga4/docs/snaga_ljubljana_eng (accessed on 25 May 2021).

[38] Eurostat Statistics Explained. Waste Management Indicators. Available online: URL https://ec.europa.eu/eurostat/statistics-explained/index.php?title=Waste_management_indicators. (accessed on 05 March 2021).

[39] Cherinko O., Balanyuk A. Waste Management in Ukraine. Opportunities for Dutch Companies: Final Report. Ministry of Foreign Affairs. Available online: URL https://www.rvo.nl/sites/default/files/2019/02/Waste-management-in-Ukraine.pdf (accessed on 06 March 2021)

[40] PwC. From the third world in the first. Waste management reform in Ukraine. Available online: URL https://www.pwc.com/ua/en/survey/2020/waste-management.pdf (accessed on 13 May 2021).

[41] Sustainable Development Goals Knowledge Platform. Available online: URL https://sustainabledevelopment.un.org/index.php?page=view&type=99&nr=81&menu=1449 (accessed on 10 May 2021).

The calculations of the efficency of the lightweight floor heating according to nordtest method NT VVS 127

Abstract: The suitability of Nordest Method NT VVS 127 for determining the operational parameters of the lightweight floor heating with a dry screed was tested. The methodology of surface temperature and heat flux density determination according to Nordest Method NT VVS 127 was presented. The calculations were made for lightweight floor heating with a dry screed of various thickness and variable water temperature. The results were compared with the numerical calculations made with ANSYS Steady-State Thermal Solver. The operational parameters of the floor heating were also determined using the method presented in PN-EN 1264 standard. The difference between the surface temperature determined according to Nordest Method NT VVS 127 and the numerical values does not exceed 5,68 K, for the heat flux density the error is up to 55,5%. The difference between the surface temperature determined according to PN-EN 1264 and the numerical value does not exceed 0,2 K, for the heat flux density the error is up to 8,5%. It was found, that the PN-EN 1264 standard is more applicable to determining the operational parameters of lightweight floor heating with a dry screed than Nordest Method NT VVS 127.

Introduction

In recent years, due to the increase in the use of low-temperature heat sources, i.e. heat pumps, condensing gas boilers, the use of surface heating has increased. Among the surface heating systems, floor, wall and ceiling heating can be distinguished. The most popular is floor heating in a wet system, especially in single-family houses [3]. In a wet system, pipes are laid on a thermal insulation layer in a cement or anhydrite screed. The finishing layer is placed directly on the screed. This system is characterized by a considerable height (the minimum height of the screed over the pipes is 45 mm) and a long assembly time. Due to its large mass, this solution is characterized by high thermal inertia, which causes control problems and a long response time to changing heat demand [15].

A solution that eliminates these disadvantages is lightweight floor heating, also known as a dry floor heating system. The dry system in relation to the wet one is characterized by lower thermal inertia [8, 14], shorter assembly time, and lower assembly height. It is a system used especially in renovated buildings, as well as in sacred and historic buildings, where interference in the building structure must be as small as possible.

In a lightweight floor heating system, pipes are laid in a ribbed channels in thermal insulation, or on a flat plate made of thermal insulation. Ducts in thermal insulation are dimensioned to the outer diameter of the pipe. A plate is mounted on the layer with pipes, whose task is to transfer mechanical loads. It is made among others from a dry screed or wood-like boards. These are most often used materials intended for installation on floor heating, they are characterized by variable height and heat conduction coefficients. The finishing layer, e.g. tiles, panels or a carpet, is placed on this layer. In order to increase the efficiency of the floor heating, heat-conducting plates made of a material with high heat conductivity, e.g. aluminium, are used on the surface of the thermal insulation and under the pipes. Radiant sheets made of metalized polyethylene are also used, but compared to aluminium sheets, they are much less efficient [11]. The heat conducting plate does not always adhere perfectly to the thermal insulation and to the pipes, which creates air spaces in the floor heating cosnstuction. Hence, the thermal resistance to heat transfer between the pipes and other layers of the floor heating is greater than for floor heating in a wet system, in which the pipes are completely surrounded by the screed.

Due to the complexity of the heat transfer process in lightweight floor heating systems, methods for calculating the efficiency of these systems are being developed. Zhang et al. in Ref. [13] developed a mathematical model to determine the efficiency of dry system. The model was developed for a system where the pipes are in the air layer. The pipes lie on a thermal insulation covered with aluminum foil. The thermal insulation board is flat without channels. The finishing layer is supported by the keels. Weitzmann et al. in Ref. [10] developed a two-dimensional model

to calculate the lightweight floor heating. Qiu and Li in Ref. [7] used the finite difference method to determine the performance of the lightweight floor heating system and to compare it with the wet system. The tested floor heating consisted of pipes arranged in profiled channels with an aluminium radiant sheet. Thomas et al. [8] developed a numerical model to study heat transfer in a lightweight system in cooling and heating mode. The model was developed for a construction in which pipes are arranged in wood planks. The pipes are laid in the aluminum clips, that do not completely cover the surface of the thermal insulation. Wang et al. [9] carried out a numerical simulation of a new construction of floor heating in a dry system: an enhanced-convection overhead radiant floor heating system. Anna Werner-Juszczuk in Ref. [12], used the numerical simulation in the ANSYS software to investigate the influence of aluminium thickness on the lightweight floor heating. The analysis took into account three structures of the floor heating in dry mode: wood-like board, dry screed and pipes embedded in the adhesive layer. The pipes were placed in channels in layer of a thermal insulation completely covered with aluminium of different thickness.

Most publications in the field of the performance of the lightweight floor heating systems contain experimental research. Zhang et al. [13] and Weitzmann [10] validated the mathematical model of the floor heating by means of experimental studies. Thomas et al. [8] also verified the proposed numerical model experimentally. Evren et al. [1] experimentally tested a system with electric fan heaters cooperating with lightweight floor heating. In the tested system, PE-Xa pipes were laid in channels made in 30 mm thick thermal insulation, the thickness of the aluminum radiant sheet was 0.5 mm. Werner-Juszczuk [11] investigated experimentally a lightweight floor heating system with radiant sheets made of metalized polyethylene sheet: heat flux emitted from the surface and surface temperature. The floor heating construction without radiant sheet was also tested. In the tested structures, the pipes were covered with a screed layer and laid in profiled channels in thermal insulation. Wang et al. [9] compared the performance of two lightweight floor heating systems by means of measurements in the artificial climate chamber: enhanced-convection overhead radiant floor heating system and overhead radiant floor heating system. Żukowski and Karpiesiuk [17] tested type B of floor hating in a dry system experimentally. A floor heating was tested with pipes placed in a plate with channels in different variants: with and without a diffusing plate, with variable dry screed thickness, with pipes in the adhesive layer or pipes in the air layer. Żukowski and Salmanowicz experimentally determined the heating efficiency of wall heating in dry mode [18].

The literature review confirms that there are few publications on modeling the performance of lightweight floor heating.

In Poland, the standards PN-EN 1264 [6] and PN-EN ISO 11855 [5] are used to design and determine the operational parameters of surface heating and cooling systems. Both standards described the types of radiant heating to which the standard applies, they are mainly used for the design of the wet systems. These standards can, inter alia, be used for type B of the floor heating. Type B is characterized

by the arrangement of the pipes in the layer of thermal insulation. The insulating layer along with the pipes is covered by a weight bearing layer made of timber or screed (dry or wet). Pipes may be stacked above the heat diffusion device. The methodology for calculating this type of lightweight floor heating is presented in [16].

Nordtest Method NT VVS 127 [4] is a standard that can also be used to determine the efficiency of lightweight floor heating. This standard is intended only for lightweight floor heating with a heat conduction device. This is not the Polish standard. The application of this standard was presented in [2], where the thermal efficiency of the ultra-thin floor heating construction was calculated. The tested lightweight floor heating consisted of pipes placed in the channels in thermal insulation on the aluminum radiant sheet layer. The construction does not use a dry screed, the pipes are directly covered with a layer of adhesive for fixing ceramic tiles.

Due to the lack of analysis of the possibility of using the Nordtest Method NT VVS 127 to calculate the efficiency of lightweight floor heating with a dry screed, this problem is analysed in this paper. First, the methodology of calculating the density of the heat flux and surface temperature according to the Nordtest Method NT VVS 127 is presented. Then, in order to assess the compliance of analysed method, calculations of the heat flux density and surface temperature will be performed according to the Nordtest Method NT VVS 127, PN-EN1264 standard and numerically. Numerical calculations will be performed using the ANSYS Steady-State Thermal Solver software (Workbench 19.2). The analysis is performed for the lightweight floor heating with pipes in thermal insulation, covered with dry screed of different thickness. An aluminium radiant sheet of thickness 0.3 mm is taken into account, with 10 mm gap between the sheets. A comparative analysis of the determined parameters of floor heating with those three methods is carried out.

Methodology of Nordtest Method NT VVS 127

The method applies to the lightweight floor heating with mounted radiant sheet and to electric floor heating systems. The heat conduction plate must have a much greater thermal conductivity than the other materials in the construction. This condition is described by the formula (1):

$$\lambda_{WL} \geq 10 \cdot \lambda_{surrounding\ materials},$$ (1)

where: λ_{WL} – thermal conductivity of radiant sheet [W/mK], $\lambda_{surrounding\ materials}$ – the highest thermal conductivity of materials surrounding the radiant sheet [W/mK].

At the same time, the product of thermal conductivity of radiant sheet and its thickness must satisfy the condition (2):

$$s_{WL} \cdot \lambda_{WL} \geq 0,01, \tag{2}$$

where: s_{WL} – thickness of a radiant sheet [m].

The first step is to calculate the parameters considering the construction of the lightweight floor heating: materials with their thicknesses and thermal properties. In the case of floor heating in a dry system, it is important to determine which layers are above the radiant sheet and which are below.

The thermal resistance of the layers above the pipes, including the contact thermal resistance of radiant sheet is defined as R_i. It can be calculated from the formula (3):

$$R_i = R_o + R_{con,i} + R_{si} \ \ [m^2K/W], \tag{3}$$

where: R_o – thermal resistance of the layers above the radiant sheet [m^{2}K/W], R_{si} – thermal resistance of the heat transfer from the surface of the floor heating [m^{2}K/W], $R_{con,i}$ – the contact thermal resistance of the radiant sheet (heat conducting plate) [m^{2}K/W].

Value of the contact thermal resistance of the radiant sheet depends on how the pipes are arranged in the radiant sheet. The standard gives two resistance values:
- 0,15 m^{2}K/W – for standard constructions,
- 0,10 m^{2}K/W – when the radiant sheet adheres tightly to the pipe and other materials in the floor heating constructions.

The resistance of the heat transfer R_{si} is determined in the same way as for wet systems. The value recommended by the Nordtest Method NT VVS 127 is 0,093 m^{2}K/W.

The resistance of the layers above the pipe R_o is determined by the height and the thermal conductivity of materials from the formula (4):

$$R_o = \sum_{i=1}^{n} \frac{d_i}{\lambda_i} \ \ [m^2K/W], \tag{4}$$

where: d_i – thickness of the i-th layer of the floor heating [m], λ_i – thermal conductivity of the i-th layer of the floor heating [W/mK].

In order to calculate the lightweight floor heating efficiency, it is also necessary to know the resistance of the layers below the radiant sheet defined as R_e. Since, in dry systems, pipes are usually laid in profiled channels made in a thermal insulation layer, covered with a radiant sheet, the resistance R_e should be calculated taking into account the geometric dimensions of these channels. For this purpose, the following formula should be used (5):

$$R_e = R_u + R_{se} - 2\frac{a}{\lambda_{ins}}\frac{b}{T} \ \ [m^2K/W], \tag{5}$$

where: a – the depth of the channel [m], b – the width of the channel [m], T – pipe spacing [m], R_u – thermal resistance of the layers below the radiant sheet, R_{se} – thermal resistance of the heat transfer from the bottom surface of the floor heating (R_{se} =0,17 m^{2}K/W).

Based on the calculated resistances R_i and R_e, it is possible to calculate the fictitious thermal resistance of the conducting layer R_{CL} from the relation (6):

$$R_{CL} = \frac{1}{\dfrac{1}{R_i} + \dfrac{1}{R_e}} \left(\frac{1}{k_{CL}} - 1 \right) \ [\text{m}^2\text{K/W}], \tag{6}$$

where: k_{CL} – parameter characterizing the radiant sheet [–].

The fin method was used in the method of calculating the parameter k_{CL}. The value of this parameter can be determined from the formula (7):

$$k_{CL} = \frac{d_{out} + 2L_{fin}k_{fin} + 0,01L_G \left(\dfrac{1}{cosh\left(\dfrac{L_{fin}}{l}\right)} \right)}{T} \ [–], \tag{7}$$

where: L_{fin} – the width of fin (the horizontal part of the radiant sheet seen as a heating fin) [m], k_{fin} – parameter characterizing the heating fin [–], l – and characteristic length of the fin [m], d_{out} – the outer diameter of the pipe [m], L_G – the distance between the radiant sheets [m].

Characteristic length of the fin l is calculated from formula (8):

$$l = \sqrt{\frac{s_{WL} \cdot \lambda_{WL}}{\dfrac{1}{R_i} + \dfrac{1}{R_e}}} \ [\text{m}], \tag{8}$$

where: s_{WL} – the thickness of the radiant sheet [m], λ_{WL} – the thermal conductivity of the radiant sheet [W/mK].

The width of the fin L_{fin} is calculated from relation (9):

$$L_{fin} = \frac{T - d_{out} - L_G}{2} \ [\text{m}]. \tag{9}$$

Based on the values of l and L_{fin}, it is possible to determine the coefficient characterizing the fin k_{fin} from the formula (10):

$$k_{fin} = \frac{l}{L_{fin}} tanh\left(\frac{L_{fin}}{l}\right) \ [-]. \tag{10}$$

The value *of* R_{CL} calculated on the basis of the formula (6) is necessary to calculate the R_{HC}. R_{HC} denotes the thermal resistance from the heating medium to the heat-conducting layer. This value strongly depends on the type of the pipes used in the floor heating construction and the pipe spacing. It is the sum of the thermal resistance of the pipes, contact resistance between the pipe and the radiant sheet, thermal resistance of the radiant sheet and thermal resistance which occurs due to assembling the pipes in channels made in radiant aluminum sheet. R_{HC} can be determined from formula (11):

$$R_{HC} = T \cdot R_p' + T \cdot R_{p,con}' + \frac{T}{2} R_U' + R_{CL} \ [\text{m}^2\text{K/W}], \tag{11}$$

where: R_p' – linear thermal resistance through the pipe wall [mK/W], $R_{p,con}'$ – linear thermal contact resistance between the conducting plate and the pipe [mK/W], R_U' – resistance in the U-section of the radiant sheet [mK/W].

It should be noted that the values of thermal resistance with the index ' are given in mK/W and not in m²K/W. This is because these linear resistance values are multiplied by the spacing of the pipes. The particular resistance values listed in formula (11) are calculated from the formulas (12–14):

$$R_p' = \frac{1}{2\pi\lambda_p} ln\left(\frac{d_{out}}{d_{in}}\right), \tag{12}$$

$$R_{p,con}' = \frac{0,01}{d_a}, \tag{13}$$

$$R_U' = \frac{0,008}{d_a}, \tag{14}$$

where: d_{out} – the outer diameter of the pipe [m], d_{in} – the inner diameter of the pipe [m], λ_p – thermal conductivity of the pipe [W/mK], d_a – the diameter of the pipe [m].

In formulas (13) and (14) the value of pipe diameter d_a is given, but it is not specified, whether it is inner or outer diameter. For analysis performed in this paper the outer diameter is taken into account.

After determining the parameters characterizing the structure of the lightweight floor heating, the density of the heat flux emitted from the surface q_i of the can be determined from the relation (15):

$$q_i = K_H \left(T_H - T_i\right) \ [\text{W/m}^2], \tag{15}$$

where: K_H – the equivalent heart transmission coefficient [W/m^{2}K], T_H – the temperature of the heating medium [°C], T_i – the room temperature [°C].

Equivalent heat transmission coefficient K_H can be calculated from formula (16):

$$K_H = \frac{q_i^{max}}{T_H^{max} - T_i}, \tag{16}$$

where: T_H^{max} – maximum permissible mean temperature of the heating medium [°C], q_i^{max} – maximum heat flow density [W/m^2].

Maximum permissible mean temperature of the heating medium T_h^{max} is calculated from relation (17):

$$T_H^{max} = T_i + q_i^{max} \left(R_i + \frac{1}{\eta} R_{HC}\right). \tag{17}$$

According to the Nordtest Method NT VVS 127, coefficient of $1/\eta$ is equal to 1,1. Maximum heat flow density q_i^{max} is determined according to formula (18):

$$q_i^{max} = 8,92 \left(T_F^{av,max} - T_i\right)^{1,1}, \tag{18}$$

where the maximum permissible average surface temperature $T_f^{av,max}$ can be calculated from formula (19):

$$T_F^{av,max} = T_i + k_{CL} \left(T_F^{max} - T_i\right) \ [\text{°C}]. \tag{19}$$

As it can be observed, for determination of maximum allowable heat flux density there is a necessity to know value of maximum permissible floor surface temperature T_F^{max}. Value of this temperature is described in standards PN-EN 1264 and PN-EN ISO 11855 and is obligatory also for the floor heating made in wet technology. The maximum allowable temperature at the floor heating surface in dry rooms is 29°C in areas of permanent human habitation and 31°C in the edge areas. In wet rooms, such as bathrooms, the maximum temperature is respectively 33°C and 35°C.

After determining the heat flux density, the average surface temperature of the lightweight floor heating can be determined from the relation (20), presented in standards PN-EN 1264 and PN-EN ISO 11855, after appropriate transformations (21):

$$q_i = 8,92 \left(T_F - T_i\right)^{1,1}, \tag{20}$$

$$T_F = \left(\frac{q_i}{8,92}\right)^{\frac{10}{11}} + T_i \ \ [°C].$$
(21)

Model of lightweight floor heating

The analysis was made for a lightweight floor heating with a dry screed, due to the lack of calculations of this type of floor heating with methodology presented in Nordtest Method NT VVS 127. The scheme of the model is shown in Figure 1. The properties and thicknesses of each element of the floor heating are summarized in Table 1. The ceramic tiles were chosen as finishing layer. Two thicknesses of a dry screed were taken into account: 20 and 25 mm.
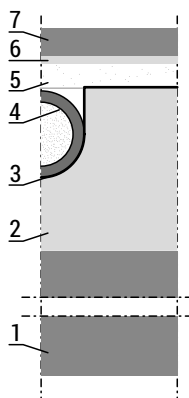

FIG. 1. **Scheme of the lightweight floor heating (markings according to Table 1)**
SOURCE: **own study**

TABLE 1. **Specifications of the materials**

No	Material	λ [W/(m·K)]	Thickness [mm]
1	reinforced concrete slab	1,7	150
2	EPS	0,04	30
3	aluminium	230	0,3
4	pipe PE-Xc	0,35	2
5	dry screed	0,32	20/25
6	tile adhesive	0,8	4
7	ceramic tiles	1,05	10

The calculations were made for a pipe spacing of 0,125 m and five temperatures of the heating medium in the range of 25–45°C. The thickness of aluminium was assumed to be 0.3 mm in accordance to recommendations in Ref. [12]. In order to obtain compatibility between the numerical model and the calculation model in the standards, the same boundary conditions inside the pipe and on the upper and lower surface of the floor heating were adopted. The constant temperature inside the pipe was assumed as average temperature of the heating medium. A heat transfer coefficient of 10,8 W/m^{2}K was assumed on the upper surface of the lightweight floor heating. A heat transfer resistance of 0,17 m^{2}K/W was assumed on the bottom surface of the floor heating. The adopted values are in line with the requirements of the Polish standards PN-EN 1264, PN-EN ISO 11855 and requirements of Nordest Method NT VVS 127.

Results and discussion

The heat flux density and the surface temperature of the lightweight floor heating were determined using three methods: Nordest Method NT VVS 127, the method presented in PN-EN 1264 and the numerical method. Numerical calculations were performed with the ANSYS Steady-State Thermal Solver software (Workbench 19.2).

The absolute error ΔT_F in the determination of the surface temperature T_F was calculated, taking the numerically calculated temperature as the reference value (22):

$$\Delta T_F = \left| T_F^x - T_F^{ANSYS} \right| \; [\text{K}], \tag{22}$$

where: $T_F^{\,x}$ – surface temperature of the lightweight floor heating calculated using particular method: PN-EN 1264 ($T_F^{\,1264}$) or Nordest Method NT VVS 127 ($T_F^{\,N}$) [°C], $T_F^{\,ANSYS}$ – surface temperature of the lightweight floor heating calculated numerically using ANSYS [°C].

The relative error ε_{qi} in determining the surface heat flux density q_i was calculated, taking the numerically calculated heat flux as a reference value (23):

$$\varepsilon_{qi} = \frac{\left| q_i^x - q_i^{ANSYS} \right|}{q_i^{ANSYS}} \cdot 100\% \;, \; [-] \tag{23}$$

where: $q_i^{\,x}$ – heat flux density of the lightweight floor heating calculated using particular method: PN-EN 1264 ($q_i^{\,1264}$) or Nordest Method NT VVS 127 ($q_i^{\,NT}$) [W/m^2], $q_i^{\,ANSYS}$ – heat flux density of the lightweight floor heating calculated numerically using ANSYS [W/m^2].

The calculation results for lightweight floor heating with a 20 mm thick dry screed are gathered in Table 2 and for construction with a 25 mm thick dry screed in Table 3. The results are given for the variable water temperature T_H.

TABLE 2. **Results for lightweight floor heating with dry screed 20 mm thick**

T_H	ANSYS		PN-EN 1264		NT vvs 127		Errors			
	T_F	q_i	T_F	q_i	T_F	q_i	ΔT_F^{1264}	ΔT_F^{NT}	ε_{qi}^{1264}	ε_{qi}^{NT}
°C	°C	W/m²	°C	W/m²	°C	W/m²	K	K	%	%
25	22,11	22,86	22,21	21,31	21,13	10.18	0,10	0,98	6,8	55,5
30	24,22	45,72	24,42	45,82	22,12	20,35	0,20	2,10	0,2	55,5
35	26,33	68,58	26,47	69,57	23,06	30,53	0,14	3,27	1,4	55,5
40	28,45	91,44	28,43	93,14	23,97	40,70	0,02	4,48	1,9	55,5
45	30,56	114,30	30,35	116,64	24,87	50,88	0,21	5,69	2,0	55,5

TABLE 3. **Results for lightweight floor heating with dry screed 25 mm thick**

T_H	ANSYS		PN-EN 1264		NT vvs 127		Errors			
	T_F	q_i	T_F	q_i	T_F	q_i	ΔT_F^{1264}	ΔT_F^{NT}	ε_{qi}^{1264}	ε_{qi}^{NT}
°C	°C	W/m²	°C	W/m²	°C	W/m²	K	K	%	%
25	21,97	21,28	22,03	19,48	21,09	9,85	0,06	0,88	8,5	53,7
30	23,94	42,57	24,08	41,90	22,05	19,69	0,15	1,89	1,6	53,7
35	25,90	63,85	25,97	63,62	22,97	29,54	0,07	2,93	0,4	53,7
40	27,87	85,13	27,78	86,17	23,86	39,39	0,09	4,01	1,2	53,7
45	29,84	106,41	29,54	106,67	24,72	49,23	0,30	5,12	0,2	53,7

The difference between the surface temperature calculated numerically and with method presented in PN-EN 1264 does not exceed the value of 0,20 K for a construction with a 20 mm thick dry screed, and 0,30 K for construction with a 25 mm thick screed. The difference between the temperature calculated with ANSYS and Nordest Method NT VVS 127 increases with increasing water temperature T_H. For floor heating with a screed with a thickness of 20 mm, the absolute surface temperature error varies from 0,98 K for water temperature of 25°C to 5,68 K for water temperature of 45°C. For construction with a dry screed with a thickness of 25 mm values of absolute error are smaller and range from 0,88 to 5,12 K.

The relative error of the heat flux density for values determined with PN-EN 1264 is in the range of 0,2–6,8% for the construction with a 20 mm thick screed, and in the range of 0,2–8,5% for the construction with a 25 mm thick screed. The value

of the relative heat flux depends on the water temperature. The relative error of heat flux density for the values determined with Nordest Method NT VVS 127 is several times greater. It is equal to 55,5% for floor heating with a 20 mm thick screed and 53,7% for floor heating with a 25 mm thick screed.

A high convergence of the calculation results using the numerical method with the method presented in the PN-EN 1264 standard can be observed. The average surface temperature determined by these two methods does not differ by more than 0,2 K. The difference between the heat flux density does not exceed 8,5%.

The results of the calculations according to the Nordest Method NT VVS 127 differ significantly from those determined numerically. Significant error values were obtained even though the tested floor heating structure met the requirements specified in the standard on the applicability of the standard. These conclusions are consistent with the results presented by Karpiesiuk in [2], where ultra-thin lightweight floor heating was analysed. Karpiesiuk [2] obtained high values of errors between the results of the Nordest Method NT VVS 127 and the results of experimental tests. Karpiesiuk indicated an error in the formulas presented in the standard as the cause of the errors.

Summary

The surface temperature and the heat flux density were determined for lightweight floor heating construction using three methods: numerically with ANSYS, PN-EN 1264 standard and Nordest Method NT VVS 127. The methodology presented in Nordest Method NT VVS 127 aims to determine the operational parameters of lightweight floor heating with heat conduction devices, i.e. radiant sheets. Thus, its applicability for lightweight floor heating with dry screed was tested.

The large differences occur between the results obtained by numerical calculations and the Nordest Method NT VVS 127: temperature error up to 5,68 K, heat flux density error up to 55,5%. Smaller differences are observed for the results determined by the PN-EN 1264 standard and numerically: temperature error up to 0,2 K, heat flux density error up to 8,5%. It can therefore be conclude that the PN-EN 1264 standard is more suitable for determining the operational parameters of lightweight floor heating with a dry screed than Nordest Method NT VVS 127.

The research was carried out with the use of program ANSYS 19.2, which is provided to the Bialystok University of Technology on the basis of an agreement between Bialystok University of Technology and ANSYS Inc. (Canonsburg, USA) and MESco Sp. z o.o. (Tarnowskie Góry, Poland).

Literature

[1] Evren M.F., Özsunar A., Kılkıs B., *Experimental investigation of energy-optimum radiant-convective heat transfer split for hybrid heating systems*, Energy and Buildings 2016, 127, p. 66–74.

[2] Karpiesiuk J., *Thermal performance of the Light Surface Heating System*. GlobeEdit 2019. In Polish.

[3] Myhren JA, Holmberg S., *Flow patterns and thermal comfort in a room with panel, floor and wall heating*, Energy and Buildings 2008, 40, p. 524–536.

[4] Nordtest Method NT VVS 127 *Floor heating systems: Design and type testing of waterborne heat systems for lightweight structures.*

[5] PN-EN ISO 11855-2:2015-10 – *Building environment design – Design, dimensioning, installation and control of embedded radiant heating and cooling systems – Part 2: Determination of the design heating and cooling capacity.*

[6] PN-EN 1264-2+A1:2013-05 – *Water based surface embedded heating and cooling systems – Part 2: Floor heating: Prove methods for the determination of the thermal output using calculation and test methods.*

[7] Qiu L., Li Q., *Analyses on two paving types of floor heating*, International Conference on Computer Distributed Control and Intelligent Environmental Monitoring 2011.

[8] Thomas S., Franck P.Y., Andre P., *Model validation of a dynamic embedded water base surface heat emitting system for buildings*, Building Simulation 2011, 4 (1), p. 41–48.

[9] Wang D., Wu Ch., Liu Y., Chen P., Liu J., *Experimental study on the thermal performance of anenhanced-convection overhead radiant floor heating system*, Energy and Buildings 2017, 135, p. 233–243.

[10] Weitzmann P., Svendsen S., *Method for calculating thermal properties of lightweight floor heating panels based on an experimental setup*, International Journal of Low Energy and Sustainable Buildings 2005, 3, p. 1–15.

[11] Werner-Juszczuk A.J., *Experimental and numerical investigation of lightweight floor heating with metallised polyethylene radiant sheet*, Energy and Buildings 2018, 177, p. 23–32.

[12] Werner-Juszczuk A.J., *The influence of the thickness of an aluminium radiant sheet on the performance of the lightweight floor heating*, Journal of Building Engineering 2021, w druku.

[13] Zhang D., Cai N., Wang Z., *Experimental and numerical analysis of lightweight radiant floor heating system*, Energy and Buildings 2013, 61, p. 260–266.

[14] Zhao K., Liu X.-H., Jiang Y., *Dynamic performance of water-based radiant floors during start-up and high-intensity solar radiation*, Solar Energy 2014, 10, p. 232–244.

[15] Zhou Z., Wang Ch., Sun X., Gao F., Feng W., Zillantee G., *Heating energy saving poten-tial from building envelope design and operation optimization in residential buildings: A case study in northern China*, Journal of Cleaner Production 2018, 174, p. 413–423.

[16] Żukowski M., *Characteristics and design methodology of the dry screed floor heating system – type B*, Instal 2015, 6, p. 31–35. In Polish.

[17] Żukowski M., Karpiesiuk P., *Experimental testing of the floor heating system – ultra flat*, Instal 2015, 10, p. 38–41. In Polish.

[18] Żukowski M., Salmanowicz M., *Experimental Testing of the Wall Heating System Integrated into Dry Construction Panel*, Ciepłownictwo, Ogrzewnictwo, Wentylacja 2016, 47(9), p. 358–364. In Polish.